

**Investigating neuromodulation with theta burst stimulation to primary visual cortex and subsequent effects on resting state networks: A multi-echo fMRI study**

Remy Cohan

A THESIS SUBMITTED TO THE FACULTY OF GRADUATE STUDIES IN PARTIAL FULFILLMENT OF  
THE REQUIREMENTS FOR THE MASTER OF ARTS

Faculty Of Graduate Studies  
Department of Psychology (Brain, Behaviour and Cognitive Sciences)  
York University, Toronto

JUNE 2023

© Remy Cohan, 2023

## Abstract

Theta burst stimulation (TBS) is a type of repetitive transcranial magnetic stimulation (rTMS) protocol which has the advantage of a shorter delivery time over traditional rTMS. When applied to motor cortex, intermittent TBS (iTBS) has been shown to yield excitatory aftereffects, whereas continuous TBS (cTBS) may lead to inhibitory aftereffects, both lasting from minutes to hours. The majority of TBS research has targeted motor, frontal, and parietal regions, and to date very few studies have examined its efficacy at visual areas. In this thesis, we designed a sham-controlled study to investigate the immediate post-stimulation and short-term (1 hr post-stimulation) effects of iTBS and cTBS targeting the primary visual cortex (V1). Using multi-echo functional magnetic resonance imaging, we compared resting state functional connectivity (FC) in whole-brain networks before and after stimulation, with seeds from V1 (stimulation site) and neighbouring occipital and parietal visual networks. In addition, we also measured pre- to post-TBS phosphene thresholds (PTs) to examine the modulatory effects of TBS on cortical excitability. We found no changes in FC for iTBS, cTBS or sham stimulation conditions from baseline to post-stimulation timepoints. Additionally, cTBS and iTBS had no effect on post-stimulation PTs. Our results indicate that unlike previous studies in our lab which used low frequency rTMS to V1 and found widespread FC changes up to 1 hr after stimulation, TBS to V1 does not affect FC. Contrary to the studies showing comparable TBS and rTMS aftereffects in motor and non-motor frontal regions, our findings suggest that in a clinical setting, a single session of cTBS or iTBS to V1 may not be an effective therapy if targeting FC is the clinical goal.

*Keywords:* transcranial magnetic stimulation (TMS), theta burst stimulation (TBS), resting state, visual networks, multi echo fMRI, functional connectivity

## Acknowledgment

I would like to express my profound gratitude to all those who have supported me during this project. Foremost, I am truly indebted to my supervisor, Dr. Jennifer Steeves, for her unwavering guidance, mentorship, and encouragement. Her extensive knowledge, expertise, and dedication have been invaluable to my progress, and I am deeply appreciative of her willingness to devote time from her hectic schedule to address my inquiries and offer insightful feedback. Dr. Steeves' support has been instrumental in the successful completion of this project, and I am truly fortunate to have had the opportunity to learn and grow under her expert supervision.

I am immensely grateful to my committee member Dr. Peter Kohler for his invaluable feedback, guidance, and support. I would also like to express my appreciation to my mentor, Dr. Joseph DeSouza, for his continuous guidance and support during my academic journey. I am deeply thankful to Dr. Diana Gorbet for her exceptional neuroimaging support. Additionally, I extend my special thanks to my committee members, Dr. Christine Till and Dr. William Gage. Thank you all for generously sharing your knowledge and expertise with me.

I would like to extend my heartfelt gratitude to my family and friends, particularly my devoted mother and my late father, for their unconditional love and unwavering encouragement throughout my life. Although I may not have articulated my appreciation and emotions as frequently as I should have, I want you to know that every fibre of my being is deeply grateful for your support. Your love has been my guiding light, and I cherish you all. Love you!

I am deeply appreciative of the amazing former and current lab mates who have provided support and motivation throughout this journey. Special thanks to Dr. Sara Rafique, Dr. Stefania Moro, and Karlene Stoby for their help, encouragement, and friendship.

Table of contents

**Table of Contents**

**ABSTRACT .....II**

**ACKNOWLEDGMENT.....III**

**TABLE OF CONTENTS..... IV**

**LIST OF FIGURES ..... VIII**

**LIST OF TABLES .....IX**

**LIST OF ABBREVIATIONS .....X**

**CHAPTER 1 : GENERAL INTRODUCTION ..... 1**

**1.1 A BRIEF HISTORY OF TRANSCRANIAL MAGNETIC STIMULATION..... 3**

**1.2 SYNAPTIC PLASTICITY, HEBBIAN LEARNING, AND NEUROMODULATION ..... 5**

**1.4 THE BIENENSTOCK, COOPER AND MUNROE THEORY, META PLASTICITY AND TMS ..... 9**

**1.5 BIOPHYSICAL PARAMETERS AFFECTING TMS OUTCOMES..... 11**

**1.5.1 THETA BURST STIMULATION ..... 12**

**1.6 MEASURING CORTICAL EXCITABILITY VIA MOTOR AND PHOSPHENE THRESHOLDS ..... 13**

<b>1.7 CONSECUTIVE TMS-NEUROIMAGING TECHNIQUES .....</b>	<b>15</b>
<b>1.7.1 TMS-FMRI .....</b>	<b>15</b>
<b>1.8 CONNECTOMICS: EVALUATING STIMULATION OUTCOMES WITH FUNCTIONAL CONNECTIVITY .....</b>	<b>17</b>
<b>1.9 TARGETING RESTING STATE NETWORKS WITH TMS .....</b>	<b>18</b>
<b>1.9.1 LIMITATIONS OF RS-FMRI: SUSCEPTIBILITY TO MOTION AND PHYSIOLOGICAL NOISE .....</b>	<b>20</b>
<b>1.10 NOISE REDUCTION WITH MULTI-ECHO MRI AND RS-FMRI ANALYSIS METHODS .....</b>	<b>21</b>
<b>1.10.1 MULTI-ECHO MRI ACQUISITION .....</b>	<b>21</b>
<b>1.10.2 VOLUMETRIC VS. SURFACE-BASED FMRI ANALYSES .....</b>	<b>24</b>
<b>1.10.3 THE IMPORTANCE OF SPATIAL SMOOTHING .....</b>	<b>25</b>
<b>1.11 CURRENT LITERATURE: OCCIPITAL TMS .....</b>	<b>27</b>
<b>1.12 CURRENT LITERATURE: CONSECUTIVE TBS-FMRI IN VISUAL BRAIN AREAS .....</b>	<b>29</b>
<b>1.13 MOTIVATION AND DIRECTION OF THE CURRENT THESIS .....</b>	<b>31</b>
<b><u>CHAPTER 2 : CONTINUOUS AND INTERMITTENT THETA BURST STIMULATION OF PRIMARY</u></b>	
<b><u>VISUAL CORTEX DO NOT MODULATE RESTING STATE FUNCTIONAL CONNECTIVITY: A SHAM-</u></b>	
<b><u>CONTROLLED MULTI-ECHO FMRI STUDY .....</u></b>	<b><u>33</u></b>
<b>2.1 ABSTRACT .....</b>	<b>34</b>
<b>INTRODUCTION.....</b>	<b>34</b>
<b>METHODS .....</b>	<b>34</b>
<b>RESULTS.....</b>	<b>34</b>
<b>CONCLUSION.....</b>	<b>34</b>
<b>2.2 INTRODUCTION .....</b>	<b>35</b>

<b>2.3</b>	<b>METHODS AND MATERIALS .....</b>	<b>38</b>
<b>2.3.1</b>	<b>PARTICIPANTS.....</b>	<b>38</b>
<b>2.3.2</b>	<b>EXPERIMENTAL DESIGN OVERVIEW .....</b>	<b>39</b>
<b>2.3.3</b>	<b>PHOSPHENE THRESHOLDS .....</b>	<b>40</b>
<b>2.3.4</b>	<b>THETA BURST STIMULATION .....</b>	<b>42</b>
<b>2.3.5</b>	<b>MAGNETIC RESONANCE IMAGING.....</b>	<b>43</b>
<b>2.3.6</b>	<b>VISION AND COGNITIVE ASSESSMENT .....</b>	<b>44</b>
<b>2.3.7</b>	<b>fMRI DATA PREPROCESSING .....</b>	<b>44</b>
<b>2.3.8</b>	<b>fMRI DATA ANALYSIS .....</b>	<b>45</b>
<b>2.4</b>	<b>RESULTS.....</b>	<b>53</b>
<b>2.4.1</b>	<b>VISUAL ACUITY AND NEUROLOGICAL ASSESSMENTS.....</b>	<b>53</b>
<b>2.4.2</b>	<b>PHOSPHENE THRESHOLDS .....</b>	<b>55</b>
<b>2.4.3</b>	<b>VOLUMETRIC SEED-BASED CONNECTIVITY ANALYSIS IN MNI SPACE .....</b>	<b>55</b>
<b>2.4.4</b>	<b>SURFACE-BASED ROI-TO-ROI ANALYSIS USING GPIP PARCELLATION .....</b>	<b>57</b>
<b>2.5</b>	<b>DISCUSSION .....</b>	<b>58</b>
<b>2.6</b>	<b>LIMITATIONS AND FUTURE DIRECTIONS .....</b>	<b>65</b>
<b>2.7</b>	<b>CONCLUSION.....</b>	<b>66</b>
 <b>CHAPTER 3 : GENERAL DISCUSSION.....</b>		 <b>67</b>
<b>3.1</b>	<b>SUMMARY.....</b>	<b>68</b>
<b>3.2</b>	<b>LIMITATIONS AND FUTURE DIRECTIONS .....</b>	<b>69</b>
<b>3.2.1</b>	<b>TBS IN V1 VS. OTHER BRAIN AREAS.....</b>	<b>70</b>

3.2.2	NEURODIVERSITY AND STATE-DEPENDENCY.....	71
3.2.3	EXPERIMENTAL DESIGN .....	72
<b>3.3</b>	<b>FINAL THOUGHTS.....</b>	<b>73</b>
<b>4</b>	<b><u>REFERENCES.....</u></b>	<b><u>75</u></b>
<b>5</b>	<b><u>APPENDIX.....</u></b>	<b><u>113</u></b>

## List of Figures

<b>FIGURE 1.1-1:</b> LTP- AND LTD-LIKE RESPONSES OF PRE AND POSTSYNAPTIC NEURONS. ....	9
<b>FIGURE 1.1-2 :</b> DIFFERENT rTMS PROTOCOLS WITH VARYING PARAMETERS.....	13
<b>FIGURE 1.1-3:</b> EFFECTS OF SHORT AND LONG TE ON BOLD CONTRAST .....	22
<b>FIGURE 1.1-4:</b> MULTI ECHO ACQUISITION AND ENHANCEMENT OF SIGNAL TO NOISE RATIO.....	23
<b>FIGURE 1.1-5:</b> EXAMPLE OF THE SPM ANALYSIS OF A SIMULATED HEMODYNAMIC RESPONSE FUNCTION (HRF) SIGNAL IN PRE AND POST CENTRAL GYRI.....	27
<b>FIGURE 1.1-6:</b> PUBMED SEARCH RESULTS CONDUCTED IN DECEMBER 2023 BY THE AUTHOR OF THIS THESIS: PERCENTAGE OF TMS EXPERIMENTS BASED ON THEIR TARGETED LOBES PUBLISHED BETWEEN 1975-2022..	29
<b>FIGURE 2-1 :</b> AN OVERVIEW OF THE EXPERIMENTAL DESIGN AND TBS PARAMETERS. ....	40
<b>FIGURE 2-2 :</b> MNI COORDINATES OF 18 ROIS USED IN ROI-ROI ANALYSIS BASED ON THE HARVARD-OXFORD ATLAS.....	48
<b>FIGURE 2-3 :</b> EXAMPLE OF INDIVIDUAL PARCELLATION AND CONNECTIVITY MATRICES IN THREE RANDOMLY SELECTED SUBJECTS FROM EACH OF THE THREE STIMULATION GROUPS AT BASELINE (DAY 1).....	52
<b>FIGURE 2-4 :</b> PRE- AND POST-TBS GROUP MEAN WITH INDIVIDUAL DATA POINTS PHOSPHENE THRESHOLDS.....	55
<b>FIGURE 2-5 :</b> SEED TO TARGET WITHIN- AND BETWEEN-GROUP RESULTS. ....	57
<b>FIGURE 2-6 :</b> UNCORRECTED CONNECTIVITY MATRICES USING FISHER Z-TRANSFORMATION OF THE PEARSON CORRELATION COEFFICIENT VALUES FOR EACH GROUP AND TIMEPOINT. ....	58
<b>FIGURE A-1:</b> INDIVIDUAL PRE- TO POST-STIMULATION PHOSPHENE THRESHOLDS. ....	119

## List of Tables

<b>TABLE 1-1 : OVERVIEW OF THE CURRENT BEHAVIOURAL AND NEUROIMAGING TBS LITERATURE IN THE PRIMARY VISUAL CORTEX AND OTHER VISUAL NETWORKS.....</b>	<b>31</b>
<b>TABLE 2-1 : ANALYSIS OF VARIANCE (ANOVA) OF PHOSPHENE THRESHOLDS, VISION, AND COGNITIVE ASSESSMENTS DATA BEFORE AND AFTER TBS.....</b>	<b>54</b>
<b>TABLE A-1: SCHAEFER-200 NODE CONVERSION TO MNI COORDINATES.....</b>	<b>113</b>
<b>TABLE A-2: RESULTS OF THE RS-fMRI SEED-TO-TARGET DATA ANALYSIS AT THREE TIMEPOINTS (DAY 1 PRE-TBS, DAY 2 IMMEDIATELY POST-TBS AND DAY 2 1 HR POST-TBS). .....</b>	<b>115</b>

## List of abbreviations

<b>AMPA</b>	$\alpha$ -amino-3-hydroxy-5-methyl-4-isoxazolepropionic acid
<b>aMT</b>	Active motor threshold
<b>ANOVA</b>	Analysis of variance
<b>BCM</b>	Bienenstock, Cooper and Munroe theory
<b>BOLD</b>	Blood-oxygen-level-dependent
<b>Ca<sup>2+</sup></b>	Calcium ion
<b>CBS</b>	Charles Bonnet syndrome
<b>CNS</b>	Central nervous system
<b>CSF</b>	Cerebrospinal fluid
<b>cTBS</b>	Continuous theta burst stimulation
<b>DMN</b>	Default mode network
<b>EEG</b>	Electroencephalography
<b>EMG</b>	Electromyography
<b>FC</b>	Functional connectivity
<b>FDA</b>	Federal food and drug administration
<b>FDR</b>	False discovery rate
<b>fMRI</b>	Functional magnetic resonance imaging
<b>FWER</b>	Family wise error
<b>FWHM</b>	Full width half maximum
<b>GABA</b>	Gamma aminobutyric acid

<b>GLM</b>	Generalised linear model
<b>GM</b>	Grey matter
<b>GPIP</b>	Group prior individual parcellation
<b>HRF</b>	Hemodynamic response function
<b>iTBS</b>	Intermittent theta burst stimulation
<b>K<sup>+</sup></b>	Potassium ion
<b>LTD</b>	Long term depression
<b>LTP</b>	Long term potentiation
<b>M1</b>	Primary motor cortex
<b>MDD</b>	Major depressive disorder
<b>ME-ICA</b>	Multi-echo independent component analysis
<b>MEP</b>	Motor evoked potential
<b>Mg<sup>2+</sup></b>	Magnesium ion
<b>MoCA</b>	Montreal Cognitive Assessment
<b>MPRAGE</b>	Magnetisation-prepared rapid gradient echo
<b>MRS</b>	Magnetic resonance spectroscopy
<b>MSO</b>	Maximum stimulator output
<b>MT</b>	Motor threshold
<b>Na<sup>2+</sup></b>	Sodium ion
<b>NIBS</b>	Non-invasive brain stimulation
<b>NMDA</b>	N-methyl-D-aspartate
<b>PCA</b>	Principle component analysis

<b>PT</b>	Phosphene threshold
<b>ROI</b>	Region of interest
<b>rs-fMRI</b>	Resting state functional magnetic resonance imaging
<b>rTMS</b>	Repetitive transcranial magnetic stimulation
<b>SBC</b>	Seed based connectivity
<b>SNR</b>	Signal to noise ratio
<b>SPM</b>	Statistical parametric mapping
<b>TBS</b>	Theta burst stimulation
<b>TE</b>	Time to echo
<b>TMS</b>	Transcranial magnetic stimulation
<b>TR</b>	Repetition time
<b>V1</b>	Primary visual cortex
<b>VA</b>	Visual acuity
<b>VOI</b>	Volume of interest
<b>WM</b>	White matter

## **Chapter 1 : General Introduction**

The study of lesions of the central nervous system (CNS) in neurological patients has played a pivotal role in our understanding of the relationship between structure and function. The advent of transcranial magnetic stimulation (TMS), however, has given us the ability to temporarily induce lesion-like states in individuals without neurological disorders, have reduced our reliance on lesion studies while contributing to new theories and novel therapies for neurological and psychiatric disorders.

In the past few decades, studies utilising repetitive TMS (rTMS) have advanced the field of non-invasive brain stimulation (NIBS) and improved TMS technology as a tool capable of both inducing transient aftereffects and inducing long-term changes at neuronal levels. For example, in clinical settings, high (e.g., 10 Hz) and low (e.g., 1 Hz) rTMS protocols have been widely used to treat various neurological and neuropsychiatric disorders. Other variations of rTMS such as theta burst stimulation (TBS) have also become popular, mainly because they can potentially produce the same effects (Blumberger et al., 2018; Voigt et al., 2021) in a much shorter time (a single TBS session takes less than three minutes while a single rTMS session can last up to 30 minutes). Similar to high and low frequency rTMS protocols, intermittent TBS (iTBS) and continuous TBS (cTBS) incorporate different frequencies and wave patterns while requiring much shorter stimulation durations to induce aftereffects that may be comparable to rTMS that can last beyond the stimulation time.

Despite a vast literature exploring the potential research and clinical applications of different TMS protocols, exploring TMS as a tool for targeting motor and non-motor regions of the frontal and parietal lobes in research and clinical applications, very few studies have explored TMS effects in primary visual cortex (V1). Although decades of vision research have

contributed to our understanding of nodes and networks in the visual brain, outstanding research questions and various visual disorders with neurological origin highlight the need for developing NIBS techniques capable of improving the efficiency and efficacy of current protocols.

As TBS has been an under-investigated protocol in visual areas of the brain, the primary focus of this thesis is centred on examining the effects of TBS to the primary visual cortex and its modulatory aftereffects in resting state brain networks. In the following sections and chapters I compile and present an updated summary of TBS research across different brain regions, the body of literature regarding TBS in V1, and current neuroimaging and behavioural techniques for studying the neural implications of TMS-based protocols in targeted regions (Chapter 1). In Chapter 2, I detail our recent rTMS experiment, which used TBS to V1 and functional magnetic resonance imaging (fMRI) to induce changes in resting-state functional networks of healthy individuals. Chapter 3 brings together the existing TBS literature and the results of our experiment, followed by a broad discussion, identification of limitations, and suggestions for future work.

## **1.1 A brief history of transcranial magnetic stimulation**

TMS technology relies on the basic principles of bioelectricity and electromagnetism. In the 18<sup>th</sup> century scientists such as Galvani and Volta discovered that electricity is an intrinsic property of biological tissues, and through a set of experiments they were able to show that muscle tissues (in a dead frog) could be re-activated through the application of electricity (reviewed in Walsh, 1998). Around the same time, Faraday and Maxwell discovered that the alternation of currents through a conductor (e.g., coil) can lead to the production of an electric

field near the conductor (described in Piccolino, 1998; Walsh, 1998). Fast forward to several centuries later, these foundational discoveries set the stage for breakthroughs in NIBS techniques. The new era of NIBS began with Merton and Morton's (1980) seminal work, where they demonstrated the possibility of inducing motor-evoked potentials (MEPs) in a human brain by non-invasive transcranial electrical stimulation at the scalp above the postcentral gyrus (motor cortex; M1), and phosphenes (flashes of light) by stimulating V1. Using a direct electrical stimulation, however, induced strong spasms of scalp muscles and was reportedly painful and uncomfortable (Merton & Morton, 1980). Shortly after, Polson et al., (1982) and Barker et al., (1985) demonstrated that by utilising the principle of electromagnetism, stimulation can induce an electric field in the brain tissue passing through the scalp and the skull, which led to the invention of TMS. While TMS still causes weak spasms in scalp muscles, it proved to be effective and well-tolerated, and repetitive TMS (rTMS) became an indispensable tool for studying the relationship between structure and function in the brain and mapping neural networks (Polson et al., 1982). Eventually in 2008, high frequency (10 Hz) rTMS targeting dorsolateral prefrontal cortex was approved by the U.S Food and Drug Administration (FDA) for the treatment of medication-resistant major depressive disorder (MDD; Lisanby et al., 2009). More recently, a patterned variation of rTMS, namely theta burst stimulation (TBS) has gained popularity both in research and clinical settings, and has also been given the FDA approval for MDD (Blumberger et al., 2018; Cole et al., 2020). TBS involves the delivery of bursts consisting of three stimuli at 50 Hz, repeated at a frequency of 5 Hz, which mirrors the pattern of theta rhythms. It has the advantage of modulating targeted neural populations with comparable efficacy as traditional 1 Hz and 10 Hz rTMS while requiring much shorter stimulation duration (Huang et al., 2005,

2011). The following sections will focus on the neurophysiology of neuromodulation in various TMS protocols in different brain regions both in health and disease.

## **1.2 Synaptic plasticity, Hebbian learning, and neuromodulation**

Neurons that fire together, wire together (Shatz, 1992). One of the hallmarks of the brain is its ability to change. In response to an everchanging world, a flexible nervous system has enabled us to learn and adapt in order to successfully navigate the environment around us. It was not until the past century, however, that psychologists and neuroscientists began to probe the theoretical and neural underpinnings of neuroplasticity and learning. Before modern neuroimaging techniques, Donald Hebb purposed the associative learning hypothesis, in which he argued that, when neurons are repeatedly activated together, the strength of the synaptic connections between them increases (Hebb, 1949). Hebb proposed that clusters of neurons that are repeatedly activated at the same time tend to become functionally associated, and therefore form a network (Keysers & Gazzola, 2014). Almost a decade later, Hebbian plasticity was supported by the discovery of long-term potentiation (LTP) and long-term depression (LTD) in hippocampal neurons of rabbits and sea slugs (Bliss & Lomo, 1973; Kandel & Tauc, 1965).

Although both LTP and LTD are hallmarks of plasticity, It has been proposed that LTP is involved in synaptic plasticity and learning after repeated exposures to specific stimuli, and the formation of new connections between neurons (Bliss & Lomo, 1973), while LTD triggers synaptic pruning, a process which prior research has deemed important in conservation of resources and dismantling unwanted connections in neural networks (Pittenger & Duman, 2008). Physiological changes in synaptic plasticity such as suboptimal LTP and LTD mechanisms and lack of balance between the two have been implicated in ageing, as well as a range of

neurological and neuropsychiatric disorders such as Alzheimer's disease and depression (Auffret et al., 2010; Pittenger & Duman, 2008).

TMS provides a tool to explore the underlying physiological mechanisms of plasticity in various brain networks (Hallett, 2007; Rafique & Steeves, 2022; Thomson et al., 2020). The main advantage of TMS is its ability to non-invasively induce transient excitatory or inhibitory aftereffects in targeted brain regions (Caparelli et al., 2012, p. 1; Dombrowe et al., 2015; Ganaden et al., 2013; Huang et al., 2005, 2011; Mullin & Steeves, 2013). However, the underlying neural mechanisms of these aftereffects are not well-understood. Earlier studies hypothesised that the application of 10 Hz rTMS results in a series of physiological events in targeted neurons leading to excitation (Chai et al., 2019), triggering action potentials and the release of neurotransmitters into the postsynaptic membrane (Huerta & Volpe, 2009). Despite uncertainties surrounding the exact mechanism of action in neural tissue, TMS-based protocols are gaining traction as treatment modalities across a wide spectrum of neurological conditions (for examples see: Bai et al., 2022; Cole et al., 2020; Kondo et al., 2017; Mi et al., 2020). It is now widely recognised that a full understanding of the underlying mechanisms of TMS-based protocols is critical for their potential use as treatments for neurological and neuropsychiatric disorders. Recent in-vivo electrophysiology studies in awake non-human primates performing visuomotor tasks have shown that TMS to V1 induces transient disruptions in thalamocortical pathways, with a dramatic reduction in single-cell firing in lateral geniculate neurons of the thalamus involved in visual information processing (Wang, 2010). These aftereffects can last up to six minutes post-stimulation (Wang, 2010; Ziemann et al., 2006). In humans on the other hand, despite the fact that a mounting body of behavioural evidence points to the effectiveness

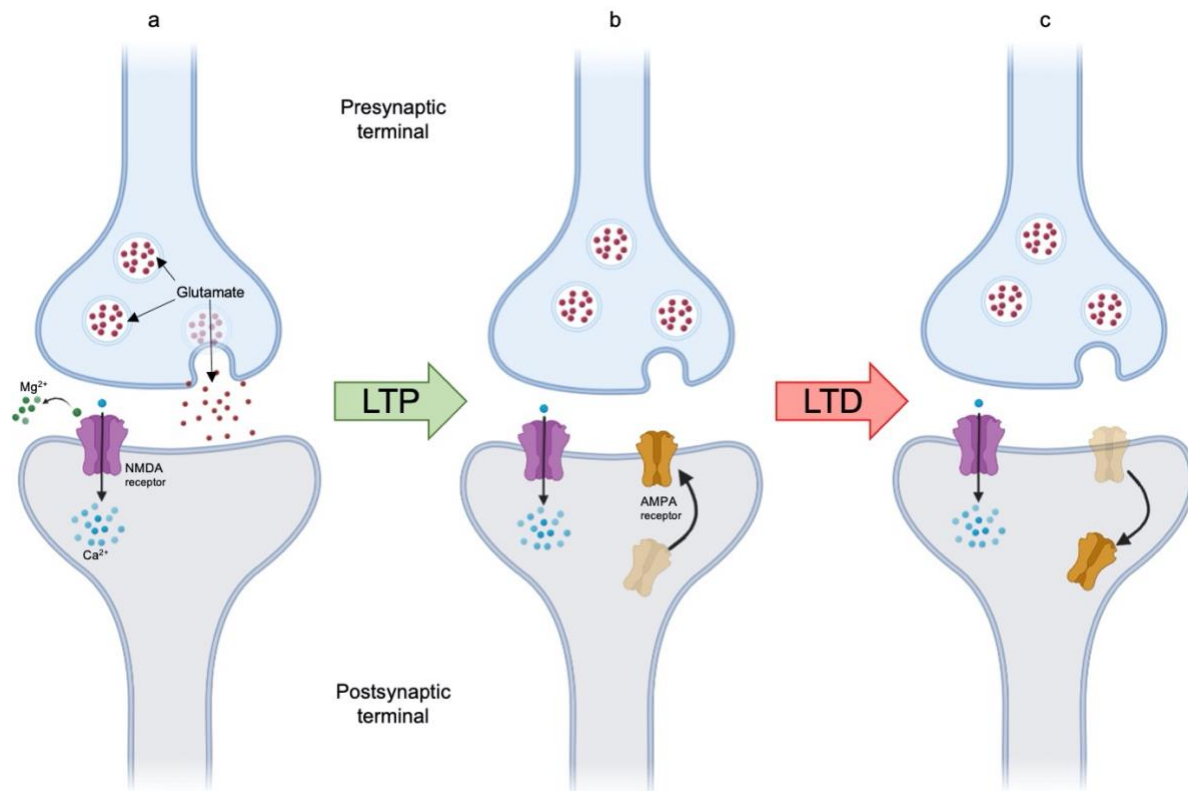
of TMS-based protocols (Ganaden et al., 2013; Liu et al., 2010; Mullin & Steeves, 2011; Solomon-Harris et al., 2016), the underlying mechanisms of these aftereffects remain complex and not fully understood

### **1.3 Physiological basis of synaptic plasticity**

After years of experimentation, the cellular and molecular mechanisms involved in the formation of new connections between neurons (synaptogenesis) and synaptic plasticity have been identified, and specific excitatory molecules and receptors have been found to facilitate the processes that lead to synaptogenesis. Glutamate, a major excitatory neurotransmitter in the brain, is thought to influence a number of important cell receptors, namely N-methyl-D-aspartate (NMDA) and  $\alpha$ -amino-3-hydroxy-5-methyl-4-isoxazolepropionic acid (AMPA) receptors. NMDA receptors are generally blocked by magnesium ions ( $Mg^{2+}$ ) and these voltage-gated receptors can only become activated with bursts of action potentials coming from presynaptic neurons to depolarise the postsynaptic neuron where the targeted NMDA receptors are housed (Cheyne & Montgomery, 2020; Curtis & Watkins, 1960; Munno & Syed, 2003; Watkins & Jane, 2006). This is because, in order for the  $Mg^{2+}$  in the postsynaptic NMDA receptor to be removed, the postsynaptic neurons must be activated (depolarised). This activation requires the presynaptic neuron to provide glutamate to the postsynaptic neuron (Munno & Syed, 2003). As the postsynaptic neuron becomes activated, the influx of sodium ( $Na^{2+}$ ) and calcium ( $Ca^{2+}$ ) ions activates various protein kinases (e.g., calcium-calmodulin and tyrosine). As shown in Figure 1.1-1, after repetitive activation between a pre and a postsynaptic neuron. It is the selective increase of AMPA receptors' response on the postsynaptic neuron that turns this associative "firing" into permanent "wiring" until LTD processes modify or

remove the connection (Kandel, 2012; Kauer et al., 1988; Lynch et al., 1983). This suggests that, over time, while repeated activity between two neurons enhances connectivity, a decrease in activity or lack of it can also alter synaptic strengths, even to the extent of dismantling these connections. Studies discussed in the following sections describe the processes involved in LTP and synaptogenesis that closely follow the mechanisms involved in learning and retention of memories (Kandel, 2012).

**Figure 1.1-1:** LTP- and LTD-like responses of pre and postsynaptic neurons.



**Note.** a) After the release of glutamate from the activated presynaptic neuron, the removal of the  $Mg^{2+}$  from the NMDA receptor leads to an intracellular influx of  $Ca^{2+}$  (and  $Na^{2+}$  not shown here). b) Repeated activation of the postsynaptic neuron eventually increases surface AMPA receptors leading to the formation and retention of connectivity between the two neurons (LTP). c) Depending on the location of the neurons, after long periods of stimulation deprivation, surface AMPA receptors become scarce, which in turn dismantles the connection between the two neurons (LTD). Image was created in BioRender.com.

#### 1.4 The Bienenstock, Cooper and Munroe theory, meta plasticity and TMS

It is now widely accepted that sensory experience and repetitive stimulation (i.e., sensory stimuli) can modify neural connectivity and future responsiveness of neurons to incoming stimuli, and that this modification is bi-directional (LTP and LTD). In 1982, Bienenstock, Cooper and Munroe proposed an eponymous (BCM) theory based on experimental evidence from rat visual cortex, to explain synaptic changes involved in LTD-like

sensory deprivation and LTP-like sensory stimulation (Bienenstock et al., 1982; Cooper & Bear, 2012). The BCM theory relies heavily on behavioural experiments showing that binocular deprivation lowers the frequency of stimulation required to induce LTP-like responses in primary visual cortex, while the restoration of normal vision reversed this phenomenon (Bienenstock et al., 1982; Kirkwood et al., 1995; Ziemann et al., 2006). This experience-dependent modification of LTP and LTD thresholds is called metaplasticity, or the plasticity of synaptic plasticity (Abraham & Bear, 1996). It has been proposed that, this occurs in circumstances where periods of low frequency stimulation led to the reduction in NMDA receptor-mediated excitatory post-synaptic potentials (EPSP). This process, in turn, decreases synaptic thresholds, increases EPSP summation and the influx of intracellular influx of  $Ca^{2+}$  and drastically enhances the likelihood of LTP-like events (Citri & Malenka, 2008; Philpot et al., 2001; Ziemann et al., 2006), meaning that LTP-like processes are more likely to occur after periods of low postsynaptic activities. This may explain why learning a task in general (consolidation and retention) is enhanced when practice is spaced out over time (Ziemann et al., 2006).

Given the assumptions of the BCM theory, early adopters of NIBS proposed, that if synaptic LTP-like activities are the precursors for learning, and if previous LTD-like processes lead to enhanced LTP-like activities, priming synaptic mechanisms with rTMS protocols that lead to inhibition (e.g., 1Hz rTMS) can increase the likelihood of subsequent activation (whether via practice or TMS). Experiments in rat's hippocampal neurons and the human motor cortex have confirmed this notion, and these assumptions have played a pivotal role in designing TMS protocols with optimised parameters to successfully enhance learning (Abraham & Bear, 1996;

Lefaucheur et al., 2004). These strategies have helped change the trajectory of the TMS technology from a “virtual lesion” tool to a technology capable of inducing long-lasting changes at the synaptic level, where it continues to help neurological and psychiatric patients suffering from a range of disorders such as stroke and depression (Bai et al., 2022; Kondo et al., 2017). In the following sections the role of different TMS parameters and their importance in inducing LTP- and LTD-like aftereffects will be discussed.

### **1.5 Biophysical parameters affecting TMS outcomes**

The electromagnetic current induced by TMS depends on both the physiology of the CNS and the stimulation parameters. In general, the synaptic history of an individual such as medication intake, substance abuse, prior history of brain stimulation or the presence of neuropsychiatric disorders should also be taken into account (Ridding & Ziemann, 2010). However, TMS optimisation studies have identified additional parameters such as frequency, pulse number, wave pattern and the intensity of stimulation to be of importance when designing experiments or stimulating patients (Di Lazzaro et al., 2011; Rossini et al., 2015). These parameters are usually determined prior to each stimulation session, and factors such as the location of stimulation targets (e.g., target’s depth) and their functional characteristics are important variables to be accounted for (McConnell et al., 2001).

In the past few decades, experiments manipulating TMS parameters have led to development of new rTMS protocols with different inhibitory and excitatory outcomes. For instance, low frequency (1 Hz) rTMS have shown to induce inhibitory aftereffects in motor and non-motor areas of frontal lobes (Caparelli et al., 2012), temporal and parietal lobes (Kashiwagi et al., 2018), and visual occipital areas (Boroojerdi et al., 2000; Rafique et al., 2015, 2016;

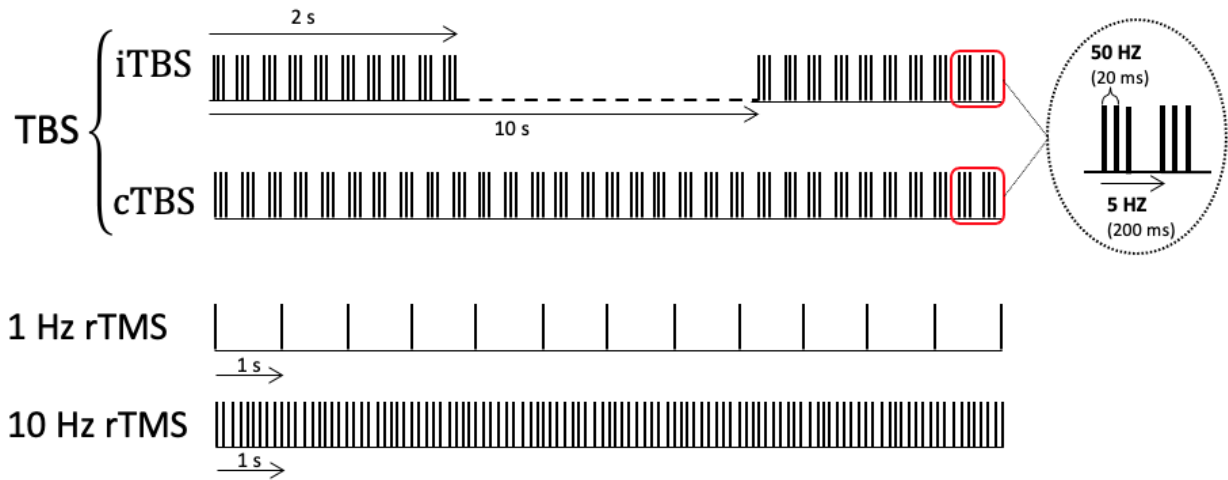
Solomon-Harris et al., 2016). In contrast, high frequency (10 Hz) rTMS leads to excitatory aftereffects in frontal and parietal lobes (Blumberger et al., 2018a; Dombrowe et al., 2015; Lisanby et al., 2009). By changing frequencies and wave patterns, researchers have also been able to develop rTMS protocols that require shorter stimulation time with comparable efficacy such as theta burst stimulation (TBS).

### **1.5.1 Theta burst stimulation**

As discussed earlier, the discovery of synaptic LTP has led to intense interest in covering the neural basis of learning and inevitably led to experimental approaches to reverse engineer LTP-like events in the human brain. Although previously neuron spike recordings had suggested the role of theta oscillations in memory storage and plasticity, it was not until the 1980's that patterned stimulation protocols in hippocampal CA1 neurons led to our better understanding of these mechanisms in the brains of human and other complex animals (Larson et al., 1986; Larson & Munkácsy, 2015). Intracellular TBS mimics important features of hippocampal neurons, such as the discharge patterns in pyramidal neurons and the theta rhythms (4-7 Hz) recorded from hippocampal neurons in the excited state (Larson et al., 1986).

As shown in Figure 2, TBS is a form of patterned rTMS with bursts of pulses at 50 Hz (20 ms, or delta oscillation range) which are repeated every 200 ms (5Hz, or theta oscillation range). There are two TBS patterns that are widely used. Intermittent TBS (iTBS) contains a 2 s train of theta bursts that is repeated every 10 s for a total of 190 seconds or 600 pulses. Continuous TBS (cTBS) contains a 40 s train of uninterrupted TBS for the total of 600 pulses (Huang et al., 2005).

**Figure 1.1-2 : Different rTMS protocols with varying parameters.**



**Note.** TBS = theta burst stimulation, iTBS = intermittent TBS, cTBS = continuous TBS, rTMS = repetitive transcranial magnetic stimulation. Image created in Adobe Illustrator.

In 2005, Huang and colleagues were the first group to use cTBS and iTBS to target M1 and investigate their aftereffects in nine healthy volunteers. They found that cTBS to M1 lowered the amplitude of MEPs, while the application of iTBS to M1 increased the amplitude of MEPs with aftereffects lasting up to 60 minutes (Huang et al., 2005). This paved the way for developing various research and clinical protocols currently used in multiple different settings (For example: Cole et al., 2020; Moisset et al., 2015; Nardone et al., 2016; Talelli et al., 2007).

## 1.6 Measuring cortical excitability via motor and phosphene thresholds

Depending on the location of the stimulation target or the purpose of the stimulation, in TMS research, motor threshold (MT) and phosphene threshold (PT) are used both to measure TMS outcomes and to determine optimal stimulation intensities tailored based on individual thresholds. MTs are defined as the minimum stimulator output (MSO) required to produce a measurable motor response after stimulating a specific target on the primary motor cortex (M1) and measured MTs in a specific muscle. Several methods can be used to measure the MT,

including electromyography (EMG; Deblieck et al., 2007; Franca et al., 2006; Rossini et al., 2015; Stewart et al., 2001). In EMG-based measurements, surface electrodes are placed over the target muscle, and the amplitude of MEPs is recorded in response to TMS stimulation (Day et al., 1989). Amplitude refers to the size or magnitude of the MEPs recorded from the target muscle which reflects the number of activated motor neurons and the degree of cortical excitability (Day et al., 1989; Rossini & Rossi, 1998). Higher amplitudes typically indicate greater cortical excitability, while lower amplitudes suggest decreased cortical excitability. MTs also can be measured, using the observation method, which involves stimulating the hand knob area of M1 and then increasing the MSO in a staircase fashion until a thumb twitch is observed (Boroogerdi et al., 2002).

Another measure of cortical excitability with TMS is the PT, which is the minimum stimulation intensity required to produce a phosphene, a transient visual sensation that can be elicited by stimulating the occipital cortex with TMS (Antal et al., 2003; Boroogerdi et al., 2000). PT estimation involves the participants' subjective reporting of the intensity of the phosphene perception, and it can be done using the staircase method in which TMS pulses are presented with increasing or decreasing intensities until a phosphene is perceived or disappears, respectively (Gerwig et al., 2003).

In summary, the use of TMS for assessing cortical excitability through motor and phosphene thresholds is a valuable approach for exploring the neural underpinnings of diverse neurological and neuropsychiatric disorders, monitoring the impact of TMS, and enabling tighter control of TMS stimulation (Kammer et al., 2003). MTs and PTs offer distinct perspectives on cortical excitability profile for each person. These methods can facilitate a more

individual-based approach to determining TMS stimulation intensity, tailoring optimal TMS intensities for each person according to their cortical excitability values, while taking into account the stimulation target and the specific research question at hand (Lee et al., 2021; McCalley et al., 2021).

## **1.7 Consecutive TMS-neuroimaging techniques**

In the past few decades, the combination of different TMS protocols and different neuroimaging techniques such as electroencephalography (EEG), functional magnetic resonance imaging (fMRI), MR spectroscopy (MRS), functional near-infrared spectroscopy or positron emission tomography has enabled researchers to investigate the causal relationship between brain activity and behaviour (Curtin et al., 2019; Krieg et al., 2013; Solomon-Harris et al., 2016; Stoby et al., 2022). By temporarily modulating neural activity in specific brain regions while measuring changes in neural networks and behaviours, these techniques have provided valuable information about the neural mechanisms underlying a wide range of cognitive processes and behaviours in both health and disease. Consecutive TMS and fMRI techniques will be discussed in more detail in the following section.

### **1.7.1 TMS-fMRI**

fMRI is a non-invasive neuroimaging technique that enables researchers to investigate brain activity by measuring a proxy of brain activity, namely changes in blood oxygenation levels. This method is based on the blood-oxygen-level-dependent (BOLD) contrast, which reflects the difference in magnetic properties of oxygenated and deoxygenated hemoglobin (Damadian et al., 1974; Gore, 2003; Lauterbur, 1973; Mansfield & Grannell, 1975; Ogawa et al., 1990; Pauling & Coryell, 1936). As neural activity increases in a specific brain region, local

oxygen consumption rises, leading to a subsequent increase in blood flow to the area (Gore, 2003; Mansfield & Grannell, 1975). This results in a higher concentration of oxygenated hemoglobin and a detectable BOLD signal. By capturing these signals, fMRI provides indirect measurements of neural activity, allowing researchers to map brain function and identify regions associated with specific cognitive processes or behaviours (Constable et al., 1993; Gore, 2003; Ogawa et al., 1990). The technique has become widely used in neuroscience for its ability to non-invasively produce high-resolution images and its compatibility with various experimental paradigms (e.g., concurrently with TMS), making it a versatile tool for studying both healthy and diseased brains.

### ***1.7.2 Task-based vs. Resting-state fMRI***

Task-based fMRI and resting-state fMRI (rs-fMRI) are two distinct approaches to functional magnetic resonance imaging, each with its own specific goals and methodology. Task-based fMRI involves presenting participants with a structured series of tasks or stimuli, typically organised in single events, or blocks of events interleaved with periods of rest (Constable et al., 1993). By comparing the BOLD signals during active task periods to those during rest periods, researchers can identify patterns of brain activity engaged in the specific cognitive processes or behaviours associated with the task (Constable et al., 1993; Gore, 2003). In contrast, rs-fMRI examines spontaneous fluctuations in brain activity while participants are not engaged in any specific task and at rest with their eyes closed or fixated on a fixation point. This approach allows for the identification of functionally connected brain networks, referred to as resting-state networks, which reveal the intrinsic functional organisation of the brain at rest. While task-based fMRI focuses on understanding the brain's response to external stimuli,

resting-state fMRI provides insights into the brain's intrinsic functional architecture (Constable et al., 1993; Kundu et al., 2012). Both task-based and rs-fMRI methods have been extensively used in combination with different TMS protocols and have played instrumental roles in the development of validated research and clinical protocols (Blumberger et al., 2018; Cole et al., 2020; Rafique et al., 2016; Rafique & Steeves, 2022; Solomon-Harris et al., 2016; Talelli et al., 2007).

### **1.8 Connectomics: Evaluating stimulation outcomes with functional connectivity**

Connectomics is a rapidly emerging field in neuroscience that aims to map and analyse the complex network of connections within the brain, referred to as the connectome (Craddock et al., 2015; Van Essen, Ugurbil, et al., 2012; Van Essen & Ugurbil, 2012). This comprehensive approach studies both structural and functional connections, covering the intricate web of neural pathways and the patterns of activity. By elucidating the brain's connectivity at various scales, from small ensembles of neurons to large-scale networks, Connectomics offers valuable insights into the principles governing brain organisation and function. Whether TMS is used as a “virtual lesion” to study the intrinsic FC or used as a treatment modality, connectome-based TMS seems to have gained popularity as a validated technique for studying the underlying mechanisms of various brain functions in healthy brains, as well as different neurological and psychiatric disorders (Balderston et al., 2022; Cole et al., 2020; Xia & He, 2022). I will now review common evidence-based techniques to measure and quantify resting state FC networks before and after NIBS.

## 1.9 Targeting resting state networks with TMS

Using fMRI, researchers have identified several resting state networks ranging from sensorimotor, auditory, visual, central executive and default mode networks (W. H. Lee & Frangou, 2017; Whitfield-Gabrieli & Nieto-Castanon, 2012). One of the most studied networks is the default mode network (DMN) which is a well-established resting-state network identified through rs-fMRI studies (Biswal et al., 1995). It comprises a set of brain regions, including the medial prefrontal cortex, posterior cingulate cortex, precuneus, and bilateral inferior parietal lobules, that exhibit synchronous activity when individuals are not engaged in any specific task (Biswal et al., 1995; Raichle & Snyder, 2007; Zhang et al., 2018). The DMN is thought to be involved in various cognitive processes, such as self-referential thinking, mind-wandering, and the consolidation of memories (Chen et al., 2013; Dunkley et al., 2018; Raichle & Snyder, 2007). It has also been implicated in numerous psychiatric and neurological disorders, including Alzheimer's disease, depression, and schizophrenia, as alterations in DMN connectivity have been observed in these conditions (Cecchetti et al., 2021; Hafkemeijer et al., 2015; Jafri et al., 2008). Aside from the DMN, rs-fMRI studies have shown that the brain hosts several other resting state networks that play vital roles in cognition and behaviour. For example, the salience network, involving the dorsal anterior cingulate cortex, bilateral insula, and presupplementary motor area, regulates dynamic changes in other networks and behavioural changes (Menon & Uddin, 2010; Smitha et al., 2017; Uddin, 2015). The auditory network encompasses primary auditory cortices and associated regions, processing auditory information (Andoh et al., 2015). The basal ganglia network, closely associated with Parkinson's disease, controls motor areas, emotion, and cognition (Afifi, 2003; Rolinski et al., 2015; Smitha et al., 2017). The visual

network, which includes the calcarine sulcus, lingual gyrus, and lateral geniculate nucleus of the thalamus, processes visual stimuli (Damoiseaux et al., 2006). The visuospatial network, based in the posterior parietal cortex, is implicated in spatial attention. (Greicius et al., 2003; Gusnard et al., 2001; Raichle, 2011). The language network, extending beyond Broca's and Wernicke's areas to prefrontal, temporal parietal, and subcortical regions, is responsible for various language functions (Skipper et al., 2007). The executive network, including the dorsolateral prefrontal cortex and posterior parietal cortex, is activated during tasks needing cognitive control (Seeley et al., 2007). The precuneus network, part of the DMN, contributes to mental imagery, memory retrieval, and emotional processing (Fransson & Marrelec, 2008). Finally, the sensorimotor network, which represents motor areas of the body, was the first RSN studied. Resting state functional MRI (rs-fMRI) has shown promise for understanding cognitive studies and has potential clinical applications (Bharath et al., 2015; Smitha et al., 2017).

Given the facilitatory and inhibitory properties of TMS, previous studies have been able to confirm the modulatory effects of TMS in various resting state networks. Examples include 10 Hz rTMS (excitatory protocol) that has been successfully used to treat depression by modulating the activity of the medial prefrontal cortex, a key region in the DMN (Cole et al., 2020). Other studies have been able to dampen connectivity between different DMN regions using 1Hz rTMS (inhibitory protocol; Chen et al., 2013). Other research groups have also shown the modulatory effects of low and high frequency rTMS protocols for treating alcohol use disorder targeting the salience network (for review: [Padula et al., 2022](#)), or sensorimotor and basal ganglia networks in stroke and Parkinson's disease just to name a few (Bai et al., 2022; Kashiwagi et al., 2018; Kondo et al., 2017; Mi et al., 2020; Rolinski et al., 2015). Given these results, the application of

TMS in modulating the activity of various neural networks holds promise for advancing our understanding of brain connectivity and its role in various psychiatric and neurological disorders.

### **1.9.1 Limitations of rs-fMRI: Susceptibility to motion and physiological noise**

Even though rs-fMRI has contributed immensely to our understanding of the underlying brain networks, it is not without limitations. Two notable limitations of rs-fMRI are its susceptibility to motion and physiological noise (Behzadi et al., 2007; Chang & Glover, 2009).

Participant motion during the scanning process can introduce significant artifacts in rs-fMRI data. Even small head movements can lead to spurious correlations or the loss of genuine connectivity patterns (Behzadi et al., 2007; Whitfield-Gabrieli & Nieto-Castanon, 2012). This issue is particularly challenging when working with certain populations, such as children, elderly individuals, or patients with movement disorders, who may find it difficult to remain still for extended periods (Power et al., 2014). Various preprocessing strategies, such as motion correction, scrubbing, and regression of motion parameters, have been developed to mitigate motion artifacts (Alves et al., 2019; Behzadi et al., 2007; Chang & Glover, 2009). However, these methods may not fully eliminate the impact of motion on rs-fMRI data (Kundu et al., 2013).

rs-fMRI is also sensitive to physiological noise, which refers to fluctuations in the BOLD signal caused by non-neuronal factors. Sources of physiological noise include cardiac and respiratory cycles, blood pressure changes, and variations in blood flow and oxygenation (Kundu et al., 2012, 2013). These factors can introduce confounding signals that obscure or mimic neural activity patterns, leading to inaccurate inferences about brain connectivity.

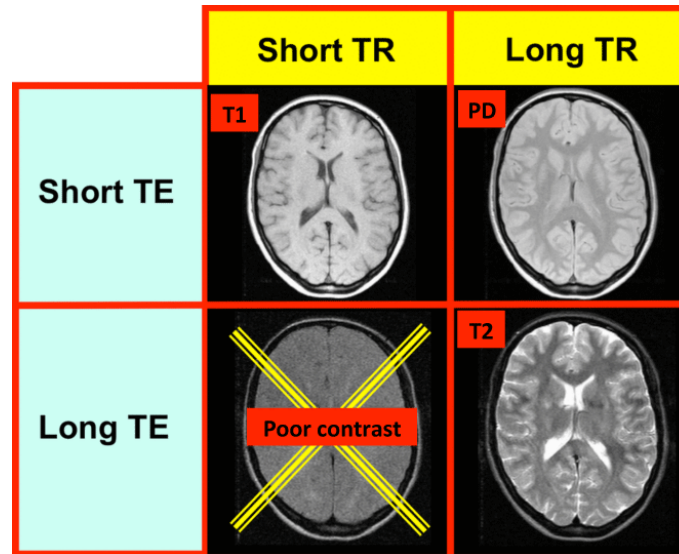
Various techniques have been developed to address physiological noise, such as the use of independent component analysis (ICA), RETROICOR (retrospective image correction; Behzadi et al., 2007). Researchers have also utilised physiological recordings during scanning (i.e., heart rate, blood pressure and capnography), with the goal of regressing out these physiological parameters during preprocessing steps (Murphy et al., 2013; Zhu et al., 2015).

## **1.10 Noise reduction with multi-echo MRI and rs-fMRI analysis methods**

### ***1.10.1 Multi-echo MRI acquisition***

In MRI scanning protocols, time to echo (TE) refers to the time elapsed between the application of the radiofrequency pulse and the acquisition of the signal echo. In simple terms, it is the time it takes for the MRI to read out the returning signal after exciting the protons in the tissues with a radiofrequency pulse. Another important parameter is repetition time (TR), which is the time interval between two successive radiofrequency pulses (Nitz & Reimer, 1999). The choice of TR depends on the type of MRI sequence being used and the desired trade-off between SNR and imaging time (Gore, 2003). Together, TE and TR play a critical role in determining the image contrast and quality in MRI. TE influences image contrast, particularly the weighting of the image in terms of T2 or T2\* relaxation properties. In the context of fMRI, T2\*-weighted images are predominantly used to determine BOLD contrast (Nitz & Reimer, 1999). Shorter TEs typically result in images with less susceptibility-induced signal loss and reduced sensitivity to physiological noise (as shown in Figure 1.1.3). However, it may also lead to lower BOLD contrast (Kundu et al., 2012; Nitz & Reimer, 1999). Conversely, a longer TE increases BOLD contrast but may also increase susceptibility artifacts and sensitivity to noise (Gore, 2003).

**Figure 1.1-3: Effects of short and long TE on BOLD contrast**



**Note.** TE = echo time, T1 = T1 weighting, T2 = T2 weighting, PD = proton density weighting.

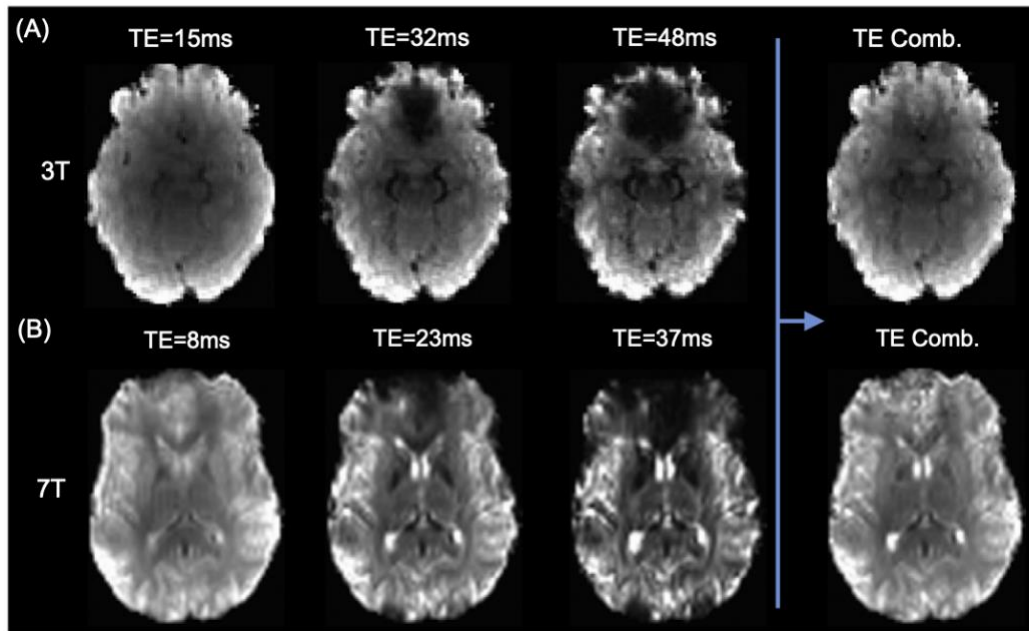
Reused with written permission from Dr. Alan Elster (author and owner;

<http://mriquestions.com/image-contrast-trte.html>).

By leveraging the unique decay properties of BOLD and non-BOLD signals at different echo times, multi-echo functional magnetic resonance imaging (ME-fMRI) allows for multiple snapshots that are gathered at varying echo intervals (multiple TEs) within one cycle of repetition during functional MRI scans (Posse et al., 1999). This enhances the balance between signal and noise and allows for the more precise quantification of fluctuations in the BOLD signal, thus refining the integrity of fMRI results and the depth of subsequent data interpretation (Power et al., 2018). In turn, this enables researchers to better isolate the neural signal of interest and reduce the impact of confounding factors such as physiological noise and magnetic field inhomogeneities (Posse et al., 1999). This improved SNR and specificity of the BOLD signal contribute to enhanced sensitivity in detecting brain activity, which can be particularly advantageous for studies involving challenging populations or experimental designs

(Posse et al., 1999; Power et al., 2018). Additionally, the multi-echo approach provides greater flexibility in data analysis, facilitating the use of advanced denoising and preprocessing techniques (Kundu et al., 2012; Power et al., 2018).

**Figure 1.1-4:** *Multi echo acquisition and enhancement of signal to noise ratio*



**Note.** Example of acquiring images at multiple echo times (TE) and combining them to remove physiological noise (and areas with short  $T2^*$ ) and improving signal-to-noise ratio throughout the brain at two different magnetic field strengths at 3 and 7 Tesla (Kundu et al., 2017). Reused with written permission from the publisher (Elsevier).

As the number of echoes increases, however, it poses challenges in terms of image processing and data analysis. Given that ME-fMRI obtains three (or more) separate images at each TE per volume, optimal combination of these images is an important step in order to identify signals originating from physiological noise such as the heart rate, breathing or head motion (Dipasquale et al., 2017; Kundu et al., 2012, 2013; Posse et al., 1999). For this purpose, Kundu and colleagues (2012), developed multi-echo independent component analysis (ME-ICA) which is a statistical pipeline that deals with removal of noise, improving SNR and the optimal combination of echoes. ME-ICA is a preprocessing method for fMRI data that applies motion

correction and standard preprocessing to ME datasets, calculates motion parameters based on the image with the highest contrast, and then uses principal component analysis (PCA) and ICA with TE-dependence analysis to extract independent components that represent BOLD signal and noise sources (Kundu et al., 2017). Both PCA and ICA are statistical techniques for separating mixed signals into their original sources, to decompose the ME-fMRI data into a set of spatial and temporal components (Cox & Hyde, 1997; Meszlényi et al., 2017). The resulting components are used to denoise the fMRI data, providing a cleaner and more accurate representation of the BOLD signal (Kundu et al., 2017). At this stage, optimally combined data are ready to be entered in first- and second-level analysis stages.

### ***1.10.2 Volumetric vs. Surface-based fMRI analyses***

After obtaining optimally combined images that have been preprocessed and denoised through ME-ICA, the choice of subsequent analytical methodology largely depends on the nature of the research question and factors such as interindividual anatomical and functional variability. Typically, two primary strategies are employed: volumetric and surface-based analysis.

Volumetric analysis, a widely used method, necessitates the registration and normalisation of individual brain images to a standard anatomical space, employing an atlas such as the Talairach or MNI-152 (Talairach & Tournoux, 1988; Collins et al., 1994; Podgórski et al., 2021). This technique includes the entire brain volume, thus facilitating the inclusion of subcortical (and white matter) regions in the analysis. Group analysis in this approach can then leverage parcellation methods and functional atlases, such as the Harvard-Oxford Atlas, for brain segmentation, enabling the study of specific regions of interest in a standard space

(Desikan et al., 2006). However, volumetric analysis generally involves the application of a three-dimensional Gaussian filter to the whole brain, a process known as smoothing. This process can lead to signal contamination between neighboring regions due to the intricate folding patterns of the brain (Anticevic et al., 2008; Khan et al., 2011; Podgórski et al., 2021; Whitfield-Gabrieli & Nieto-Castanon, 2012).

In contrast, surface-based analysis initially involves the segmentation and inflation of individual anatomical images. For group analysis, these individual brains are subsequently aligned and projected onto a common surface template, such as the fsaverage in FreeSurfer or Conte-69 (Fischl et al., 1999; Glasser & Van Essen, 2011; Van Essen, Glasser, et al., 2012). This projection facilitates the alignment of cortical folding patterns across individuals (Van Essen, Glasser, et al., 2012). Tools like GPIP (Group Prior Individual Parcellation) that are specifically designed to be used with surface-based approaches are beneficial for resting state fMRI as they enhance the accuracy of parcel boundaries for each individual accounting for the uniqueness of their rs-fMRI data (Chong et al., 2017). For instance, unlike traditional methods, GPIP maintains inter-subject consistency while optimising for individual variations in functional specialisation. This surface-based analysis tool thus enables more precise estimations of individual functional areas, enhancing the quality of group analysis (Chong et al., 2017) .

### ***1.10.3 The importance of spatial smoothing***

Although surface-based and volume-based techniques have various pros and cons, preparatory stages before further analysis steps can also impact SNR and therefore the analysis outcome (Andrade et al., 2001; Blazejewska et al., 2019; Mikl et al., 2008). Spatial smoothing is one of the standard preprocessing steps in fMRI analysis, used to increase the SNR and facilitate

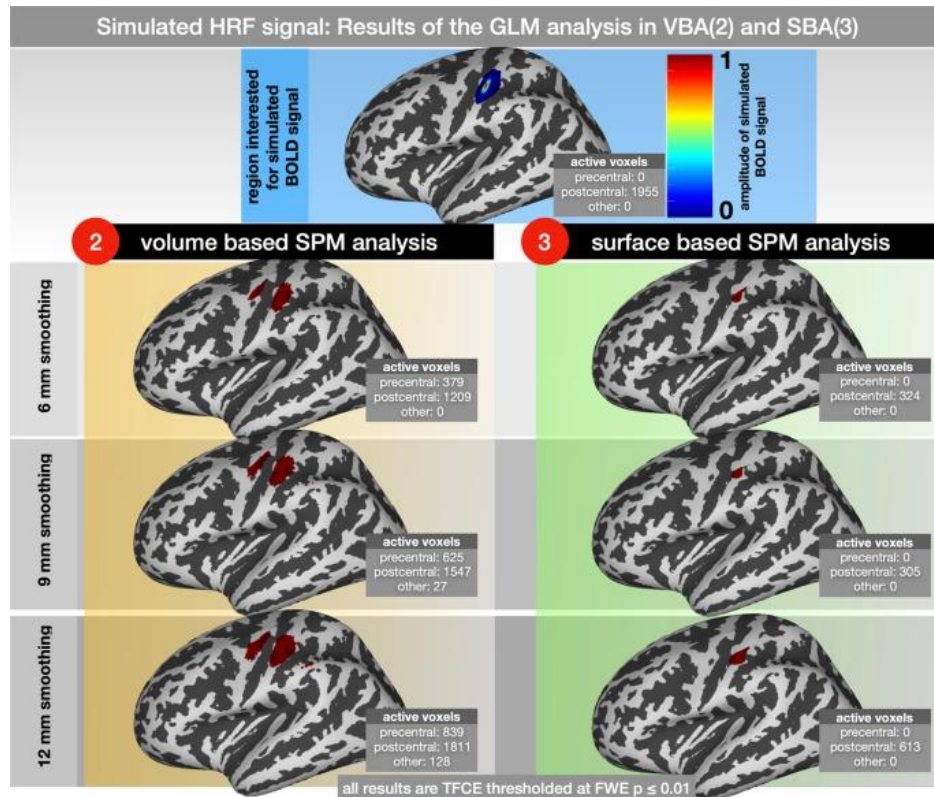
comparisons across subjects (Brodoehl et al., 2020; Mikl et al., 2008; Power et al., 2014). It involves applying a filter, typically a three-dimensional Gaussian filter with a specific full width at half maximum (FWHM) size, to the data. This process averages the signal time courses of nearby voxels, which can be beneficial if they belong to the same functional region (Andrade et al., 2001; Blazejewska et al., 2019; Brodoehl et al., 2020; Mikl et al., 2008; Power et al., 2014). However, as mentioned earlier, due to the complex folding of the brain, spatial smoothing with certain FWHM sizes can also lead to signal contamination between adjacent functional areas, impacting the results of activity and connectivity analyses.

One potential improvement to address this issue is the use of two-dimensional smoothing on the unfolded cortex, which considers the FWHM size in relation to the cortical surface. This approach, known as surface-based smoothing, may provide more sensitive results for cortical activations by restricting smoothing to smoothing in distances that are defined in terms of the cortical surface geometry and excluding white matter and cerebrospinal fluid (Blazejewska et al., 2019). Surface-based smoothing has been proposed in the past but is not yet a standard procedure in neuroimaging data preprocessing, partly due to usability and variations in the quality of surface modelling (Brodoehl et al., 2020; Mikl et al., 2008).

For example, in a study, Brodoehl et al., (2020) compared the effects of volume-based and surface-based smoothing with different FWHM sizes, they found that surface-based smoothing reduced signal contamination between neighbouring functional brain regions, improving the validity of activity and connectivity results. This study utilised fMRI data from 19 subjects during a tactile stimulation paradigm and simulated data to better understand the

effects of spatial smoothing and the choice of FWHM sizes on different areas of the precentral gyrus (See Figure 1.1-5).

**Figure 1.1-5:** Example of the SPM analysis of a simulated hemodynamic response function (HRF) signal in pre and post central gyri



Note. The simulated BOLD signal occurred every 10 s and lasted 1 s. GLM-results were smoothed using 6, 9 and 12 mm FWHM; 2nd level results were corrected for multiple comparisons and adjusted at  $p \leq 0.05$  FWE. The number of active voxels within the precentral and postcentral gyri are displayed for each separate analysis (Brodoehl et al., 2020). Reused under the open access Creative Commons license 4.0.

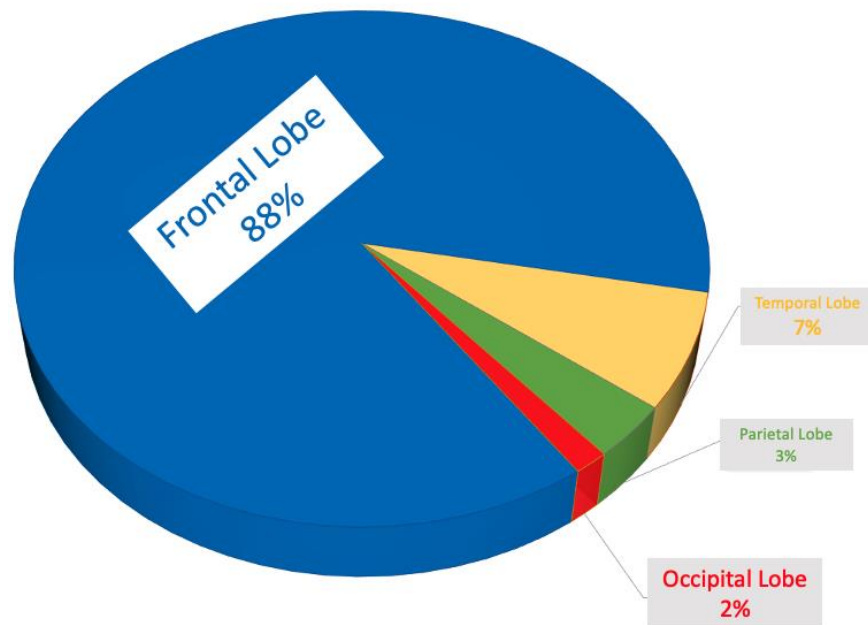
### 1.11 Current literature: Occipital TMS

Although TMS technology has been available for several decades, the majority of TMS-based research has primarily focused on frontotemporal brain regions. This trend is understandable given the recent development of TMS-based treatments for various neuropsychiatric disorders such as major depressive disorder targeting non-motor areas in the

frontal lobe, and the traditional study of brain networks in motor cortices (also in frontal brain areas). As shown in Figure 1.1-6, to investigate the distribution of TMS research across different brain regions, a PubMed search was conducted, revealing nearly 1700 papers published between 1975 and the present day that utilised an rTMS protocol (including cTBS and iTBS) in various brain areas.

Upon categorising these papers based on the targeted brain lobes, it is evident that occipital lobe studies constitute only a small fraction of rTMS research (around 2%). In fact, 88% of the studies examined rTMS effects in the frontal lobes, highlighting the need for a broader exploration of rTMS applications in other brain regions. Despite the wealth of rTMS research focusing on frontotemporal regions, it is important to consider the possibility that different brain regions may respond differently to rTMS. The occipital lobe, which primarily handles visual processing, could exhibit unique characteristics in response to rTMS stimulation that may require distinct optimisation and dose parameters. There are inherent differences in neural architecture, connectivity, and function between the occipital lobe and the frontal lobes, where most rTMS research has been conducted. Expanding our understanding of rTMS effects on the occipital lobe is crucial for developing targeted treatments and interventions for visual processing disorders or other conditions that involve the occipital region. Furthermore, a comprehensive investigation into the outcome of occipital visual areas to rTMS could reveal the underlying mechanisms of action and the potential synergistic effects of rTMS with other treatments or therapies.

**Figure 1.1-6:** PubMed search results conducted in December 2022: Percentage of TMS experiments based on their targeted lobes published between 1985-2022.



### 1.12 Current literature: Consecutive TBS-fMRI in visual brain areas

Although the behavioural effects of TBS to V1 have been explored in the past (Brückner & Kammer, 2015, 2016; Franca et al., 2006), only one rs-fMRI study has investigated the effects of TBS in the primary visual cortex (V1; Rahnev et al., 2013). Rahnev and colleagues (2013) applied cTBS, iTBS, and sham TBS to the scalp of five subjects at V1 using a stimulation intensity of 80% PT, followed by rs-fMRI. They found that iTBS did not have a significant effect on functional FC, however, they did observe a significant decrease in FC between retinotopically defined early visual areas (i.e., V1, V2, and V3) after cTBS. Similarly, other studies have reported no change in PTs following iTBS but a reduction in PTs measured 2 minutes post-cTBS (80% PT, 600 pulses; Franca et al., 2006). However, other TBS studies targeting visual brain areas outside V1, have shown that when cTBS targeted the right occipital face area and the posterior superior temporal sulcus (pSTS) at 80% active motor threshold (aMT) employing 900 pulses, cTBS

reduced BOLD signal in face-selective areas (Pitcher et al., 2014) and reduced FC between pSTS and the amygdala (Pitcher et al., 2014, 2017). Other studies using the same stimulation parameters (80% aMT and 900 pulses) demonstrated that cTBS reduced FC between pSTS and other vision and non-vision ROIs (Handwerker et al., 2020) and reduced BOLD signal in the occipital place area (Groen et al., 2021). As shown in Figure 1.1-7, additionally, a few neuroimaging studies have also examined the effects of TBS to specific nodes within the visual network (in areas beyond V1; e.g., in visual category-selective areas) to measure changes at the stimulation site and FC between different vision-related cortical and subcortical regions before and after TBS (Groen et al., 2021; Handwerker et al., 2020; Lasagna et al., 2021; Rahnev et al., 2013).

**Table 1-1 : Overview of the current behavioural and neuroimaging TBS literature in the primary visual cortex and other visual networks**

Authors	Sample	Methodology	Outcome measure	Outcome
<b>Franca et al., (2006)</b>	N = 18	cTBS and iTBS to V1 at 80% PT intensity and 600 pulses. Pre and post PT measurement	PTs	No iTBS effects, cTBS increased phosphene thresholds (inhibitory effect)
<b>Brückner &amp; Kammer (2015)</b>	N = 53	cTBS and iTBS to V1 at 100% PT and 600 pulses	PTs	No cTBS or iTBS aftereffects on phosphene thresholds
<b>Rahnev et al., (2013)</b>	N = 5	iTBS and cTBS to V1 at 80% PT and 600 pulses.	rs-fMRI (combined with retinotopy)	iTBS effects were null, cTBS decreased resting state FC between V1, V2 and V3.
<b>Allen et al., (2014)</b>	N = 15	cTBS to V1 at 80-120% MT	MRS	Post cTBS measurements: GABA increased, non-specific oscillatory changes. cTBS increased inhibitory MRS markers.
<b>Pitcher et al., (2014)</b>	N = 15	cTBS (80 % active MT, 900 pulses) to right occipital face area	rs-fMRI	Reduced BOLD signal in face selective areas
<b>Pitcher et al., (2017)</b>	N = 17	cTBS at 80 % active M and 900 pulses to posterior superior temporal sulcus (pSTS)	rs-fMRI	cTBS to pSTS reduced FC between pSTS and amygdala
<b>Handwerker et al., (2020)</b>	N = 17	cTBS at 80 % active M and 900 pulses to pSTS	rs-fMRI	cTBS to pSTS reduced FC between pSTS and other vision and non-vision ROIs
<b>Groen et al., (2021)</b>	N = 16	cTBS at 80 % active M and 900 pulses to occipital place area	rs-fMRI	cTBS to the occipital place area reduced BOLD signal in the target and other ROIs

*Note.* All the above studies recruited healthy individuals.

### 1.13 Motivation and direction of the current thesis

As discussed in this chapter, the application of TBS, a variant of rTMS, has shown to be effective in modulating neural activity in motor and non-motor frontal regions, and parietal regions. However, the research on its effects on visual areas, particularly the primary visual cortex (V1), is limited to only a few studies. This gap in knowledge has motivated the current thesis to explore the immediate and short-term effects of iTBS and cTBS on V1 and its FC with

other brain regions. The primary goal of this thesis is to advance our understanding of the modulatory effects of TBS on cortical excitability and functional connectivity in V1. To achieve this, we designed a sham-controlled study using multi-echo fMRI to compare resting state FC before and after stimulation (to V1). We looked at changes in whole-brain networks based on seeds in V1 and neighbouring occipital and parietal visual networks. We also compared PTs before and after stimulation to assess the impact of TBS on cortical excitability. The independent variables consisted of the groups (type of stimulation) including cTBS, iTBS, and sham (3 levels) in addition to the time of measurements which included: pre-TBS, post-TBS, and 1 hr post-TBS (3 levels). The main hypotheses are as follows:

**1-** We hypothesised that distinct differences in resting-state functional connectivity throughout the brain and the neighbouring seeds in the targeted brain region (V1) before and after stimulation should be observed across all three groups. We predicted that both immediate and short-term (1-hour post-stimulation) effects of TBS on V1 and other brain areas will be discernible with inhibitory effects observed in the cTBS group, excitatory effects in the iTBS, and minimal to no effects in the sham group.

**2-** We anticipated directional changes in PTs, where cTBS increases the PTs (consistent with inhibitory effect) and iTBS decreases PTs (consistent with excitatory effect).

## **Chapter 2 : Continuous and intermittent theta burst stimulation of primary visual cortex do not modulate resting state functional connectivity: A sham-controlled multi-echo fMRI study<sup>1</sup>**

---

<sup>1</sup> Adapted from the published manuscript: Cohan, R., Rafique, S. A., Stoby, K. S., Gorbet, D. J., &

Steeves, J. K. E. (2023). *Brain and Behavior*, 13(5), e2989. <https://doi.org/10.1002/brb3.2989>

## 2.1 Abstract

### **Introduction**

Theta burst stimulation (TBS) is a type of rTMS protocol which has the advantage of a shorter delivery time over traditional rTMS. When applied to motor cortex, intermittent TBS (iTBS) has been shown to yield excitatory aftereffects, whereas continuous TBS (cTBS) may lead to inhibitory aftereffects, both lasting from minutes to hours. The majority of TBS research has targeted motor, frontal, and parietal regions, and to date very few studies have examined its efficacy at visual areas. We designed a sham-controlled study to investigate the immediate post-stimulation and short-term (1 hr post-stimulation) effects of iTBS and cTBS to V1.

### **Methods**

Using multi-echo functional magnetic resonance imaging, we measured the direct and indirect effects of TBS by comparing resting state functional connectivity (FC) before and after stimulation in whole-brain networks, and seeds from V1 (stimulation site) and neighbouring occipital and parietal visual networks. In addition, we also measured pre- and post-TBS phosphene thresholds (PTs) to examine the modulatory effects of TBS on cortical excitability.

### **Results**

We found no changes in FC for iTBS, cTBS or sham stimulation conditions from baseline to post-stimulation timepoints. Additionally, cTBS and iTBS had no effect on visual cortical excitability.

### **Conclusion**

Our results indicate that unlike our previous low frequency rTMS to V1 study which resulted in widespread FC changes up to at least 1 hr after stimulation, TBS to V1 does not affect

FC. Contrary to the studies showing comparable TBS and rTMS aftereffects in motor and frontal regions, our findings suggest that a single session of cTBS or iTBS to V1 at 80% PT using a standard protocol of 600 pulses may not be effective in targeting FC especially in clinical settings where therapy for pathological networks is the goal.

## **2.2 Introduction**

Since the advent of non-invasive brain stimulation (NIBS), transcranial magnetic stimulation (TMS) has proven to be a powerful tool for inducing transient alteration of neural activity and has allowed for causal mapping of nodes within neural networks (Barker et al., 1985; Day et al., 1989; Kobayashi & Pascual-Leone, 2003; Rafique et al., 2015; Solomon-Harris et al., 2016). Commonly employed TMS protocols such as low (1 Hz) and high (10 Hz) frequency repetitive TMS (rTMS) have been shown to alter focal neural activity at the stimulation site as well as remote neural networks with effects lasting from minutes to days (Fox et al., 2012; Pascual-Leone et al., 2000; Rafique et al., 2016; Rafique & Steeves, 2022). Although the mechanism is not fully understood, they have been attributed to long-term potentiation (LTP) and long-term depression (LTD) involved in synaptic plasticity (Barker et al., 1985; Bliss & Lomo, 1973; Day et al., 1989).

rTMS has shown to be effective both as a research tool and a treatment modality in neurological and neuropsychiatric disorders (Mi et al., 2020; Rafique et al., 2016). The quest for shorter stimulation time and lasting aftereffects however has led to a modified variation of rTMS, namely theta burst stimulation (Hill, 1978; Huang et al., 2011; Larson et al., 1986). Since its inception, research employing TBS protocols have shown that modifying traditional stimulation parameters (i.e., frequency, intensity, pattern and duration) can lead to focal

dissociable inhibitory and excitatory effects (Gilio et al., 2007; Hess & Donoghue, 1996). These effects, however, have been mostly examined in primary motor cortex (M1) via motor evoked potentials (MEPs) measured using electromyography (EMG) to evaluate the efficacy of stimulation and to determine optimal stimulation intensity levels at M1 (Huang et al., 2011; Rossini & Rossi, 1998).

With a growing number of confirmatory studies, TBS has gained a foothold in research and clinical settings mainly due to its shorter (~ 3min) delivery time over rTMS (~28 min), which can drastically improve efficiency of empirical research in the lab and patient compliance in clinical settings. Nevertheless, it is assumed that for any TMS-based protocol to be considered an effective treatment, its therapeutic effects should last long enough to induce measurable changes at the neural and behavioural levels. Thus far, TBS has proven to be effective in treating depression, and has shown promising results in neurorehabilitation and chronic pain (Blumberger et al., 2018a; Moisset et al., 2015; Talelli et al., 2007). However, the neural underpinnings of TBS aftereffects beyond the stimulation time remains an open area of research. Moreover, the efficacy of TBS targeting visual cortex and, therefore, its value and use in visual disorders is poorly documented. Pilot data in the therapeutic effects of occipital (and cerebellar) TBS in ameliorating symptoms of patients with Mal de Débarquement syndrome (Cha et al., 2019) has been explored and shown promising results. This patient population suffers from the chronic phantom perception of oscillating vertigo thought to be caused by changes in neural excitability in the balance system, in the absence of movement or vestibular and ocular inputs (Van Ombergen et al., 2016). Both cTBS and iTBS have been explored in phantom limb sensation after spinal cord injury, and cTBS proved effective in suppressing

phantom sensations (Nardone et al., 2016). TBS is also a potentially viable candidate as an investigative tool to study the aetiology of visual disorders, including cortical blindness and post-stroke or post-enucleation visual hallucination such as Charles Bonnet syndrome (CBS; Cox & ffytche, 2014; Gothe et al., 2002; Wen et al., 2018) and phosphenes (Rafique et al., 2018), and to develop neuromodulation based therapies for these conditions in the future.

To probe TMS effects at the neuronal level, neuroimaging techniques such as resting state fMRI (rs-fMRI) can measure whole brain and regional changes in connectivity of stimulated targets, respectively. Using blood oxygenation level dependent (BOLD) imaging, rs-fMRI is an indirect measure of physiological dependencies between different anatomical locations determined through various functional connectivity (FC) data analysis techniques (Biswal et al., 1995; Fox et al., 2005; Friston, 1994). rs-fMRI can track changes in the brain's networks both in health and disease, for example previous studies have demonstrated distinct alterations in visual networks and the default mode network (DMN) of patients with strabismus and amblyopia (Peng et al., 2021; Shao et al., 2019), late blindness (Wen et al., 2018) and CBS (ffytche et al., 1998). Additionally, studies using rs-fMRI investigating the inhibitory and excitatory effects of cTBS and iTBS to motor, parietal and frontal brain regions have shown that these protocols modulate opposite connectivity patterns in focal and remote brain areas (Cocchi et al., 2015; de Wandel et al., 2020; Gratton et al., 2013). To date, however, only one rs-fMRI study investigated the effects TBS to primary visual cortex (V1; Rahnev et al., 2013), and a few neuroimaging studies have examined the effects of TBS to specific nodes within the visual network (in areas beyond V1), e.g., at the occipital cortex in visual category-selective areas to measure changes at the stimulation site and FC between different vision-related cortical and

subcortical regions before and after TBS (Groen et al., 2021; Handwerker et al., 2020; Lasagna et al., 2021; Rahnev et al., 2013).

In our lab, we previously examined the effects of a single session of 1 Hz rTMS to V1 using MRI-guided neuronavigation and rs-fMRI to determine immediate and short-term effects of stimulation and found no immediate effects on FC following a single 20-minute session of 1 Hz rTMS but widespread changes in FC were observed at 1 hr following stimulation (Rafique & Steeves, 2022). In the present study, to determine whether TBS offers a shorter protocol with equivalent effects compared to traditional TMS at V1, we similarly examined the immediate and short-term (up to 1 hr post-TBS) effects of cTBS and iTBS to V1 on whole-brain FC as well as nodes in occipital and parietal visual networks using MRI-guided neuronavigation. Parietal areas, such as the precuneus cortex were chosen mainly due to their interconnectivity with occipital visual areas and their involvement in resting state networks such as the DMN (Fox et al., 2005; Raichle, 2011; Zhang et al., 2018). Additionally, we also set out to determine TBS aftereffects on phosphene thresholds (PTs; a measure of cortical excitability in V1), and monocular and binocular visual acuity by comparing baseline and 1 hr post-TBS data.

## **2.3 Methods and materials**

### **2.3.1 Participants**

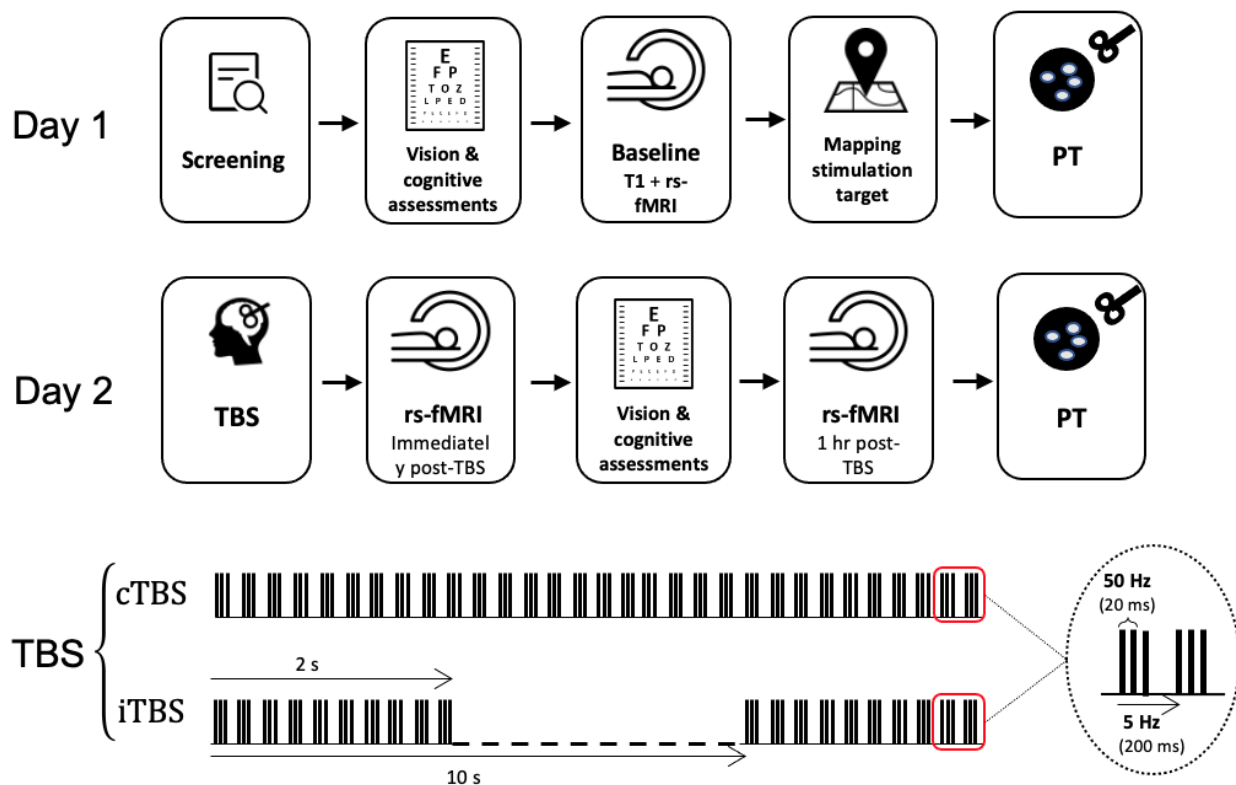
Thirty-one right-handed participants (14 males and 17 females,  $M_{\text{age}} = 23$   $SD = 4$  years) with no history of medical, neurological, or psychological disorders and no contraindications to TMS and MRI consented to participate. Participants had normal or corrected-to-normal vision and underwent screening including eligibility questionnaires, vision, and cognitive assessments.

Data from one participant was omitted due to high motion artefacts detected during image preprocessing.

### **2.3.2 Experimental design overview**

This study was approved by the Office of Research Ethics at York University and took place over two sessions separated by one week. In a pseudo random fashion, and naïve to TMS, participants were assigned to one of three conditions: cTBS, iTBS or sham. As shown in Figure 2-1, on day 1, at approximately 1 pm, each participant completed the screening, including eligibility questionnaires, vision assessment and the Montreal Cognitive Assessment (MoCA) versions 7.1-7.3 (Nasreddine et al., 2005). At approximately 1:30 pm, baseline anatomical MRI and rs-fMRI were obtained, and subsequently PTs were measured. In order to prevent residual effects from PT and to minimise diurnal effects, participants were tested one week following the baseline session at approximately the same time of the day. On day 2, participants underwent TBS and post-stimulation MRI scans were acquired at two different timepoints—immediately following TBS (within five minutes) and 1 hr after TBS. PTs were then re-measured after scans were completed.

**Figure 2-1** : An overview of the experimental design and TBS parameters.



Note. TBS = theta burst stimulation, iTBS = intermittent TBS, cTBS = continuous TBS, Phosphene thresholds = PTs, rs-fMRI = resting-state functional magnetic resonance imaging.

### 2.3.3 Phosphene thresholds

A phosphene is the experience of light in the absence of visual stimuli. PT is a measure of visual cortex excitability that is accomplished by stimulation of visual cortex leading to a subjective percept of light in participant's visual field. Visual cortex excitability thresholds can vary greatly across individuals (Stewart et al., 2001) presumably reflecting individual cortical excitability. As such, PTs can be used to determine appropriate individual stimulation intensity for TMS administration at the visual cortex in the same way that motor threshold (MT) is used to determine TMS intensity when applied to the motor cortex. Phosphenes are elicited when

stimulation is applied from 1–5 cm above theinion and 0–3 cm laterally, in either hemisphere being tested (Elkin-Frankston et al., 2010). Participants sat in a dimly lit room while wearing a blindfold with eyes closed. Four locations including theinion, 2 cm above theinion, 2 cm to the left of theinion, and 2 cm above the 2 cm to the left of theinion marker were identified as the stimulation grid. Using single-pulse TMS with the coil centre held tangential to the scalp and handle orientated 90° laterally to the midline, individual PTs were measured for each subject. The minimum stimulator output intensity was set at 50%, and 10 pulses were delivered to the marker 2 cm above theinion. Each pulse was 6 s apart. Upon delivery of a single TMS pulse, participants were instructed to respond “yes/no/maybe” corresponding to whether a phosphene was perceived. At each location, the stimulator output was increased in 5% increments until a phosphene was evoked. For safety, we limited the maximum output setting to 90% intensity (Wassermann, 1998). If no phosphenes were evoked after 10 pulses, the coil was moved to a new position in the stimulation grid until the participant responded “yes”, which was then marked as the hotspot. Subsequently, at the hotspot, the threshold was modified by 1% increments to refine the PT. A threshold was defined as the intensity at which 50% of pulses (5/10 pulses) resulted in a “yes” response. The blindfold was removed every 10–15 min, when necessary, for a minimum of 3-5 min, to prevent dark adaption (Boroojerdi et al., 2000b). PTs were analysed using R statistical software (v 3.3.3; R Foundation for Statistical Computing, Vienna, Austria; [www.R-project.org](http://www.R-project.org)) and the *lmer* package for multilevel modelling. The independent variable was “Group”, which included the cTBS, iTBS, and Sham conditions. Meanwhile, PTs measured at baseline and 1-hr post-stimulation were designated as the dependent variable.

#### **2.3.4 Theta burst stimulation**

Participants underwent one of the three TBS stimulation conditions (cTBS, iTBS or Sham). TMS was delivered with a Magstim Rapid<sup>2</sup> Plus 1 stimulator and an air-cooled figure-of-eight stimulation coil (Magstim, Whiteland, Wales, UK). Participants were stimulated at 80% individual PT that was initially determined on Day 1. The cTBS protocol consisted of bursts containing three pulses at 50 Hz with a 20 ms inter-stimulus interval (ISI) repeated at 5 Hz intervals with 200 ms ISI, applied continuously for 40 s, providing a total of 600 pulses (Huang et al., 2005). The iTBS protocol consisted of the same bursts containing three pulses at 50 Hz, repeated at 5 Hz intervals, however applied in 2 s trains repeated every 10 s for a total of 190 s, providing a total of 600 pulses (Huang et al., 2005). The sham TBS protocol was the same as the active conditions, except it was performed using the placebo sham coil. Four participants received sham iTBS and six received sham cTBS. The sham coil is equipped with a shield that attenuates the magnetic field while mimicking auditory and stimulation effects of an active coil.

TMS was delivered using Brainsight's neuronavigation system to ensure the accuracy of the coil position throughout stimulation (Rogue Research, Montreal, QC, Canada). Participants' anatomical MR images were reconstructed and co-registered to their three-dimensional cortical surfaces in Brainsight. The stimulation site corresponded to the volume of interest (VOI) in V1 in our previously published magnetic resonance spectroscopy (MRS) study of the same cohort (Stoby et al., 2022). The stimulation site was mapped on each participant's corresponding anatomical image in Brainsight by manually matching the anatomical landmarks to the centre of the MRS VOI images. The neuronavigation system precisely maps individually targeted stimulation sites and accounts for anatomical variability across participants. We used the same

coil both for determining phosphene thresholds and for TBS, however, for TBS the coil was held parallel to the midline with the handle pointing downwards and the coil centre tangential to the head to minimise coil to cortex distance. This coil orientation was necessary due to the fact that we stimulated the calcarine sulcus (V1) by placing the centre of the coil 1-2 cm around the centre of theinion. The exact stimulation location differed for each participant due to individual anatomical differences observed on T1 images in Brainsight neuronavigation system.

Participants sat upright with their eyes open, and their chin stabilised by a chin rest, and while TBS was delivered with the coil placed 2 cm above the centre of theinion, PTs were measured at varying locations around theinion (2 cm radius).

### **2.3.5 Magnetic resonance imaging**

Both anatomical and functional sequences were obtained at baseline, immediately post-TBS, and 1 hr post-TBS using a 3 Tesla Siemens Magnetom Prisma magnetic resonance scanner with a 32-channel high resolution array head coil (Siemens, Erlangen, Germany). Participants were instructed to remain motionless with their eyes closed while refraining from falling asleep.

Anatomical high-resolution T-weighted magnetisation-prepared rapid gradient echo (MPRAGE) sequence was acquired first [number of slices = 192, in-plane resolution = 1 mm x 1 mm, slice thickness = 1 mm, imaging matrix = 256 x 256, repetition time (TR) = 2300 ms, echo time (TE) = 2.26 ms, inversion time (TI) = 900 ms, flip angle = 8°, field of view (FoV) = 256 mm, acquisition time = approximately 5 min]. Resting state functional imaging was acquired with T2\* weighted whole-brain echo planar ME imaging [number of contiguous axial slices = 43; in-plane resolution = 3.4 x 3.4 mm; slice thickness = 3 mm; imaging matrix = 64 x 64; TR = 3000 ms; TE<sub>1</sub> =

14.0 ms, TE<sub>2</sub> = 30.08 ms, TE<sub>3</sub> = 46.16 ms; flip angle = 83°; FoV = 216 mm; acquisition time = 10 min].

### **2.3.6 Vision and cognitive assessment**

All participants were required to complete and pass three basic visual assessments for eligibility for normal or corrected-to-normal vision (> 0.04 LogMAR; stereoacuity ≥ 50", normal colour vision). Monocular and binocular visual acuities were measured using the standardised ETDRS LogMAR vision chart (precision Vision, La Salle, IL), stereo acuity was measured using the Titmus Stereoacuity test (Stereo Optical Company Inc., Chicago, IL), and colour vision was assessed using the Ishihara Colour Plates (Kanehara Trading Inc., Tokyo, Japan).

Participants were also required to complete and pass the MoCA (v7.1-7.3). The MoCA is a screening tool that detects cognitive impairment with scores ranging from 0-30. It evaluates attention, concentration, and executive function (Nasreddine et al., 2005). The inclusion cut-off was set at scores equal and greater than 26 (Yeung et al., 2020). All participants were able to meet the cut-off. Statistical analyses for visual acuity and MoCA scores were performed using R statistical software (v 3.3.3; R Foundation for Statistical Computing, Vienna, Austria; [www.R-project.org](http://www.R-project.org)) and the *lmer* package for multilevel modelling (Kuznetsova et al., 2017).

### **2.3.7 fMRI data preprocessing**

Preprocessing and denoising were performed in AFNI (Cox & Hyde, 1997) using multi-echo independent component analysis (ME-ICA, v3.2). ME-ICA uses the TE-dependence of the BOLD signal to separate true BOLD signal from non-TE-dependent fluctuations that result from sources of noise (Kundu et al., 2012b). Prior to denoising with ME-ICA, data preprocessing

steps included discarding the first five volumes of each resting-state fMRI time-series. Images were skull-stripped, and image intensity was normalised (3dSkullStrip). The functional images were de-obliques (3dWarp). Large signal transients were removed via interpolation (“despiking”, 3dDespike) and slice time correction was applied (3dTshift). Motion correction parameters were calculated using the middle echo ( $TE_2 = 30.08$  ms, 3dvolreg). Skull-stripped anatomical and functional images were coregistered by registering the middle echo image from the first time point to the anatomical image using an affine alignment procedure with the local Pearson correlation and  $T2^*$  weights (3dAllineate). Anatomical and functional images were kept in native space. After the three TEs were optimally combined, ME-ICA denoising was applied. BOLD signal was identified as independent components having linearly TE-dependent percentage signal changes. Non-BOLD noise components were removed from the time-series by ME-ICA using linear regression. The output of this process included a functional time-series reconstructed to include only the BOLD signal components of the data. This preprocessed and denoised time-series was used in all subsequent stages of the data analysis. Subject- and session-specific quality checks were performed after preprocessing and denoising by inspecting plots of estimated head motion and anatomical-functional alignment. In addition, inclusion of subjects in further stages of analysis required the identification of at least 10 BOLD-like components by ME-ICA. Images from one subject were omitted due to excessive motion and few detected BOLD-like components.

### **2.3.8 fMRI data analysis**

To analyse the rs-fMRI data, we used two different approaches, 1) Volumetric seed-based FC analysis in MNI space, and 2) Surface-based FC analysis with individual parcellation.

For each analysis, an exploratory stepwise approach was used to first determine group-level whole brain seed-to-voxel connectivity profiles followed by ROI-to-ROI and seed-to-target analyses in occipital and parietal visual areas to probe group differences at different timepoints. Given the individual variability in response to stimulation and statistical stringencies involved in exploratory analyses, this approach was deemed critical in order to detect TBS aftereffects at the connectome level.

#### ***2.3.8.1 Analysis 1: Volumetric seed-based analysis in MNI space***

For this analysis we used MATLAB R2019a (MathWorks, Natick, MA, USA), and CONN toolbox v20.b ([www.nitrc.org/projects/conn](http://www.nitrc.org/projects/conn)). The preprocessed and denoised rs-fMRI images and the preprocessed anatomical scans for each subject and each session were input into CONN. Functional and anatomical scans were normalised into standard MNI space and segmented into grey matter (GM), white matter (WM) and cerebrospinal fluid (CSF) tissue classes using SPM12 unified segmentation and normalisation procedure (Ashburner & Friston, 2005). Functional images were then spatially smoothed by a 6 mm Gaussian kernel of full width at half-maximum. Using an anatomical component-based noise correction (CompCor) five principal components from CSF, GM, and WM were extracted (Behzadi et al., 2007) and confound regression was performed via principal component analysis (PCA) in order to remove non-BOLD signals (Power et al., 2014b).

Using an exploratory whole-brain seed-based connectivity (SBC) approach, subject-specific cross-correlation matrices between the seed and the whole brain, as well as non-BOLD confounds were fitted to a first-level model (Whitfield-Gabrieli & Nieto-Castanon, 2012). We explored SBC in two seeds, the stimulation site and the precuneus cortex based on the Harvard-

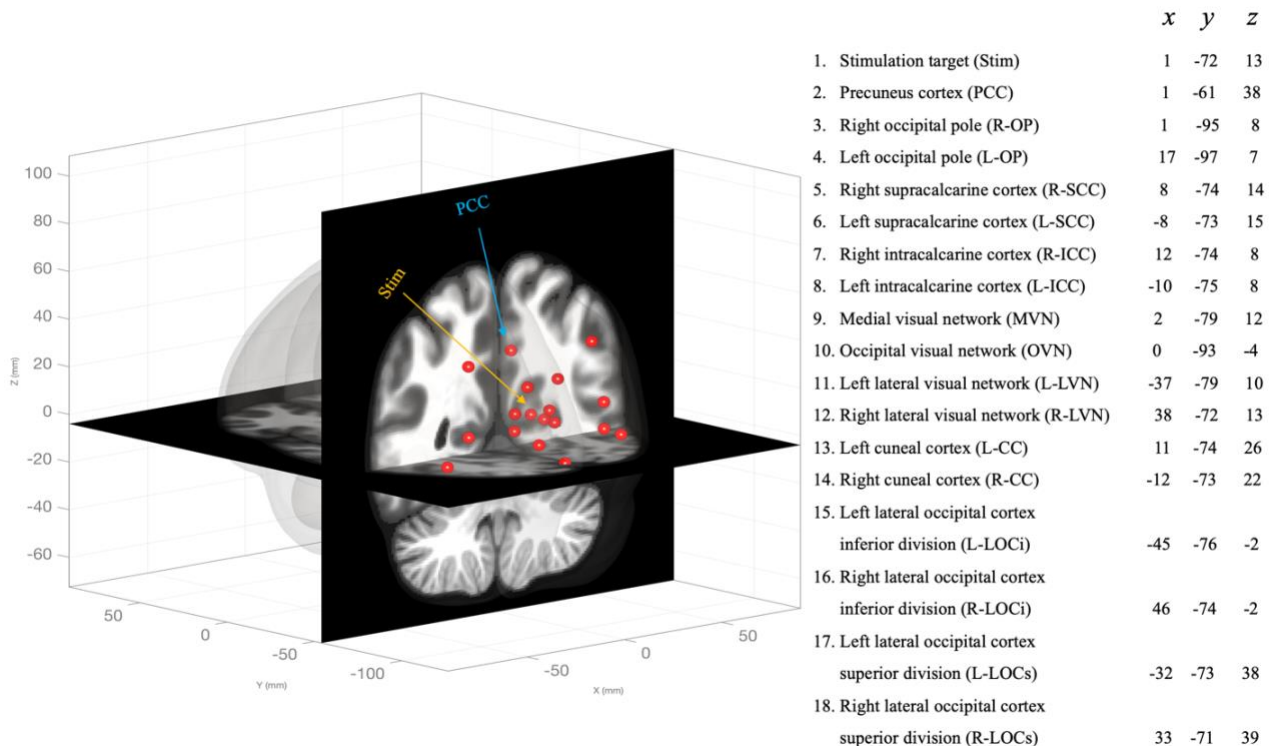
Oxford atlas coordinates (Desikan et al., 2006). For the stimulation site, a 10 mm spherical seed ROI was centred at the average stimulation site coordinates ( $x = 1$ ,  $y = -72$ ,  $z = 13$ ). The subject-specific standardised stimulation site coordinates were extracted following manual co-registration of individual anatomical scans to the MNI template in Brainsight neuronavigation system using the anterior commissure (AC)-posterior commissure (PC) technique. SBC maps were computed as the Fisher-transformed bivariate correlation coefficients between the seeds' timeseries and each individual voxel timeseries. Given the non-normal nature of the data, non-parametric (permutation-randomisation with 1000 simulations) statistics were chosen for further analyses. To control for multiple comparisons, we implemented family wise error rate (FWER) and false discovery rate (FDR) methods. FWER methods are ideal when controlling for the probability of even one false positive (Type I error). On the other hand, FDR-controlled procedures are suitable when a certain number of false positives is tolerable to avoid excessive false negatives (Eklund et al., 2016; Kang et al., 2015). In essence, FDR control is more lenient, allowing for some proportion of false positives in exchange for a decrease in false negatives (Nichols & Hayasaka, 2003). In this analysis, as noted above, permutation testing was chosen as the method to control the FWER. The advantage of permutation tests is that they make fewer assumptions about the underlying data, making them suitable for non-parametric data (i.e., rs-fMRI data), and they can accurately control the Type I error rate even when conducting a large number of tests (Bullmore et al., 1999).

For ROI-to-ROI analyses, with lower number of comparisons, FDR is chosen to control for multiple comparisons. FDR was calculated by sorting the statistical significance measures (p-values) from smallest to largest and then comparing each one to a threshold that gradually

increases with the rank of the p-value. If the p-value was smaller than this threshold, the null hypothesis was rejected (Benjamini & Hochberg, 1995).

In addition to the whole-brain FC analysis described above, we also examined the FC between 18 occipital and parietal ROIs in order to investigate post-TBS changes in specific visual networks (see Figure 2-2). These ROIs were mainly chosen based on their proximities to the stimulation site seed ROI (covering bilateral focal and remote areas surrounding the stimulation ROI). The ROI-to-ROI connectivity matrices were computed with bivariate Pearson’s correlation coefficients of BOLD signal for each pair of ROIs. The Pearson’s correlation coefficients were then transformed to Fisher Z values for further statistical analyses. In order to correct for multiple comparisons, the cluster-level p-value was set at  $p < 0.05$  (FDR-corrected).

**Figure 2-2 :** MNI coordinates of 18 ROIs used in ROI-ROI analysis based on the Harvard-Oxford atlas.



Lastly, we focused on the connections between the stimulation site and the 17 other chosen ROIs using a seed-to-target analysis. The 17 other ROIs were the same as the ROI-to-ROI analysis, but this approach is inherently different from the previous ROI-to-ROI analysis in that one seed was compared to the chosen targets (targets are not compared to one another), therefore requiring fewer comparisons to address a specific hypothesis. Using a mixed-design analysis of variance (ANOVA) with FDR-corrected p-values  $< 0.05$  we then examined between-group differences in FC. The independent variables consisted of the groups (type of stimulation) including cTBS, iTBS, and sham (3 levels) in addition to the time of measurements which included: pre-TBS, post-TBS, and 1 hr post-TBS (3 levels).

#### *2.3.8.2 Analysis 2: Surface-based ROI-to-ROI analysis using GPIP parcellation*

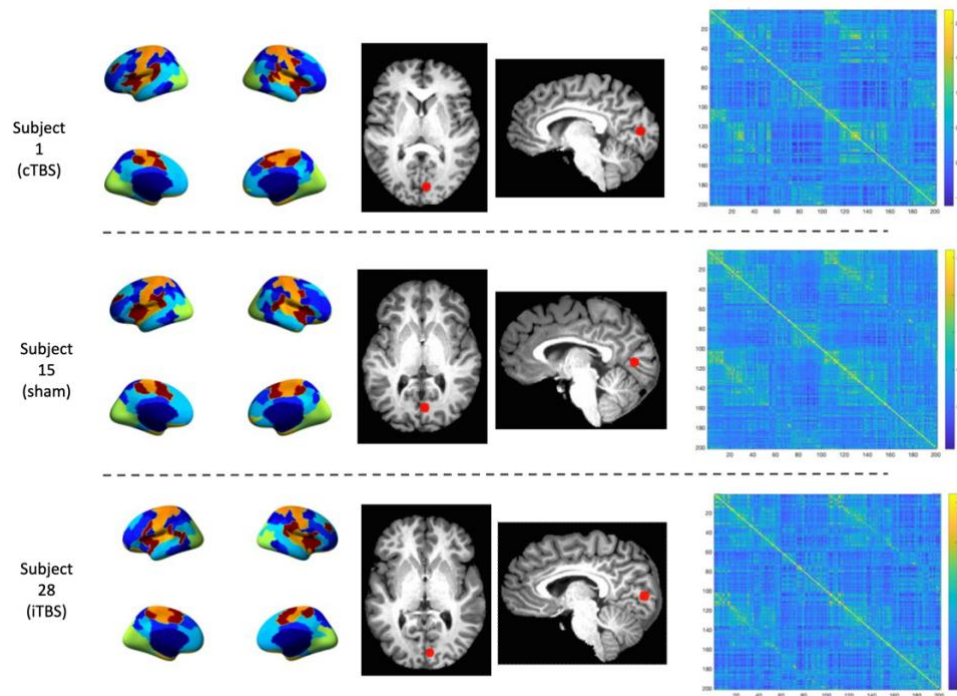
In this analysis, individual T1 images were parcellated into anatomical regions using the *recon-all* pipeline in FreeSurfer v6.0.1 (<http://surfer.nmr.mgh.harvard.edu/>). Within FreeSurfer, the preprocessed and denoised timeseries output by ME-ICA were coregistered to the T1-weighted anatomical images output by *recon-all* for each subject and session (*bbregister*). Next, the functional data were resampled to the *fsaverage5* template image using trilinear volume-to-surface interpolation (*mri\_vol2surf*). Spatial smoothing was applied using a full width half max kernel of 6mm (*mri\_surf2surf*). Using the surface space functional data, the time course of each resting state imaging run was normalised to a mean of 0 and a standard deviation of 1. Group Prior Individual Parcellation (GPIP; Chong et al., 2017) was used to output subject-specific functional parcellations of the resting state data. Within GPIP, the data were first initialised using the 200-parcel 7-Network Schaefer atlas (Schaefer et al., 2018; for more information see Table A1 in Appendix) resulting in a common set of parcellation labels for all

subjects. After initialisation, GPIP uses each subject's resting state functional images to optimise the boundaries of each parcel, resulting in subject-specific functional parcellations of resting state networks. The quality of GPIP parcellations for each subject was assessed by calculating the homogeneity of parcels at each of the 20 GPIP iterations. Homogeneity was calculated as the mean correlation coefficient of all pairs of vertices within each parcel and then averaged over all parcels in the brain for each subject to verify that these values increased over iterations and then plateaued in value prior to the final GPIP iteration.

Spherical ROI masks 5 mm in diameter were created for each subject/session using the coordinates of their stimulation site within V1 in AFNI. These ROI masks were then resampled to fsaverage5 surface space and inspected for accuracy of placement in each subject. The mean timeseries of each stimulation site ROI was extracted from the functional data (mri\_segstats). Similarly, for each subject/session, the mean timeseries was extracted for each GPIP parcel. Pair-wise Pearson correlation coefficients were calculated for all extracted mean time-series and then Fisher r-to-z transformed resulting in cross-correlation functional connectivity matrices for each subject and session (see Figure 3 for examples of individual parcellation and connectivity matrices). Group analyses of parcel functional connectivity were performed using the Network Based Statistics toolbox (NBS; Zalesky et al., 2010). NBS V.2.0 (<https://www.nitrc.org/projects/nbs>) is a nonparametric method that controls the family-wise error rate (FWER) when multivariate models are applied to neuroimaging data in order to compare functional or structural connectivity between pairs of ROIs or networks of ROIs. After setting up between- and within-group contrasts and using the default FWER-corrected significance level of 0.05, a whole brain FC analysis was first conducted. Using a 2 x 2 mixed

effect ANOVA the Stimulation (Group) main effects were explored in each pair of conditions (e.g., cTBS > iTBS, cTBS > Sham or iTBS > Sham) across two timepoints (e.g., Day 1 < Day 2 immediately post-TBS).

**Figure 2-3 :** Example of individual parcellation and connectivity matrices in three randomly selected subjects from each of the three stimulation groups at baseline (day 1).



As the final step, and in order to choose comparable ROIs to the ones used in the volumetric analysis, the Schaefer 200-parcel-7-network atlas that was used to initialise GPIIP was overlaid on top of a standard MNI-152 template in *fsleyes* (<https://git.fmrib.ox.ac.uk/fsl/fsleyes/fsleyes/>). Labels used in the Schaefer 200-parcel 7-network atlas correspond to resting state networks but do not correspond to specific anatomical region labels. Therefore, the Harvard-Oxford cortical structural atlas was used to identify corresponding anatomical labels of the Schaefer atlas regions to facilitate comparison with the 17 ROIs used in the CONN Toolbox. Coordinates from the ROIs included in the volumetric analysis performed in CONN Toolbox and the homologous Schaefer atlas regions were manually determined and the connectivity values between the 17 selected GPIIP ROIs and the stimulation site were extracted and compared (see Appendix Table A1 for the list of ROIs).

To examine FC within the visual networks we applied a less stringent correction method of FDR correction ( $< 0.05$ ), and a series of 2 x 2 mixed effects ANOVAs were conducted to determine the effects of Stimulation and Time on FC between groups at different timepoints. This procedure was performed using the visual network subset of the Schaefer 200-parcel 7-network atlas ROIs (28 ROIs plus the stimulation site; see Table A1 in Appendix).

## **2.4 Results**

### **2.4.1 Visual acuity and neurological assessments**

For the visual acuity data (both monocular and binocular), and MoCA scores a two-way mixed effects ANOVA revealed no significant interaction between Group (cTBS, iTBS, and Sham) and Time (Pre-TBS and post-TBS). Main effects of Group and Time were also non-significant (see Table 2-1 for group-specific statistics).

**Table 2-1 : Analysis of variance (ANOVA) of phosphene thresholds, vision, and cognitive assessments data before and after TBS.**

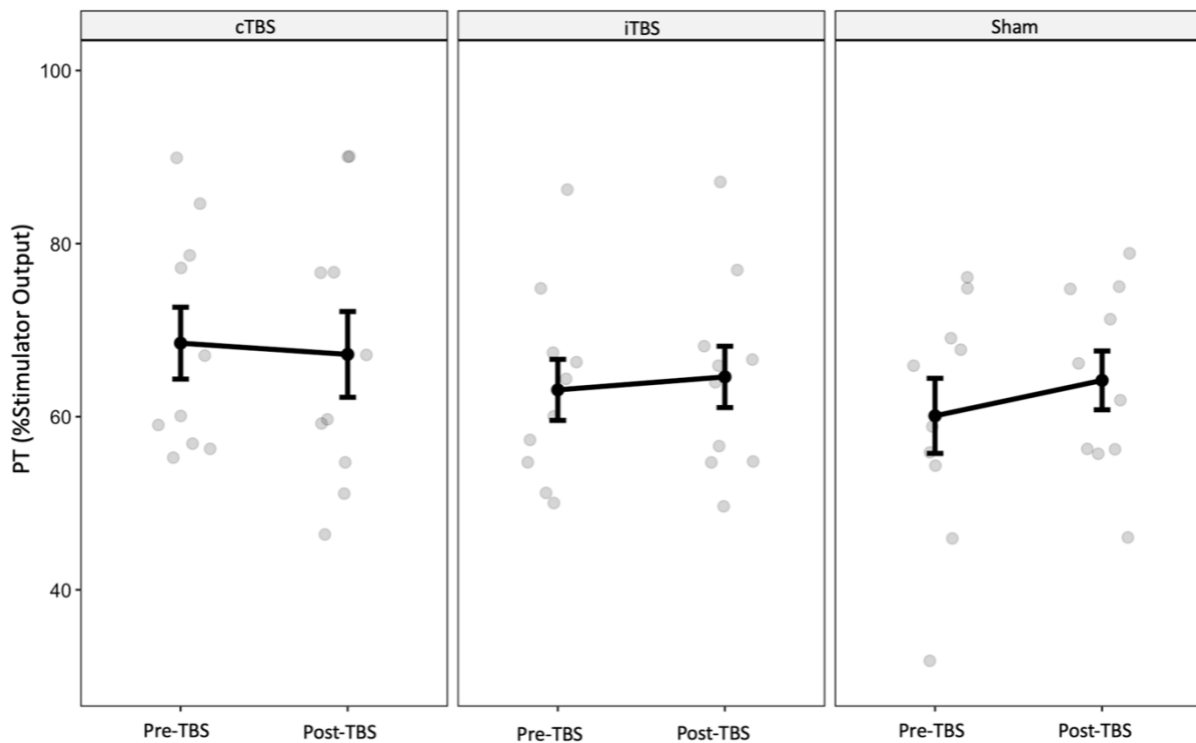
Assessment		Pre-TBS		Post-TBS		ANOVA				
Condition		<i>M</i>	<i>SD</i>	<i>M</i>	<i>SD</i>	Effect	<i>F</i> <i>ratio</i>	<i>df</i>	<i>p</i>	$\eta^2$
PT (% Stimulator output)	cTBS	68.5	13.1	67.2	15.7	G	0.552	2,27	0.58	0.004
	iTBS	63.1	11.2	64.6	11.2	T	0.552	1,27	0.14	0.038
	Sham	60.1	13.7	64.2	10.7	G x T	2.69	2,27	0.09	0.086
Binocular VA (LogMAR)	cTBS	-1.23	0.062	-0.108	0.051	G	0.167	2,27	0.85	0.011
	iTBS	-1.22	0.086	-0.146	0.077	T	0.221	1,27	0.64	0.001
	Sham	-0.13	0.11	-0.138	0.115	G x T	0.906	2,27	0.42	0.009
Right monocular VA (LogMAR)	cTBS	-0.043	0.063	-0.037	0.084	G	3.16	2,27	0.068	0.152
	iTBS	-0.078	0.051	-0.096	0.087	T	0.027	1,27	0.87	0.0002
	Sham	-0.13	0.105	-0.126	0.124	G x T	0.242	2,27	0.79	0.004
Left monocular VA (LogMAR)	cTBS	-0.089	0.07	-0.069	0.069	G	0.865	2,27	0.43	0.044
	iTBS	-0.115	0.07	-0.1	0.071	T	0.331	1,27	0.57	0.004
	Sham	-0.115	0.096	-0.123	0.112	G x T	0.283	2,27	0.76	0.006
MoCA	cTBS	27.9	1.60	27.8	1.48	G	0.019	2,27	0.98	0.001
	iTBS	27.9	0.99	28	1.25	T	0.672	1,27	0.42	0.006
	Sham	28.2	1.32	27.6	1.26	G x T	0.728	2,27	0.49	0.013

*Note.* PT = phosphene threshold, TBS = Theta burst stimulation, cTBS = continuous TBS, iTBS = intermittent TBS, VA = visual acuity, MoCA = Montreal cognitive assessment. LogMAR = logarithm of the minimum angle of resolution. Pre-TBS = Day 1, before TBS, post-TBS = Day 2, after TBS. Effect = G (Group: cTBS, iTBS or sham), T (Time: pre- or post-TBS), G x T (interaction between Group and Time). Significance level = p-values < 0.05.

## 2.4.2 Phosphene thresholds

As shown in Figure 2-4 (also see Table 2-1 for group-specific descriptive and inferential statistics), the average pre- to post-TBS PTs in all three groups did not change significantly. A two-way mixed effects ANOVA found no interaction between Stimulation Group (cTBS, iTBS and sham) and Time (pre-TBS and 1 hr post-TBS). There was no main effect of Stimulation Group.

**Figure 2-4 :** Pre- and post-TBS group mean with individual data points phosphene thresholds.



Note. cTBS = continuous theta burst stimulation, iTBS = intermittent theta burst stimulation, PT = phosphene threshold. For individual data see Figure A1 in Appendix.

## 2.4.3 Volumetric seed-based connectivity analysis in MNI space

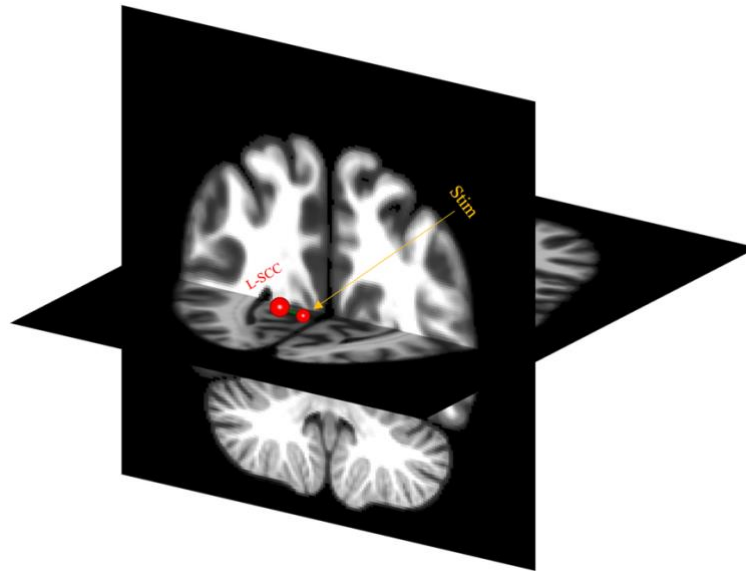
*Whole brain connectivity:* An omnibus test to detect significant seed-to-voxel FC between conditions and timepoints was conducted. No significant interaction between

Condition and Time was observed for whole brain connectivity. Similarly, there were no significant main effects of Group or Time for any of the seeds on whole brain connectivity.

*ROI-to-ROI:* At the group level, we first examined individual connectivity for each condition (iTBS, cTBS and sham) across the three timepoints. We used within-group contrasts to determine the connectivity profile for each of the 18 chosen ROIs and 153 non-overlapping connections. No significant interaction was found between Stimulation Condition (Group) and Time, and there were no significant main effects of Stimulation and Time on individual connectivity profiles.

*Seed-to-target:* A between-group analysis revealed one target ROI [Left supracalcarine cortex (L-SCC)] that survived the pre-defined threshold ( $t(18) = 3.59$ ,  $p\text{-FDR} = 0.036$ ). However, pairwise comparisons revealed no significant difference in seed-to-target connectivity for the within-condition (Stimulation effect) at different timepoints. This indicates that despite differences in FC between groups, no changes were observed in cTBS, iTBS or sham groups at different timepoints (see Table A2 in the Appendix for statistics).

**Figure 2-5 : Seed to target within- and between-group results.**



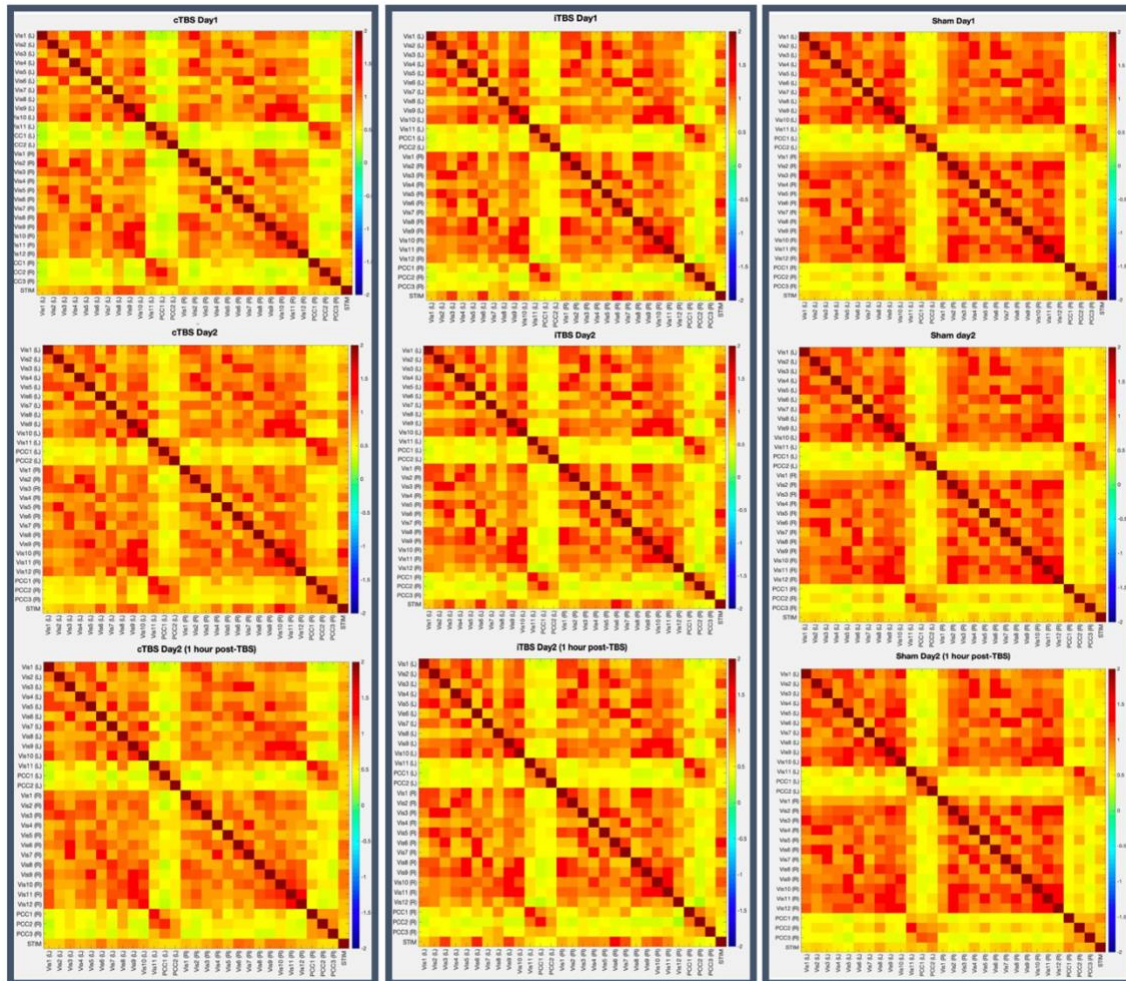
Note. L-SCC = Left supracalcarine cortex, Stim = Stimulation target

#### 2.4.4 Surface-based ROI-to-ROI analysis using GPIP parcellation

*Whole brain FC:* There were no significant differences in whole brain functional connectivity pre-and post-stimulation (FWER-corrected p-values of  $< 0.05$ ). See Figure 6 for connectivity matrices.

*ROI-to-ROI & seed-to-target:* There were no significant differences in functional connectivity for ROI-to-ROI and seed-to-target pre- to post-stimulation (FDR-corrected p-value  $< 0.05$  threshold was used).

**Figure 2-6 :** *Uncorrected connectivity matrices using Fisher Z-transformation of the Pearson correlation coefficient values for each group and timepoint.*



## 2.5 Discussion

In the current study, we determined the effects of TBS to primary visual cortex (V1) on visual cortex-associated FC and phosphene thresholds (PTs). We compared group-level FC across the entire brain and visual networks at three timepoints—baseline, immediately after stimulation and 1 hr following stimulation. Despite employing different analysis methods to explore FC, we found no significant changes in FC pre- to post-TBS. Additionally, we assessed PTs at baseline and 1 hr following TBS and found no changes in cortical excitability levels post-

TBS. Overall, we did not identify any cTBS or iTBS related aftereffects on FC and PTs. These results are consistent with our MRS study of the same cohort using the same experimental design, where cTBS and iTBS did not alter the concentration levels of GABA and glutamate at the stimulation site (see Stoby et al., 2022).

The fact that a single session of cTBS and iTBS had no effect on FC does not refute the efficacy of TBS to V1, however, it may very well highlight the challenges in determining the optimal stimulation dosage for the use of TBS to modulate FC associated with the visual cortex in clinical settings. The transient effects of traditional TMS protocols to visual regions of the brain have been reported for years (Ganaden et al., 2013; Mullin & Steeves, 2013; Solomon-Harris et al., 2016). In addition, our previous TMS-fMRI study at visual cortex using a low frequency (1Hz) rTMS paradigm (with similar methodology) found widespread FC changes 1 hr following a single session of rTMS (Rafique & Steeves, 2022). These contrasting findings may suggest that TBS is not a suitable replacement for traditional rTMS when stimulating V1 since it does not yield equivalent effects. It may be that the shorter TBS stimulation time is insufficient to reach optimal thresholds required to disturb synaptic equilibrium and neuronal status quo in order to detect TBS aftereffects with rs-fMRI. One possible mechanism to consider is the differential abilities of TBS and rTMS protocols to entrain oscillations in targeted neural populations. Oscillations have long been studied and implicated as location- and state-dependent neural signatures of the central nervous system (Buzsáki, 2004). Recent literature suggests that stimulation parameters (i.e., oscillations resembling specific brain rhythms) closer to the specific intrinsic oscillatory patterns of the stimulated location can lead to entrainment and therefore more effective stimulation outcomes (Lin et al., 2021; Okazaki et al., 2021; Thut

et al., 2011). For instance, previous studies using electro- and magneto-encephalography have shown that during memory and motor sequence learning tasks theta oscillations (~ 6-7 Hz) are the predominant recorded oscillations at the scalp electrodes closest to hippocampus and motor cortex (Meissner et al., 2018; Tesche & Karhu, 2000). Execution of already mastered motor tasks, however, is correlated with beta oscillations (~ 13-30 Hz) recorded at motor cortex (Baker, 2007; Pfurtscheller & Lopes da Silva, 1999). In addition, gamma oscillations (~ 30-50 Hz) have been recorded during high-order cognitive tasks in temporal and frontal brain regions (Buzsáki & Wang, 2012; Singh et al., 2020), and intrinsic occipital alpha oscillations (~ 8-12 Hz) have been linked to the perception of incoming visual stimuli (e.g., eyes open and closed) and attending to such inputs (Ergenoglu et al., 2004). TMS studies in V1 have been able to validate the notion of synchronicity between TMS and intrinsic brain rhythms by entraining occipital alpha oscillations via a 10 Hz rTMS protocol (Lin et al., 2021; Romei et al., 2010). Theta oscillations, however, were the basic elements upon which TBS protocols have been developed (Larson et al., 1986), and as theta oscillations are mainly recorded in frontal and motor regions, TBS may better target and manipulate M1 and frontal regions. Therefore, such oscillatory properties may also explain the efficacy of cTBS and iTBS in motor and frontal cortices but not in V1.

Our finding that a single session of TBS to V1 at 80% PT did not produce measurable effects in rs-fMRI is consistent with a study by Rahnev and colleagues (2013) where cTBS, iTBS and sham TBS were applied to the scalps of five subjects at V1 using a stimulation intensity of 80% PT followed by rs-fMRI. They also found that iTBS did not have a significant effect on FC, they did, however, find a significant decrease in FC between retinotopically defined early visual

areas (i.e., V1, V2 and V3) following cTBS. Similarly, others have observed no change in PTs following iTBS but a reduction in PTs measured 2 min post-cTBS (80% MT, 600 pulses; Franca et al., 2006). Other TBS studies, however, have adopted different dosing strategies using lower intensities and increased pulse numbers. For example, when cTBS targeted the right occipital face area and the posterior superior temporal sulcus (pSTS) at 80% active MT (or 30% maximum stimulator output; whichever was greater) delivering 900 pulses, cTBS reduced BOLD signal in face selective areas (Pitcher et al., 2014) and reduced FC between pSTS and amygdala (Pitcher et al., 2014, 2017). Other studies using the same low intensity and high number of pulses as the stimulation parameters demonstrated that cTBS reduced FC between pSTS and other vision and non-vision ROIs (Handwerker et al., 2020) and reduced BOLD signal in the occipital place area (Groen et al., 2021). This stimulation protocol may support the efficacy of cTBS in yielding inhibitory effects in visual areas, however, other TBS studies such as Abuleil et al., (2020) have shown that cTBS to V1 increases mixed percepts during binocular rivalry (excitatory effect).

Occipital TBS studies have used a variety of dosing strategies ranging from lower intensities to increased pulse numbers, and despite clear anatomical and functional distinctions between M1 and V1 (Shinomoto et al., 2009) a number of studies utilised active MTs to determine optimal TBS intensities. Previously, four studies had compared MTs (resting and active) and PTs and concluded that these two measures are not correlated, and that PTs are the most accurate measure of cortical excitability in the occipital cortex and MTs should not be utilised for non-motor TMS targets (Antal et al., 2003; Boroojerdi et al., 2002; Gerwig et al., 2003; Stewart et al., 2001). Nevertheless, Deblieck and colleagues (2008) demonstrated a significant correlation between active MTs and PTs, and the notion of a universal cortical

excitability value (based on MTs) appears to dominate TBS research in frontal, parietal and temporal regions and to some extent in the occipital visual areas (Stokes et al., 2013). However, it remains unclear whether the two thresholds (MT and PT) are comparable measures of cortical excitability, given the design and methodological limitations of MT-PT studies, and the anatomical and functional differences between M1 and V1. It is therefore plausible to speculate that whether the individual cortical excitability in V1 is measured via MTs or PTs, subthreshold intensities and increased pulse number may play a role in cTBS outcomes (Groen et al., 2021; Handwerker et al., 2020; Pitcher et al., 2014, 2017). Knowing that on average MTs are lower than PTs (Boroojerdi et al., 2002), a 30% MT translates into a much lower stimulation intensity than intensities delivered at 80% PT. As a result, in comparison to other occipital TBS studies (using 80% PT intensity such as Franca et al., 2006 and Rahnev et al., 2013), these intensities are considered sub-threshold.

Modifying the number of pulses in a stimulation protocol also can modulate TBS effects. The respective inhibitory and excitatory effects of cTBS and iTBS in M1 first observed by Huang and colleagues (2005) are reversed by doubling the number of pulses. At 1200 pulses for example, cTBS increased MEP amplitudes while iTBS lowered MEP amplitudes (Gamboa et al., 2010). It is possible that the 900-pulse protocol (e.g., Pitcher et al., 2014, 2017) allows for an increased pulse delivery without reversing the inhibitory effects of cTBS when targeting visual networks. However, at the moment, comparison studies examining different TBS parameters in occipital regions are lacking, and despite a vast literature exploring pulse numbers, sub- and supra-threshold stimulation intensities, and accelerated TBS protocols in frontal lobes (Chen et al., 2021; Lee et al., 2021; McCalley et al., 2021) only one occipital TBS study has examined the

effects of TBS intensities on visual perception (and not on PTs). When cTBS and iTBS were applied to V1 using stimulation intensities of 60, 80, 100 and 120% PT, both cTBS and iTBS had no effect on peripheral visual acuity at any of the intensity levels (Brückner & Kammer, 2014).

In addition to the variability of TBS parameters, outcome variability in TBS research may be modulated by a high individual variability in stimulation responsiveness (McCalley et al., 2021; Young-Bernier et al., 2014), leading to a statistical net-zero effect when subjects with variable responses to cTBS or iTBS are pooled in a group and outcome measures are averaged. In the present study, we also observed this pattern of variability in our FC analyses in both the cTBS and iTBS groups. To mitigate the effects of individual variability on stimulation outcomes, Ridding & Ziemann (2010) had previously identified a list of contributing factors influencing TMS outcomes. Factors such as diurnal cortisol levels, age, attention, synaptic history (pharmacological agents, and prior stimulation), and genetics were all identified to affect the stimulation outcomes to varying degrees. Although many studies including our current study have controlled for these factors, genetic variations also seem to play an important role in neural response to stimulation (Cheeran et al., 2008). Brain-derived neurotrophic factor (BDNF) is a protein that reportedly is involved in LTP and LTD processes. It is speculated that BDNF directly affects the susceptibility of synapses to undergo plasticity and change in response to learning and stimulation (Lu, 2003). Genetic polymorphism in BDNF expression factors such as the heterozygous genotype “val66met” has been linked to decreased response to non-invasive brain stimulation protocols at M1 unlike homozygous Met/Met and Val/Val carriers (Cheeran et al., 2008; Fritsch et al., 2010; Guerra et al., 2020).

In summary, our findings show no effects of cTBS or iTBS to V1 on FC across visual networks nor any effects on PTs. These findings, together with the paucity of research on TBS to V1 and the heterogeneity of protocols used in other visual regions suggest that further research is needed to refine the protocols for optimal TBS dosage in visual networks. This is especially important because the traditional rTMS studies showing lasting aftereffects generally used much longer stimulation duration, while TBS protocols have a much shorter stimulation duration. Despite the fact that multiple studies have implied the comparability of iTBS and 10 Hz rTMS in major depressive disorders (Blumberger et al., 2018) as well as cTBS and 1 Hz rTMS in fronto-parietal regions (Tupak et al., 2011; Yu-Lei et al., 2022), such comparisons have yet to be determined in TBS to V1 or occipital cortex more broadly.

While our study did not reveal any significant effects of cTBS and iTBS to V1 in healthy individuals, the potential of non-invasive brain stimulation to improve therapeutic outcomes in patients with neurological visual disorders is still a promising area of research. Our findings contribute to the growing body of literature in this field. Reporting null findings can be informative in designing future studies as it helps to rule out alternative hypotheses and refines our understanding of different TBS protocols and methodologies. Furthermore, our study underscores the need for further investigation into optimal TBS dosage by studying different stimulation parameters. As discussed in detail earlier in this section, it is crucial to study the root cause of interindividual variability in TBS outcomes by examining response variations in healthy subjects, while considering factors such as BDNF expression and the neural entrainment properties of different rTMS protocols at specific target locations. We believe that combining

insights from a growing number of TBS studies in visual brain areas, regardless of their outcomes, will open exciting avenues of research in the near future.

## 2.6 Limitations and future directions

In the present study, measuring PTs immediately after TBS could not have been achieved, mainly due to rs-fMRI timepoints (immediately and 1 hr post-TBS). Determining PTs requires stimulation, which would have prevented us from measuring the true aftereffects of TBS on resting state networks at 1 hr. We therefore opted for measuring PTs at 1 hr (after the last rs-fMRI scan). Despite this limitation, however, these results could be taken into consideration when designing future experiments. On the one hand the PT results could be interpreted as the evidence that TBS cannot modify PTs when measured 1 hr after stimulation. On the other hand, this may suggest that if cTBS or iTBS are capable of inducing directional changes to PTs, these effects wear off after 1 hr and thresholds return to baseline. This could indicate that experiments utilising within-subjects designs can consider using this 1 hr cut off when determining optimal “rest periods” required for participants undergoing multi-session TBS protocols (e.g., comparison studies).

As we highlighted in the discussion, future research should focus on optimisation of TBS protocols in V1 by designing studies that compare the ability of different TBS protocols to influence intrinsic oscillatory processes at different brain areas (e.g., M1 vs. V1). Despite a vast number of comparison studies in M1 and non-motor frontal regions, parameters such as pulse number, stimulation intensities, and accelerated TBS protocols should also be explored in V1 while taking covariates such as genetic polymorphism (i.e., BDNF expression factors) and anatomical differences (e.g., scalp to cortex distance and target depth) into account.

## 2.7 Conclusion

In the current study, we demonstrate that the application of cTBS and iTBS to V1 does not modulate resting state FC in focal or remote brain networks when measured immediately and 1 hr post-TBS. PT levels also remain unaffected by cTBS and iTBS when measured 1 hr after stimulation. These results are consistent with our MRS study, where cTBS and iTBS did not alter GABA and glutamate concentration levels (Stoby et al., 2022). Our results are also in line with others who showed iTBS did not modulate FC and PT levels. Our findings show that while cTBS and 1 Hz rTMS may have comparable effects at the motor and frontal cortices (Blumberger et al., 2018; Tupak et al., 2011; Yu-Lei et al., 2022) cTBS to V1 does not have comparable effects to low frequency (1 Hz) rTMS in our previous study (Rafique & Steeves, 2022) .

Our findings suggest that in a clinical setting, a single session of cTBS or iTBS to V1 at 80% PT using a protocol of 600 pulses may not be an effective therapy if targeting FC is the clinical goal.

## **Chapter 3 : General discussion**

### 3.1 Summary

In this thesis, in Chapter 1 we discussed the fundamentals of TMS, reviewed the TBS literature, highlighted the lack of TBS research in V1, and in Chapter 2, we demonstrated empirically that the application of cTBS and iTBS to V1 does not modulate resting state FC in focal or remote brain networks when measured immediately and 1 hour post-TBS. PT levels also remained unaffected by cTBS and iTBS when measured 1 hour after stimulation. These results are in line with others who showed that iTBS does not modulate FC and PT levels., but not with previous data showing effects of cTBS on PT. Our findings indicate that while cTBS and 1 Hz rTMS may have comparable effects on the motor and frontal cortices, cTBS to V1 does not have comparable effects to low frequency (1 Hz) rTMS in our previous study (Rafique & Steeves, 2022). Our findings suggest that a single session of cTBS or iTBS to V1 using conventional TBS parameters (e.g., 600 pulses and 80% PT MSO) may not be an effective protocol if targeting FC is the goal.

As outlined in Chapter 1, both 10 Hz rTMS and iTBS have received FDA approval for treating major depressive disorders. Further, research suggests that the modulatory aftereffects of 10Hz rTMS and iTBS are comparable; however, while a 10 Hz rTMS session can last up to thirty minutes, an iTBS session takes less than three minutes. This efficiency has significant implications for research and clinical settings. In addition, TMS protocols for other neuropsychiatric conditions (such as obsessive-compulsive disorder and addiction) and neurorehabilitation (including stroke and movement disorders) are currently being developed. A common theme among these neuropathologies is the presence of suboptimal neural networks (Boon et al., 2020; Hou et al., 2014; Larivière et al., 2018; Rao et al., 2022), and rTMS

may have potential for modulating functional connectivity and guide processing in these networks towards optimal levels.

Considering the similar aetiologies between neuropsychiatric disorders and certain visual disorders with neurological origins—specifically, extensive alterations in the functional connectivity of visual networks (ffytche et al., 1998; Martial et al., 2019; Shi et al., 2022) and the comparable aftereffects of continuous and intermittent TBS with their rTMS counterparts (i.e., 1 Hz and 10 Hz), visual disorders such as blindsight and Charles Bonnet syndrome may benefit from TBS-based interventions. Due to the limited empirical evidence investigating such protocols for visual disorders, we chose to explore TBS in healthy individuals. Our goal was to gain insight into the aftereffects of cTBS and iTBS at the network level, with the motivation of using our findings for potential future studies to determine suitable and efficient research protocols and further investigation in clinical populations.

### **3.2 Limitations and future directions**

While the efficacy of TBS in targeting V1 may vary among individuals, it is important to recognise this as an aspect of “interindividual variability” inherent in TBS research. This concept acknowledges that stimulation aftereffects may differ significantly across individuals, in both healthy and patient populations. Therefore, the potential of TBS should not be underestimated but instead calls for more in-depth investigation of stimulation parameters and responsiveness of different brain regions to such stimulation parameters.

As discussed earlier, various anatomical and physiological differences between individuals can hinder the ability of cTBS and iTBS to perturb neural networks. Whether the goal of stimulation is inhibition or facilitation, a variety of contributing factors need to be identified

and controlled for. However, studies that aim to identify and control for these factors are currently lacking. The next few sections will cover important factors that could improve and optimise TBS protocols in V1.

### 3.2.1 TBS in V1 vs. Other brain areas

We discussed the origin story of TBS in Chapter 1, Huang and colleagues (2005) applied cTBS and iTBS to M1 and measured aftereffects using MEPs, and their results indicated that iTBS facilitates and cTBS inhibits MEPs. There are, however, multiple factors to be considered when TBS is applied to non-motor brain regions. Although Hubel and Weisel (1962) discovered the functional organisation of cortical columns in V1, there is no consensus as to what role these cortical columns play in other brain areas, and therefore any comparisons between the two regions require careful consideration. For instance, we know that V1 is a somatosensory cortex featuring a dense input layer (layer IV) within its cortical columns, while M1 possesses considerably thicker output layers (layers V and VI) in its cortical columns (Hubel & Wiesel, 1963; Mountcastle, 1957). Consequently, optimal stimulation parameters for one area may not necessarily be ideal for other regions (Stokes et al., 2013).

In future research, it is essential to address these uncertainties empirically through comparative studies. The seminal TBS study by Larson and colleagues (1986) conducted on a mouse model, using single-cell recordings from the hippocampal CA1 neurons was the stepping stone for the development of current TBS protocols targeting other brain regions. With advancements in neurophysiological methods, it is possible now to use in vivo multi-array electrodes for laminar recordings. This method can be applied in animal models, targeting V1 and M1. Other in vivo options would be to compare the effects of cTBS and iTBS noninvasively

by measuring MTs and PTs or rs-fMRI to compare the differential effects of TBS in different cortical regions using within-subjects designs.

### 3.2.2 Neurodiversity and State-dependency

In addition to the anatomical and physiological variability among different cortical regions, in Chapter 2, we also delved into the role of intrinsic oscillatory brain rhythms and the entrainment properties of various rTMS protocols in different cortical areas. TBS was developed based on Hebbian principles, such as "neurons that fire together, wire together," and the evidence regarding the role of theta oscillations in memory storage and plasticity, which stemmed from research on hippocampal CA1 neurons (Larson et al., 1986; Larson & Munkácsy, 2015). Consequently, it is reasonable to speculate that the intrinsic oscillatory properties involved in different cortical regions may serve as markers of specific brain states, implying that successful TMS protocols should target different regions at distinct frequencies.

However, recent studies suggest that these oscillations may not necessarily be unique to a particular cortical area but rather indicative of a specific state (Baker, 2007; Buzsáki, 2004; Cha et al., 2019; Lin et al., 2021). Almost a century ago, Hans Berger's studies, for example, demonstrated that alpha power increases when an individual enters a state of mind-wandering (Adrian & Matthews, 1934; Berger, 1929). In contrast, beta oscillations increase during effortful motor learning and decrease when performing a mastered motor task (Cohan et al., 2019; Quandt et al., 2019). Theta and gamma oscillations have also been associated with cognitive and memory tasks (Buzsáki & Wang, 2012; Guerra et al., 2020; Larson & Munkácsy, 2015). State-dependency in TMS studies, therefore, emphasises the importance of considering the participant's current mental state when designing and interpreting TMS studies, as the same

stimulation parameters may yield different outcomes depending on the participant's cognitive state (Kearney-Ramos et al., 2019; Silvanto et al., 2018; Silvanto & Pascual-Leone, 2008). This highlights the need for a more tailored approach to TMS protocols, one that accounts for individual differences in brain rhythms and cognitive states to optimise the effects of brain stimulation. There is no easy solution to account for such state variabilities. Rigorous behavioural and cognitive assessments to stratify participants, and controlling for age, neurological disorders, and medications, have not been able to reduce variability. In recent years however, by combining EEG and TMS, researchers have been able to identify optimal stimulation intensities (Schaworonkow et al., 2019). In such settings, optimal TMS parameters are determined after acquiring baseline rhythmic profile at each target region. Stimulation is then delivered, taking phase and amplitude of the intrinsic oscillations into account (Glim et al., 2019). Concurrent TMS-EEG studies have shown the efficacy of this phase-amplitude coupling of the TMS and stimulation targets by modulating focal and distant neural networks (Desideri et al., 2019; Glim et al., 2019; Okazaki et al., 2021). Nevertheless, it is worth noting that concurrent TMS-EEG techniques are demanding and laborious and perhaps future research also needs to focus on creating more mainstream protocols (for examples in motor cortex and speech networks see: Daffertshofer & van Wijk, 2011; Mostame & Sadaghiani, 2020; van Wijk et al., 2012).

### 3.2.3 Experimental design

In the current study, we utilised a between-subject experimental design. While the between-subject setup remains the gold standard for demonstrating the efficacy of treatment interventions including different rTMS protocols, the individual variability across participants

highlights a key limitation. Therefore, there may be significant value in incorporating within-subject designs into TMS studies. This design allows each participant to serve as their own control, thus reducing the confounding impact of individual differences in neuroanatomy, neurophysiology, and psychological profile (Evans, 2010; Harita et al., 2022). This can lead to a more accurate representation of the effects of different TMS protocols as outcomes are less likely influenced by inherent inter-subject differences. Additionally, the within-subject design increases statistical power and often requires a smaller sample size compared to between-subject designs, making it more efficient and cost-effective (Evans, 2010; Yamasaki et al., 2018). It is essential, however, to remain cognisant of the potential challenges associated with within-subject designs, such as carry-over effects and time-related changes or attrition. Nevertheless, with careful experimental design and rigorous controls, these can be effectively managed, and perhaps future studies using similar methodologies used in our current study could potentially reveal the modulatory effects of cTBS and iTBS on neural networks.

### **3.3 Final thoughts**

In reflecting upon our study, it is important to note that the absence of significant effects when applying cTBS and iTBS to V1 in healthy individuals does not undermine the broader relevance of non-invasive brain stimulation. These techniques still hold considerable promise for neurological visual disorders. As science often builds upon both breakthroughs and roadblocks, our null findings serve an essential role. They guide future researchers by pinpointing areas of potential refinement and drawing attention to the nuances of TBS protocols and methodologies. As the field expands, such insights, even from studies yielding null results, will be pivotal in optimising therapeutic interventions and furthering our collective

understanding. Earlier in our discussion, we emphasised the importance of identifying the underlying causes of variability in TBS responses. To do this effectively, it's crucial to analyse the responses of healthy individuals while accounting for elements like genetic polymorphism and the specific interactions of different rTMS protocols with targeted neural populations. We believe that integrating the findings from various TBS studies on the visual cortex, irrespective of their outcomes, will prove beneficial in guiding future research.

## 4 References

- Abraham, W. C., & Bear, M. F. (1996). Metaplasticity: The plasticity of synaptic plasticity. *Trends in Neurosciences*, *19*(4), 126–130. [https://doi.org/10.1016/s0166-2236\(96\)80018-x](https://doi.org/10.1016/s0166-2236(96)80018-x)
- Adrian, E. D., & Mathews, B. H. C. (1934). The Berger rhythm: Potential changes from the occipital lobes in man. *Brain*, *57*(4), 355–385. <https://doi.org/10.1093/brain/57.4.355>
- Afifi, A. K. (2003). The basal ganglia: A neural network with more than motor function. *Seminars in Pediatric Neurology*, *10*(1), 3–10. [https://doi.org/10.1016/s1071-9091\(02\)00003-7](https://doi.org/10.1016/s1071-9091(02)00003-7)
- Alves, P. N., Foulon, C., Karolis, V., Bzdok, D., Margulies, D. S., Volle, E., & Thiebaut de Schotten, M. (2019). An improved neuroanatomical model of the default-mode network reconciles previous neuroimaging and neuropathological findings. *Communications Biology*, *2*(1), Article 1. <https://doi.org/10.1038/s42003-019-0611-3>
- Andoh, J., Matsushita, R., & Zatorre, R. J. (2015). Asymmetric Interhemispheric Transfer in the Auditory Network: Evidence from TMS, Resting-State fMRI, and Diffusion Imaging. *The Journal of Neuroscience*, *35*(43), 14602–14611. <https://doi.org/10.1523/JNEUROSCI.2333-15.2015>
- Andrade, A., Kherif, F., Mangin, J. F., Worsley, K. J., Paradis, A. L., Simon, O., Dehaene, S., Le Bihan, D., & Poline, J. B. (2001). Detection of fMRI activation using cortical surface mapping. *Human Brain Mapping*, *12*(2), 79–93. [https://doi.org/10.1002/1097-0193\(200102\)12:2<79::aid-hbm1005>3.0.co;2-i](https://doi.org/10.1002/1097-0193(200102)12:2<79::aid-hbm1005>3.0.co;2-i)
- Antal, A., Kincses, T. Z., Nitsche, M. A., & Paulus, W. (2003). Manipulation of phosphene thresholds by transcranial direct current stimulation in man. *Experimental Brain Research*, *150*(3), 375–378. <https://doi.org/10.1007/s00221-003-1459-8>

- Ashburner, J., & Friston, K. J. (2005). Unified segmentation. *NeuroImage*, *26*(3), 839–851.  
<https://doi.org/10.1016/j.neuroimage.2005.02.018>
- Auffret, A., Gautheron, V., Mattson, M. P., Mariani, J., & Rovira, C. (2010). Progressive Age-Related Impairment of the Late Long-Term Potentiation in Alzheimer's Disease Presenilin-1 Mutant Knock-in Mice. *Journal of Alzheimer's Disease : JAD*, *19*(3), 1021–1033. <https://doi.org/10.3233/JAD-2010-1302>
- Bai, Z., Zhang, J., & Fong, K. N. K. (2022). Effects of transcranial magnetic stimulation in modulating cortical excitability in patients with stroke: A systematic review and meta-analysis. *Journal of NeuroEngineering and Rehabilitation*, *19*(1), 24.  
<https://doi.org/10.1186/s12984-022-00999-4>
- Baker, S. N. (2007). Oscillatory interactions between sensorimotor cortex and the periphery. *Current Opinion in Neurobiology*, *17*(6), 649–655.  
<https://doi.org/10.1016/j.conb.2008.01.007>
- Balderston, N. L., Beer, J. C., Seok, D., Makhoul, W., Deng, Z.-D., Girelli, T., Teferi, M., Smyk, N., Jaskir, M., Oathes, D. J., & Sheline, Y. I. (2022). Proof of concept study to develop a novel connectivity-based electric-field modelling approach for individualized targeting of transcranial magnetic stimulation treatment. *Neuropsychopharmacology*, *47*(2), Article 2. <https://doi.org/10.1038/s41386-021-01110-6>
- Barker, A. T., Jalinous, R., & Freeston, I. L. (1985). Non-invasive magnetic stimulation of human motor cortex. *Lancet (London, England)*, *1*(8437), 1106–1107.  
[https://doi.org/10.1016/s0140-6736\(85\)92413-4](https://doi.org/10.1016/s0140-6736(85)92413-4)

- Behzadi, Y., Restom, K., Liu, J., & Liu, T. T. (2007). A component based noise correction method (CompCor) for BOLD and perfusion based fMRI. *NeuroImage*, *37*(1), 90–101.  
<https://doi.org/10.1016/j.neuroimage.2007.04.042>
- Benjamini, Y., & Hochberg, Y. (1995). Controlling the False Discovery Rate: A Practical and Powerful Approach to Multiple Testing. *Journal of the Royal Statistical Society. Series B (Methodological)*, *57*(1), 289–300.
- Berger, H. (1929). Über das Elektrenkephalogramm des Menschen. *Archiv für Psychiatrie und Nervenkrankheiten*, *87*(1), 527–570. <https://doi.org/10.1007/BF01797193>
- Bharath, R. D., Munivenkatappa, A., Gohel, S., Panda, R., Saini, J., Rajeswaran, J., Shukla, D., Bhagavatula, I. D., & Biswal, B. B. (2015). Recovery of resting brain connectivity ensuing mild traumatic brain injury. *Frontiers in Human Neuroscience*, *9*, 513.  
<https://doi.org/10.3389/fnhum.2015.00513>
- Bienenstock, E. L., Cooper, L. N., & Munro, P. W. (1982). Theory for the development of neuron selectivity: Orientation specificity and binocular interaction in visual cortex. *The Journal of Neuroscience*, *2*(1), 32–48.
- Biswal, B., Yetkin, F. Z., Haughton, V. M., & Hyde, J. S. (1995). Functional connectivity in the motor cortex of resting human brain using echo-planar mri. *Magnetic Resonance in Medicine*, *34*(4), 537–541. <https://doi.org/10.1002/mrm.1910340409>
- Blazejewska, A. I., Fischl, B., Wald, L. L., & Polimeni, J. R. (2019). Intracortical smoothing of small-voxel fMRI data can provide increased detection power without spatial resolution losses compared to conventional large-voxel fMRI data. *NeuroImage*, *189*, 601–614.  
<https://doi.org/10.1016/j.neuroimage.2019.01.054>

- Bliss, T. V., & Lomo, T. (1973). Long-lasting potentiation of synaptic transmission in the dentate area of the anaesthetized rabbit following stimulation of the perforant path. *The Journal of Physiology*, 232(2), 331–356. <https://doi.org/10.1113/jphysiol.1973.sp010273>
- Blumberger, D. M., Vila-Rodriguez, F., Thorpe, K. E., Feffer, K., Noda, Y., Giacobbe, P., Knyahnytska, Y., Kennedy, S. H., Lam, R. W., Daskalakis, Z. J., & Downar, J. (2018). Effectiveness of theta burst versus high-frequency repetitive transcranial magnetic stimulation in patients with depression (THREE-D): A randomised non-inferiority trial. *The Lancet*, 391(10131), 1683–1692. [https://doi.org/10.1016/S0140-6736\(18\)30295-2](https://doi.org/10.1016/S0140-6736(18)30295-2)
- Boon, L. I., Hepp, D. H., Douw, L., van Geenen, N., Broeders, T. A. A., Geurts, J. J. G., Berendse, H. W., & Schoonheim, M. M. (2020). Functional connectivity between resting-state networks reflects decline in executive function in Parkinson’s disease: A longitudinal fMRI study. *NeuroImage : Clinical*, 28, 102468. <https://doi.org/10.1016/j.nicl.2020.102468>
- Borojerdi, B., Meister, I. G., Foltys, H., Sparing, R., Cohen, L. G., & Töpper, R. (2002). Visual and motor cortex excitability: A transcranial magnetic stimulation study. *Clinical Neurophysiology*, 113(9), 1501–1504. [https://doi.org/10.1016/s1388-2457\(02\)00198-0](https://doi.org/10.1016/s1388-2457(02)00198-0)
- Borojerdi, B., Prager, A., Muellbacher, W., & Cohen, L. G. (2000a). Reduction of human visual cortex excitability using 1-Hz transcranial magnetic stimulation. *Neurology*, 54(7), 1529–1531. <https://doi.org/10.1212/wnl.54.7.1529>
- Borojerdi, B., Prager, A., Muellbacher, W., & Cohen, L. G. (2000b). Reduction of human visual cortex excitability using 1-Hz transcranial magnetic stimulation. *Neurology*, 54(7), 1529–1531. <https://doi.org/10.1212/WNL.54.7.1529>

- Brodoehl, S., Gaser, C., Dahnke, R., Witte, O. W., & Klingner, C. M. (2020). Surface-based analysis increases the specificity of cortical activation patterns and connectivity results. *Scientific Reports*, *10*(1), Article 1. <https://doi.org/10.1038/s41598-020-62832-z>
- Brückner, S., & Kammer, T. (2015). High visual demand following theta burst stimulation modulates the effect on visual cortex excitability. *Frontiers in Human Neuroscience*, *0*. <https://doi.org/10.3389/fnhum.2015.00591>
- Brückner, S., & Kammer, T. (2016). Modulation of Visual Cortex Excitability by Continuous Theta Burst Stimulation Depends on Coil Type. *PLOS ONE*, *11*(7), e0159743. <https://doi.org/10.1371/journal.pone.0159743>
- Bullmore, E. T., Suckling, J., Overmeyer, S., Rabe-Hesketh, S., Taylor, E., & Brammer, M. J. (1999). Global, voxel, and cluster tests, by theory and permutation, for a difference between two groups of structural MR images of the brain. *IEEE Transactions on Medical Imaging*, *18*(1), 32–42. <https://doi.org/10.1109/42.750253>
- Buzsáki, G. (2004). Large-scale recording of neuronal ensembles. *Nature Neuroscience*, *7*(5), Article 5. <https://doi.org/10.1038/nn1233>
- Buzsáki, G., & Wang, X.-J. (2012). Mechanisms of Gamma Oscillations. *Annual Review of Neuroscience*, *35*, 203–225. <https://doi.org/10.1146/annurev-neuro-062111-150444>
- Caparelli, E., Backus, W., Telang, F., Wang, G., Maloney, T., Goldstein, R., & Henn, F. (2012). Is 1 Hz rTMS Always Inhibitory in Healthy Individuals? *The Open Neuroimaging Journal*, *6*, 69–74. <https://doi.org/10.2174/1874440001206010069>
- Cecchetti, G., Agosta, F., Basaia, S., Cividini, C., Corsi, M., Santangelo, R., Caso, F., Minicucci, F., Magnani, G., & Filippi, M. (2021). Resting-state electroencephalographic biomarkers of

Alzheimer's disease. *NeuroImage: Clinical*, 31, 102711.

<https://doi.org/10.1016/j.nicl.2021.102711>

Cha, Y.-H., Gleghorn, D., & Doudican, B. (2019). Occipital and Cerebellar Theta Burst Stimulation for Mal De Debarquement Syndrome. *Otology & Neurotology*, 40(9), e928–e937.

<https://doi.org/10.1097/MAO.0000000000002341>

Chai, Z., Ma, C., & Jin, X. (2019). Cortical stimulation for treatment of neurological disorders of hyperexcitability: A role of homeostatic plasticity. *Neural Regeneration Research*, 14(1), 34–38. <https://doi.org/10.4103/1673-5374.243696>

Chang, C., & Glover, G. H. (2009). Effects of model-based physiological noise correction on default mode network anti-correlations and correlations. *NeuroImage*, 47(4), 1448–1459. <https://doi.org/10.1016/j.neuroimage.2009.05.012>

Cheeran, B., Talelli, P., Mori, F., Koch, G., Suppa, A., Edwards, M., Houlden, H., Bhatia, K., Greenwood, R., & Rothwell, J. C. (2008). A common polymorphism in the brain-derived neurotrophic factor gene (BDNF) modulates human cortical plasticity and the response to rTMS. *The Journal of Physiology*, 586(23), 5717–5725.

<https://doi.org/10.1113/jphysiol.2008.159905>

Chen, A. C., Oathes, D. J., Chang, C., Bradley, T., Zhou, Z.-W., Williams, L. M., Glover, G. H., Deisseroth, K., & Etkin, A. (2013). Causal interactions between fronto-parietal central executive and default-mode networks in humans. *Proceedings of the National Academy of Sciences*, 110(49), 19944–19949. <https://doi.org/10.1073/pnas.1311772110>

Chen, L., Thomas, E. H. X., Kaewpijit, P., Miljevic, A., Hughes, R., Hahn, L., Kato, Y., Gill, S., Clarke, P., Ng, F., Paterson, T., Giam, A., Sarma, S., Hoy, K. E., Galletly, C., & Fitzgerald, P.

- B. (2021). Accelerated theta burst stimulation for the treatment of depression: A randomised controlled trial. *Brain Stimulation: Basic, Translational, and Clinical Research in Neuromodulation*, 14(5), 1095–1105.  
<https://doi.org/10.1016/j.brs.2021.07.018>
- Cheyne, J. E., & Montgomery, J. M. (2020). The cellular and molecular basis of in vivo synaptic plasticity in rodents. *American Journal of Physiology. Cell Physiology*, 318(6), C1264–C1283. <https://doi.org/10.1152/ajpcell.00416.2019>
- Chong, M., Bhushan, C., Joshi, A. A., Choi, S., Haldar, J. P., Shattuck, D. W., Spreng, R. N., & Leahy, R. M. (2017). Individual Parcellation of Resting fMRI with a Group Functional Connectivity Prior. *NeuroImage*, 156, 87–100.  
<https://doi.org/10.1016/j.neuroimage.2017.04.054>
- Citri, A., & Malenka, R. C. (2008). Synaptic Plasticity: Multiple Forms, Functions, and Mechanisms. *Neuropsychopharmacology*, 33(1), Article 1.  
<https://doi.org/10.1038/sj.npp.1301559>
- Cocchi, L., Sale, M. V., Lord, A., Zalesky, A., Breakspear, M., & Mattingley, J. B. (2015). Dissociable effects of local inhibitory and excitatory theta-burst stimulation on large-scale brain dynamics. *Journal of Neurophysiology*, 113(9), 3375–3385.  
<https://doi.org/10.1152/jn.00850.2014>
- Cohan, R., Bearss, K. A., & DeSouza, J. F. X. (2019). Frequency-Specific Biomarkers in Neurodegenerative Disorders: Implications of Alpha and Beta Oscillations in Motor Behaviour. *Journal of Neurology & Neuromedicine*, 4(3).  
<https://www.jneurology.com/articles/frequencyspecific-biomarkers-in->

neurodegenerative-disorders-implications-of-alpha-and-beta-oscillations-in-motor-behaviour.html

- Cole, E. J., Stimpson, K. H., Bentzley, B. S., Gulser, M., Cherian, K., Tischler, C., Nejad, R., Pankow, H., Choi, E., Aaron, H., Espil, F. M., Pannu, J., Xiao, X., Duvio, D., Solvason, H. B., Hawkins, J., Guerra, A., Jo, B., Raj, K. S., ... Williams, N. R. (2020). Stanford Accelerated Intelligent Neuromodulation Therapy for Treatment-Resistant Depression. *American Journal of Psychiatry*, *177*(8), 716–726. <https://doi.org/10.1176/appi.ajp.2019.19070720>
- Constable, R. T., McCarthy, G., Allison, T., Anderson, A. W., & Gore, J. C. (1993). Functional brain imaging at 1.5 T using conventional gradient echo MR imaging techniques. *Magnetic Resonance Imaging*, *11*(4), 451–459. [https://doi.org/10.1016/0730-725x\(93\)90463-n](https://doi.org/10.1016/0730-725x(93)90463-n)
- Cooper, L. N., & Bear, M. F. (2012). The BCM theory of synapse modification at 30: Interaction of theory with experiment. *Nature Reviews Neuroscience*, *13*(11), Article 11. <https://doi.org/10.1038/nrn3353>
- Cox, R. W., & Hyde, J. S. (1997). Software tools for analysis and visualization of fMRI data. *NMR in Biomedicine*, *10*(4–5), 171–178. [https://doi.org/10.1002/\(sici\)1099-1492\(199706/08\)10:4/5<171::aid-nbm453>3.0.co;2-l](https://doi.org/10.1002/(sici)1099-1492(199706/08)10:4/5<171::aid-nbm453>3.0.co;2-l)
- Cox, T. M., & ffytche, D. H. (2014). Negative outcome Charles Bonnet Syndrome. *British Journal of Ophthalmology*, *98*(9), 1236–1239. <https://doi.org/10.1136/bjophthalmol-2014-304920>
- Craddock, R. C., Tungaraza, R. L., & Milham, M. P. (2015). Connectomics and new approaches for analyzing human brain functional connectivity. *GigaScience*, *4*, 13. <https://doi.org/10.1186/s13742-015-0045-x>

- Curtin, A., Tong, S., Sun, J., Wang, J., Onaral, B., & Ayaz, H. (2019). A Systematic Review of Integrated Functional Near-Infrared Spectroscopy (fNIRS) and Transcranial Magnetic Stimulation (TMS) Studies. *Frontiers in Neuroscience, 13*.  
<https://www.frontiersin.org/articles/10.3389/fnins.2019.00084>
- Curtis, D. R., & Watkins, J. C. (1960). The excitation and depression of spinal neurones by structurally related amino acids. *Journal of Neurochemistry, 6*, 117–141.  
<https://doi.org/10.1111/j.1471-4159.1960.tb13458.x>
- Daffertshofer, A., & van Wijk, B. (2011). On the Influence of Amplitude on the Connectivity between Phases. *Frontiers in Neuroinformatics, 5*.  
<https://www.frontiersin.org/articles/10.3389/fninf.2011.00006>
- Damadian, R., Zaner, K., Hor, D., & DiMaio, T. (1974). Human tumors detected by nuclear magnetic resonance. *Proceedings of the National Academy of Sciences of the United States of America, 71*(4), 1471–1473. <https://doi.org/10.1073/pnas.71.4.1471>
- Damoiseaux, J. S., Rombouts, S. a. R. B., Barkhof, F., Scheltens, P., Stam, C. J., Smith, S. M., & Beckmann, C. F. (2006). Consistent resting-state networks across healthy subjects. *Proceedings of the National Academy of Sciences of the United States of America, 103*(37), 13848–13853. <https://doi.org/10.1073/pnas.0601417103>
- Day, B. L., Dressler, D., Maertens de Noordhout, A., Marsden, C. D., Nakashima, K., Rothwell, J. C., & Thompson, P. D. (1989). Electric and magnetic stimulation of human motor cortex: Surface EMG and single motor unit responses. *The Journal of Physiology, 412*, 449–473.  
<https://doi.org/10.1113/jphysiol.1989.sp017626>

- de Wandel, L., Pulopulos, M. M., Labanauskas, V., de Witte, S., Vanderhasselt, M.-A., & Baeken, C. (2020). Individual resting-state frontocingular functional connectivity predicts the intermittent theta burst stimulation response to stress in healthy female volunteers. *Human Brain Mapping, 41*(18), 5301–5312. <https://doi.org/10.1002/hbm.25193>
- Deblieck, C., Thompson, B., Iacoboni, M., & Wu, A. D. (2007). Correlation between motor and phosphene thresholds: A transcranial magnetic stimulation study. *Human Brain Mapping, 29*(6), 662–670. <https://doi.org/10.1002/hbm.20427>
- Desideri, D., Zrenner, C., Ziemann, U., & Belardinelli, P. (2019). Phase of sensorimotor  $\mu$ -oscillation modulates cortical responses to transcranial magnetic stimulation of the human motor cortex. *The Journal of Physiology, 597*(23), 5671–5686. <https://doi.org/10.1113/JP278638>
- Desikan, R. S., Ségonne, F., Fischl, B., Quinn, B. T., Dickerson, B. C., Blacker, D., Buckner, R. L., Dale, A. M., Maguire, R. P., Hyman, B. T., Albert, M. S., & Killiany, R. J. (2006). An automated labeling system for subdividing the human cerebral cortex on MRI scans into gyral based regions of interest. *NeuroImage, 31*(3), 968–980. <https://doi.org/10.1016/j.neuroimage.2006.01.021>
- Di Lazzaro, V., Dileone, M., Pilato, F., Capone, F., Musumeci, G., Ranieri, F., Ricci, V., Bria, P., Di Iorio, R., de Waure, C., Pasqualetti, P., & Profice, P. (2011). Modulation of motor cortex neuronal networks by rTMS: Comparison of local and remote effects of six different protocols of stimulation. *Journal of Neurophysiology, 105*(5), 2150–2156. <https://doi.org/10.1152/jn.00781.2010>

- Dipasquale, O., Sethi, A., Laganà, M. M., Baglio, F., Baselli, G., Kundu, P., Harrison, N. A., & Cercignani, M. (2017). Comparing resting state fMRI de-noising approaches using multi- and single-echo acquisitions. *PLoS ONE*, *12*(3), e0173289.  
<https://doi.org/10.1371/journal.pone.0173289>
- Dombrowe, I., Juravle, G., Alavash, M., Gießing, C., & Hilgetag, C. C. (2015). The Effect of 10 Hz Repetitive Transcranial Magnetic Stimulation of Posterior Parietal Cortex on Visual Attention. *PLoS ONE*, *10*(5), e0126802. <https://doi.org/10.1371/journal.pone.0126802>
- Dunkley, B. T., Urban, K., Da Costa, L., Wong, S. M., Pang, E. W., & Taylor, M. J. (2018). Default Mode Network Oscillatory Coupling Is Increased Following Concussion. *Frontiers in Neurology*, *9*. <https://doi.org/10.3389/fneur.2018.00280>
- Eklund, A., Nichols, T. E., & Knutsson, H. (2016). Cluster failure: Why fMRI inferences for spatial extent have inflated false-positive rates. *Proceedings of the National Academy of Sciences*, *113*(28), 7900–7905. <https://doi.org/10.1073/pnas.1602413113>
- Elkin-Frankston, S., Fried, P. J., Pascual-Leone, A., Rushmore III, R. J., & Valero-Cabré, A. (2010). A Novel Approach for Documenting Phosphenes Induced by Transcranial Magnetic Stimulation. *Journal of Visualized Experiments : JoVE*, *38*, 1762.  
<https://doi.org/10.3791/1762>
- Ergenoglu, T., Demiralp, T., Bayraktaroglu, Z., Ergen, M., Beydagi, H., & Uresin, Y. (2004). Alpha rhythm of the EEG modulates visual detection performance in humans. *Brain Research. Cognitive Brain Research*, *20*(3), 376–383.  
<https://doi.org/10.1016/j.cogbrainres.2004.03.009>

- Evans, S. R. (2010). Fundamentals of clinical trial design. *Journal of Experimental Stroke & Translational Medicine*, 3(1), 19–27.
- ffytche, D. H., Howard, R. J., Brammer, M. J., David, A., Woodruff, P., & Williams, S. (1998). The anatomy of conscious vision: An fMRI study of visual hallucinations. *Nature Neuroscience*, 1(8), Article 8. <https://doi.org/10.1038/3738>
- Fischl, B., Sereno, M. I., Tootell, R. B., & Dale, A. M. (1999). High-resolution intersubject averaging and a coordinate system for the cortical surface. *Human Brain Mapping*, 8(4), 272–284. [https://doi.org/10.1002/\(sici\)1097-0193\(1999\)8:4<272::aid-hbm10>3.0.co;2-4](https://doi.org/10.1002/(sici)1097-0193(1999)8:4<272::aid-hbm10>3.0.co;2-4)
- Fox, M. D., Halko, M. A., Eldaief, M. C., & Pascual-Leone, A. (2012). Measuring and manipulating brain connectivity with resting state functional connectivity magnetic resonance imaging (fcMRI) and transcranial magnetic stimulation (TMS). *NeuroImage*, 62(4), 2232–2243. <https://doi.org/10.1016/j.neuroimage.2012.03.035>
- Fox, M. D., Snyder, A. Z., Vincent, J. L., Corbetta, M., Van Essen, D. C., & Raichle, M. E. (2005). The human brain is intrinsically organized into dynamic, anticorrelated functional networks. *Proceedings of the National Academy of Sciences of the United States of America*, 102(27), 9673–9678. <https://doi.org/10.1073/pnas.0504136102>
- Franca, M., Koch, G., Mochizuki, H., Huang, Y.-Z., & Rothwell, J. C. (2006a). Effects of theta burst stimulation protocols on phosphene threshold. *Clinical Neurophysiology*, 117(8), 1808–1813. <https://doi.org/10.1016/j.clinph.2006.03.019>
- Franca, M., Koch, G., Mochizuki, H., Huang, Y.-Z., & Rothwell, J. C. (2006b). Effects of theta burst stimulation protocols on phosphene threshold. *Clinical Neurophysiology*, 117(8), 1808–1813. <https://doi.org/10.1016/j.clinph.2006.03.019>

- Fransson, P., & Marrelec, G. (2008). The precuneus/posterior cingulate cortex plays a pivotal role in the default mode network: Evidence from a partial correlation network analysis. *NeuroImage*, *42*(3), 1178–1184. <https://doi.org/10.1016/j.neuroimage.2008.05.059>
- Fritsch, B., Reis, J., Martinowich, K., Schambra, H. M., Ji, Y., Cohen, L. G., & Lu, B. (2010). Direct current stimulation promotes BDNF-dependent synaptic plasticity: Potential implications for motor learning. *Neuron*, *66*(2), 198–204. <https://doi.org/10.1016/j.neuron.2010.03.035>
- Gamboa, O. L., Antal, A., Moliadze, V., & Paulus, W. (2010). Simply longer is not better: Reversal of theta burst after-effect with prolonged stimulation. *Experimental Brain Research*, *204*(2), 181–187. <https://doi.org/10.1007/s00221-010-2293-4>
- Ganaden, R. E., Mullin, C. R., & Steeves, J. K. E. (2013a). Transcranial magnetic stimulation to the transverse occipital sulcus affects scene but not object processing. *Journal of Cognitive Neuroscience*, *25*(6), 961–968. [https://doi.org/10.1162/jocn\\_a\\_00372](https://doi.org/10.1162/jocn_a_00372)
- Ganaden, R. E., Mullin, C. R., & Steeves, J. K. E. (2013b). Transcranial magnetic stimulation to the transverse occipital sulcus affects scene but not object processing. *Journal of Cognitive Neuroscience*, *25*(6), 961–968. [https://doi.org/10.1162/jocn\\_a\\_00372](https://doi.org/10.1162/jocn_a_00372)
- Gerwig, M., Kastrup, O., Meyer, B.-U., & Niehaus, L. (2003). Evaluation of cortical excitability by motor and phosphene thresholds in transcranial magnetic stimulation. *Journal of the Neurological Sciences*, *215*(1), 75–78. [https://doi.org/10.1016/S0022-510X\(03\)00228-4](https://doi.org/10.1016/S0022-510X(03)00228-4)
- Gilio, F., Conte, A., Vanacore, N., Frasca, V., Inghilleri, M., & Berardelli, A. (2007). Excitatory and inhibitory after-effects after repetitive magnetic transcranial stimulation (rTMS) in

normal subjects. *Experimental Brain Research*, 176(4), 588–593.

<https://doi.org/10.1007/s00221-006-0638-9>

Glasser, M. F., & Van Essen, D. C. (2011). Mapping human cortical areas in vivo based on myelin content as revealed by T1- and T2-weighted MRI. *The Journal of Neuroscience*, 31(32), 11597–11616. <https://doi.org/10.1523/JNEUROSCI.2180-11.2011>

Glim, S., Okazaki, Y. O., Nakagawa, Y., Mizuno, Y., Hanakawa, T., & Kitajo, K. (2019). Phase-Amplitude Coupling of Neural Oscillations Can Be Effectively Probed with Concurrent TMS-EEG. *Neural Plasticity*, 2019, 6263907. <https://doi.org/10.1155/2019/6263907>

Gore, J. C. (2003). Principles and practice of functional MRI of the human brain. *Journal of Clinical Investigation*, 112(1), 4–9. <https://doi.org/10.1172/JCI200319010>

Gothe, J., Brandt, S. A., Irlbacher, K., Rörich, S., Sabel, B. A., & Meyer, B.-U. (2002). Changes in visual cortex excitability in blind subjects as demonstrated by transcranial magnetic stimulation. *Brain: A Journal of Neurology*, 125(Pt 3), 479–490.

<https://doi.org/10.1093/brain/awf045>

Gratton, C., Lee, T., Nomura, E., & D’Esposito, M. (2013). The effect of theta-burst TMS on cognitive control networks measured with resting state fMRI. *Frontiers in Systems Neuroscience*, 7. <https://www.frontiersin.org/article/10.3389/fnsys.2013.00124>

Greicius, M. D., Krasnow, B., Reiss, A. L., & Menon, V. (2003). Functional connectivity in the resting brain: A network analysis of the default mode hypothesis. *Proceedings of the National Academy of Sciences of the United States of America*, 100(1), 253–258.

<https://doi.org/10.1073/pnas.0135058100>

- Groen, I. I. A., Silson, E. H., Pitcher, D., & Baker, C. I. (2021). Theta-burst TMS of lateral occipital cortex reduces BOLD responses across category-selective areas in ventral temporal cortex. *NeuroImage*, *230*, 117790. <https://doi.org/10.1016/j.neuroimage.2021.117790>
- Guerra, A., Asci, F., Zampogna, A., D'Onofrio, V., Petrucci, S., Ginevrino, M., Berardelli, A., & Suppa, A. (2020). Gamma-transcranial alternating current stimulation and theta-burst stimulation: Inter-subject variability and the role of BDNF. *Clinical Neurophysiology*, *131*(11), 2691–2699. <https://doi.org/10.1016/j.clinph.2020.08.017>
- Gusnard, D. A., Raichle, M. E., & Raichle, M. E. (2001). Searching for a baseline: Functional imaging and the resting human brain. *Nature Reviews. Neuroscience*, *2*(10), 685–694. <https://doi.org/10.1038/35094500>
- Hafkemeijer, A., Möller, C., Dopfer, E. G. P., Jiskoot, L. C., Schouten, T. M., van Swieten, J. C., van der Flier, W. M., Vrenken, H., Pijnenburg, Y. A. L., Barkhof, F., Scheltens, P., van der Grond, J., & Rombouts, S. A. R. B. (2015). Resting state functional connectivity differences between behavioral variant frontotemporal dementia and Alzheimer's disease. *Frontiers in Human Neuroscience*, *9*, 474. <https://doi.org/10.3389/fnhum.2015.00474>
- Hallett, M. (2007). Transcranial Magnetic Stimulation: A Primer. *Neuron*, *55*(2), 187–199. <https://doi.org/10.1016/j.neuron.2007.06.026>
- Handwerker, D. A., Ianni, G., Gutierrez, B., Roopchansingh, V., Gonzalez-Castillo, J., Chen, G., Bandettini, P. A., Ungerleider, L. G., & Pitcher, D. (2020). Theta-burst TMS to the posterior superior temporal sulcus decreases resting-state fMRI connectivity across the

- face processing network. *Network Neuroscience*, 4(3), 746–760.  
[https://doi.org/10.1162/netn\\_a\\_00145](https://doi.org/10.1162/netn_a_00145)
- Harita, S., Momi, D., Mazza, F., & Griffiths, J. D. (2022). Mapping Inter-individual Functional Connectivity Variability in TMS Targets for Major Depressive Disorder. *Frontiers in Psychiatry*, 13, 902089. <https://doi.org/10.3389/fpsyt.2022.902089>
- Hebb, D. O. (1949). *The organization of behavior; a neuropsychological theory* (pp. xix, 335). Wiley.
- Hess, G., & Donoghue, J. P. (1996). Long-term potentiation and long-term depression of horizontal connections in rat motor cortex. *Acta Neurobiologiae Experimentalis*, 56(1), 397–405.
- Hill, A. J. (1978). First occurrence of hippocampal spatial firing in a new environment. *Experimental Neurology*, 62(2), 282–297. [https://doi.org/10.1016/0014-4886\(78\)90058-4](https://doi.org/10.1016/0014-4886(78)90058-4)
- Hou, J.-M., Zhao, M., Zhang, W., Song, L.-H., Wu, W.-J., Wang, J., Zhou, D.-Q., Xie, B., He, M., Guo, J.-W., Qu, W., & Li, H.-T. (2014). Resting-state functional connectivity abnormalities in patients with obsessive–compulsive disorder and their healthy first-degree relatives. *Journal of Psychiatry & Neuroscience : JPN*, 39(5), 304–311.  
<https://doi.org/10.1503/jpn.130220>
- Huang, Y.-Z., Edwards, M. J., Rounis, E., Bhatia, K. P., & Rothwell, J. C. (2005a). Theta burst stimulation of the human motor cortex. *Neuron*, 45(2), 201–206.  
<https://doi.org/10.1016/j.neuron.2004.12.033>

- Huang, Y.-Z., Edwards, M. J., Rounis, E., Bhatia, K. P., & Rothwell, J. C. (2005b). Theta burst stimulation of the human motor cortex. *Neuron*, *45*(2), 201–206.  
<https://doi.org/10.1016/j.neuron.2004.12.033>
- Huang, Y.-Z., Rothwell, J. C., Chen, R.-S., Lu, C.-S., & Chuang, W.-L. (2011). The theoretical model of theta burst form of repetitive transcranial magnetic stimulation. *Clinical Neurophysiology*, *122*(5), 1011–1018. <https://doi.org/10.1016/j.clinph.2010.08.016>
- Huerta, P. T., & Volpe, B. T. (2009). Transcranial magnetic stimulation, synaptic plasticity and network oscillations. *Journal of Neuroengineering and Rehabilitation*, *6*, 7.  
<https://doi.org/10.1186/1743-0003-6-7>
- Jafri, M. J., Pearlson, G. D., Stevens, M., & Calhoun, V. D. (2008). A method for functional network connectivity among spatially independent resting-state components in schizophrenia. *NeuroImage*, *39*(4), 1666–1681.  
<https://doi.org/10.1016/j.neuroimage.2007.11.001>
- Kammer, T., Beck, S., Puls, K., Roether, C., & Thielscher, A. (2003). Motor and phosphene thresholds: Consequences of cortical anisotropy. *Supplements to Clinical Neurophysiology*, *56*, 198–203. [https://doi.org/10.1016/s1567-424x\(09\)70222-3](https://doi.org/10.1016/s1567-424x(09)70222-3)
- Kandel, E. R. (2012). The molecular biology of memory: CAMP, PKA, CRE, CREB-1, CREB-2, and CPEB. *Molecular Brain*, *5*(1), 14. <https://doi.org/10.1186/1756-6606-5-14>
- Kandel, E. R., & Tauc, L. (1965). Heterosynaptic facilitation in neurones of the abdominal ganglion of *Aplysia depilans*. *The Journal of Physiology*, *181*(1), 1–27.  
<https://doi.org/10.1113/jphysiol.1965.sp007742>

- Kang, H., Blume, J., Ombao, H., & Badre, D. (2015). Simultaneous Control of Error Rates in fMRI Data Analysis. *NeuroImage*, *123*, 102–113.  
<https://doi.org/10.1016/j.neuroimage.2015.08.009>
- Kashiwagi, F. T., El Dib, R., Gomaa, H., Gawish, N., Suzumura, E. A., da Silva, T. R., Winckler, F. C., de Souza, J. T., Conforto, A. B., Luvizutto, G. J., & Bazan, R. (2018). Noninvasive Brain Stimulations for Unilateral Spatial Neglect after Stroke: A Systematic Review and Meta-Analysis of Randomized and Nonrandomized Controlled Trials. *Neural Plasticity*, *2018*.  
<https://doi.org/10.1155/2018/1638763>
- Kauer, J. A., Malenka, R. C., & Nicoll, R. A. (1988). A persistent postsynaptic modification mediates long-term potentiation in the hippocampus. *Neuron*, *1*(10), 911–917.  
[https://doi.org/10.1016/0896-6273\(88\)90148-1](https://doi.org/10.1016/0896-6273(88)90148-1)
- Kearney-Ramos, T. E., Dowdle, L. T., Mithoefer, O. J., Devries, W., George, M. S., & Hanlon, C. A. (2019). State-Dependent Effects of Ventromedial Prefrontal Cortex Continuous Thetaburst Stimulation on Cocaine Cue Reactivity in Chronic Cocaine Users. *Frontiers in Psychiatry*, *10*, 317. <https://doi.org/10.3389/fpsyt.2019.00317>
- Keysers, C., & Gazzola, V. (2014). Hebbian learning and predictive mirror neurons for actions, sensations and emotions. *Philosophical Transactions of the Royal Society B: Biological Sciences*, *369*(1644). <https://doi.org/10.1098/rstb.2013.0175>
- Kirkwood, A., Lee, H. K., & Bear, M. F. (1995). Co-regulation of long-term potentiation and experience-dependent synaptic plasticity in visual cortex by age and experience. *Nature*, *375*(6529), 328–331. <https://doi.org/10.1038/375328a0>

- Kobayashi, M., & Pascual-Leone, A. (2003). Transcranial magnetic stimulation in neurology. *The Lancet. Neurology*, 2(3), 145–156. [https://doi.org/10.1016/s1474-4422\(03\)00321-1](https://doi.org/10.1016/s1474-4422(03)00321-1)
- Kondo, T., Yamada, N., Momosaki, R., Shimizu, M., & Abo, M. (2017). Comparison of the Effect of Low-Frequency Repetitive Transcranial Magnetic Stimulation with That of Theta Burst Stimulation on Upper Limb Motor Function in Poststroke Patients. *BioMed Research International*, 2017, 4269435. <https://doi.org/10.1155/2017/4269435>
- Krieg, T. D., Salinas, F. S., Narayana, S., Fox, P. T., & Mogul, D. J. (2013). PET-Based Confirmation of Orientation Sensitivity of TMS-Induced Cortical Activation in Humans. *Brain Stimulation*, 6(6), 898–904. <https://doi.org/10.1016/j.brs.2013.05.007>
- Kundu, P., Brenowitz, N. D., Voon, V., Worbe, Y., Vértes, P. E., Inati, S. J., Saad, Z. S., Bandettini, P. A., & Bullmore, E. T. (2013). Integrated strategy for improving functional connectivity mapping using multiecho fMRI. *Proceedings of the National Academy of Sciences*, 110(40), 16187–16192. <https://doi.org/10.1073/pnas.1301725110>
- Kundu, P., Inati, S. J., Evans, J. W., Luh, W.-M., & Bandettini, P. A. (2012a). Differentiating BOLD and non-BOLD signals in fMRI time series using multi-echo EPI. *NeuroImage*, 60(3), 1759–1770. <https://doi.org/10.1016/j.neuroimage.2011.12.028>
- Kundu, P., Inati, S. J., Evans, J. W., Luh, W.-M., & Bandettini, P. A. (2012b). Differentiating BOLD and non-BOLD signals in fMRI time series using multi-echo EPI. *NeuroImage*, 60(3), 1759–1770. <https://doi.org/10.1016/j.neuroimage.2011.12.028>
- Kundu, P., Voon, V., Balchandani, P., Lombardo, M. V., Poser, B. A., & Bandettini, P. A. (2017). Multi-echo fMRI: A review of applications in fMRI denoising and analysis of BOLD signals. *NeuroImage*, 154, 59–80. <https://doi.org/10.1016/j.neuroimage.2017.03.033>

- Kuznetsova, A., Brockhoff, P. B., & Christensen, R. H. B. (2017). lmerTest Package: Tests in Linear Mixed Effects Models. *Journal of Statistical Software*, *82*, 1–26.  
<https://doi.org/10.18637/jss.v082.i13>
- Larivière, S., Ward, N. S., & Boudrias, M.-H. (2018). Disrupted functional network integrity and flexibility after stroke: Relation to motor impairments. *NeuroImage: Clinical*, *19*, 883–891. <https://doi.org/10.1016/j.nicl.2018.06.010>
- Larson, J., & Munkácsy, E. (2015). Theta-Burst LTP. *Brain Research*, *1621*, 38–50.  
<https://doi.org/10.1016/j.brainres.2014.10.034>
- Larson, J., Wong, D., & Lynch, G. (1986). Patterned stimulation at the theta frequency is optimal for the induction of hippocampal long-term potentiation. *Brain Research*, *368*(2), 347–350. [https://doi.org/10.1016/0006-8993\(86\)90579-2](https://doi.org/10.1016/0006-8993(86)90579-2)
- Lasagna, C. A., Taylor, S. F., Lee, T. G., Rutherford, S., Greathouse, T., Gu, P., & Tso, I. F. (2021). Continuous Theta Burst Stimulation to the Secondary Visual Cortex at 80% Active Motor Threshold Does Not Impair Central Vision in Humans During a Simple Detection Task. *Frontiers in Human Neuroscience*, *15*.  
<https://www.frontiersin.org/article/10.3389/fnhum.2021.709275>
- Lauterbur, P. C. (1973). Image Formation by Induced Local Interactions: Examples Employing Nuclear Magnetic Resonance. *Nature*, *242*(5394), Article 5394.  
<https://doi.org/10.1038/242190a0>
- Lee, J. C., Corlier, J., Wilson, A. C., Tadayonnejad, R., Marder, K. G., Ngo, D., Krantz, D. E., Wilke, S. A., Levitt, J. G., Ginder, N. D., & Leuchter, A. F. (2021). Subthreshold stimulation intensity is associated with greater clinical efficacy of intermittent theta-burst

- stimulation priming for Major Depressive Disorder. *Brain Stimulation*, *14*(4), 1015–1021.  
<https://doi.org/10.1016/j.brs.2021.06.008>
- Lee, W. H., & Frangou, S. (2017). Linking functional connectivity and dynamic properties of resting-state networks. *Scientific Reports*, *7*(1), Article 1.  
<https://doi.org/10.1038/s41598-017-16789-1>
- Lefaucheur, J.-P., Drouot, X., Menard-Lefaucheur, I., Zerah, F., Bendib, B., Cesaro, P., Keravel, Y., & Nguyen, J.-P. (2004). Neurogenic pain relief by repetitive transcranial magnetic cortical stimulation depends on the origin and the site of pain. *Journal of Neurology, Neurosurgery & Psychiatry*, *75*(4), 612–616. <https://doi.org/10.1136/jnnp.2003.022236>
- Lin, Y.-J., Shukla, L., Dugué, L., Valero-Cabré, A., & Carrasco, M. (2021). Transcranial magnetic stimulation entrains alpha oscillatory activity in occipital cortex. *Scientific Reports*, *11*(1), Article 1. <https://doi.org/10.1038/s41598-021-96849-9>
- Lisanby, S. H., Husain, M. M., Rosenquist, P. B., Maixner, D., Gutierrez, R., Krystal, A., Gilmer, W., Marangell, L. B., Aaronson, S., Daskalakis, Z. J., Canterbury, R., Richelson, E., Sackeim, H. A., & George, M. S. (2009). Daily left prefrontal repetitive transcranial magnetic stimulation in the acute treatment of major depression: Clinical predictors of outcome in a multisite, randomized controlled clinical trial. *Neuropsychopharmacology*, *34*(2), 522–534. <https://doi.org/10.1038/npp.2008.118>
- Liu, J., Harris, A., & Kanwisher, N. (2010). Perception of face parts and face configurations: An fMRI study. *Journal of Cognitive Neuroscience*, *22*(1), 203–211.  
<https://doi.org/10.1162/jocn.2009.21203>

- Lu, B. (2003). BDNF and activity-dependent synaptic modulation. *Learning & Memory (Cold Spring Harbor, N.Y.)*, *10*(2), 86–98. <https://doi.org/10.1101/lm.54603>
- Lynch, G., Larson, J., Kelso, S., Barrionuevo, G., & Schottler, F. (1983). Intracellular injections of EGTA block induction of hippocampal long-term potentiation. *Nature*, *305*(5936), 719–721. <https://doi.org/10.1038/305719a0>
- Mansfield, P., & Grannell, P. K. (1975). “Diffraction” and microscopy in solids and liquids by NMR. *Physical Review B*, *12*(9), 3618–3634. <https://doi.org/10.1103/PhysRevB.12.3618>
- Martial, C., Larroque, S. K., Cavaliere, C., Wannez, S., Annen, J., Kupers, R., Laureys, S., & Di Perri, C. (2019). Resting-state functional connectivity and cortical thickness characterization of a patient with Charles Bonnet syndrome. *PLoS ONE*, *14*(7), e0219656. <https://doi.org/10.1371/journal.pone.0219656>
- McCalley, D. M., Lench, D. H., Doolittle, J. D., Imperatore, J. P., Hoffman, M., & Hanlon, C. A. (2021). Determining the optimal pulse number for theta burst induced change in cortical excitability. *Scientific Reports*, *11*(1), Article 1. <https://doi.org/10.1038/s41598-021-87916-2>
- McConnell, K. A., Nahas, Z., Shastri, A., Lorberbaum, J. P., Kozel, F. A., Bohning, D. E., & George, M. S. (2001). The transcranial magnetic stimulation motor threshold depends on the distance from coil to underlying cortex: A replication in healthy adults comparing two methods of assessing the distance to cortex. *Biological Psychiatry*, *49*(5), 454–459. [https://doi.org/10.1016/s0006-3223\(00\)01039-8](https://doi.org/10.1016/s0006-3223(00)01039-8)

- Meissner, S. N., Krause, V., Südmeyer, M., Hartmann, C. J., & Pollok, B. (2018). The significance of brain oscillations in motor sequence learning: Insights from Parkinson's disease. *NeuroImage : Clinical, 20*, 448–457. <https://doi.org/10.1016/j.nicl.2018.08.009>
- Menon, V., & Uddin, L. Q. (2010). Saliency, switching, attention and control: A network model of insula function. *Brain Structure & Function, 214*(5–6), 655–667. <https://doi.org/10.1007/s00429-010-0262-0>
- Merton, P. A., & Morton, H. B. (1980). Stimulation of the cerebral cortex in the intact human subject. *Nature, 285*(5762), Article 5762. <https://doi.org/10.1038/285227a0>
- Meszlényi, R. J., Hermann, P., Buza, K., Gál, V., & Vidnyánszky, Z. (2017). Resting State fMRI Functional Connectivity Analysis Using Dynamic Time Warping. *Frontiers in Neuroscience, 11*. <https://doi.org/10.3389/fnins.2017.00075>
- Mi, T.-M., Garg, S., Ba, F., Liu, A.-P., Liang, P.-P., Gao, L.-L., Jia, Q., Xu, E.-H., Li, K.-C., Chan, P., & McKeown, M. J. (2020). Repetitive transcranial magnetic stimulation improves Parkinson's freezing of gait via normalizing brain connectivity. *Npj Parkinson's Disease, 6*(1), Article 1. <https://doi.org/10.1038/s41531-020-0118-0>
- Mikl, M., Marecek, R., Hlustík, P., Pavlicová, M., Drastich, A., Chlebus, P., Brázdil, M., & Krupa, P. (2008). Effects of spatial smoothing on fMRI group inferences. *Magnetic Resonance Imaging, 26*(4), 490–503. <https://doi.org/10.1016/j.mri.2007.08.006>
- Moisset, X., Goudeau, S., Poindessous-Jazat, F., Baudic, S., Clavelou, P., & Bouhassira, D. (2015). Prolonged continuous theta-burst stimulation is more analgesic than “classical” high frequency repetitive transcranial magnetic stimulation. *Brain Stimulation, 8*(1), 135–141. <https://doi.org/10.1016/j.brs.2014.10.006>

- Mostame, P., & Sadaghiani, S. (2020). Phase- and amplitude-coupling are tied by an intrinsic spatial organization but show divergent stimulus-related changes. *NeuroImage*, *219*, 117051. <https://doi.org/10.1016/j.neuroimage.2020.117051>
- Mullin, C. R., & Steeves, J. K. E. (2011). TMS to the lateral occipital cortex disrupts object processing but facilitates scene processing. *Journal of Cognitive Neuroscience*, *23*(12), 4174–4184. [https://doi.org/10.1162/jocn\\_a\\_00095](https://doi.org/10.1162/jocn_a_00095)
- Mullin, C. R., & Steeves, J. K. E. (2013). Consecutive TMS-fMRI Reveals an Inverse Relationship in BOLD Signal between Object and Scene Processing. *Journal of Neuroscience*, *33*(49), 19243–19249. <https://doi.org/10.1523/JNEUROSCI.2537-13.2013>
- Munno, D. W., & Syed, N. I. (2003). Synaptogenesis in the CNS: An Odyssey from Wiring Together to Firing Together. *The Journal of Physiology*, *552*(Pt 1), 1–11. <https://doi.org/10.1113/jphysiol.2003.045062>
- Murphy, K., Birn, R. M., & Bandettini, P. A. (2013). Resting-state fMRI confounds and cleanup. *NeuroImage*, *80*, 349–359. <https://doi.org/10.1016/j.neuroimage.2013.04.001>
- Nardone, R., De Blasi, P., Höller, Y., Taylor, A. C., Brigo, F., & Trinka, E. (2016). Effects of theta burst stimulation on referred phantom sensations in patients with spinal cord injury. *Neuroreport*, *27*(4), 209–212. <https://doi.org/10.1097/WNR.0000000000000508>
- Nasreddine, Z. S., Phillips, N. A., Bédirian, V., Charbonneau, S., Whitehead, V., Collin, I., Cummings, J. L., & Chertkow, H. (2005). The Montreal Cognitive Assessment, MoCA: A Brief Screening Tool For Mild Cognitive Impairment. *Journal of the American Geriatrics Society*, *53*(4), 695–699. <https://doi.org/10.1111/j.1532-5415.2005.53221.x>

- Nichols, T., & Hayasaka, S. (2003). Controlling the familywise error rate in functional neuroimaging: A comparative review. *Statistical Methods in Medical Research*, 12(5), 419–446. <https://doi.org/10.1191/0962280203sm341ra>
- Nitz, W. R., & Reimer, P. (1999). Contrast mechanisms in MR imaging. *European Radiology*, 9(6), 1032–1046. <https://doi.org/10.1007/s003300050789>
- Ogawa, S., Lee, T. M., Kay, A. R., & Tank, D. W. (1990). Brain magnetic resonance imaging with contrast dependent on blood oxygenation. *Proceedings of the National Academy of Sciences of the United States of America*, 87(24), 9868–9872. <https://doi.org/10.1073/pnas.87.24.9868>
- Okazaki, Y. O., Nakagawa, Y., Mizuno, Y., Hanakawa, T., & Kitajo, K. (2021). Frequency- and Area-Specific Phase Entrainment of Intrinsic Cortical Oscillations by Repetitive Transcranial Magnetic Stimulation. *Frontiers in Human Neuroscience*, 15. <https://www.frontiersin.org/article/10.3389/fnhum.2021.608947>
- Padula, C. B., Tenekedjieva, L.-T., McCalley, D. M., Al-Dasouqi, H., Hanlon, C. A., Williams, L. M., Kozel, F. A., Knutson, B., Durazzo, T. C., Yesavage, J. A., & Madore, M. R. (2022). Targeting the Salience Network: A Mini-Review on a Novel Neuromodulation Approach for Treating Alcohol Use Disorder. *Frontiers in Psychiatry*, 13. <https://www.frontiersin.org/articles/10.3389/fpsyt.2022.893833>
- Pascual-Leone, A., Walsh, V., & Rothwell, J. (2000). Transcranial magnetic stimulation in cognitive neuroscience—Virtual lesion, chronometry, and functional connectivity. *Current Opinion in Neurobiology*, 10(2), 232–237. [https://doi.org/10.1016/s0959-4388\(00\)00081-7](https://doi.org/10.1016/s0959-4388(00)00081-7)

- Pauling, L., & Coryell, C. D. (1936). The Magnetic Properties and Structure of Hemoglobin, Oxyhemoglobin and Carbonmonoxyhemoglobin. *Proceedings of the National Academy of Sciences of the United States of America*, 22(4), 210–216.  
<https://doi.org/10.1073/pnas.22.4.210>
- Peng, J., Yao, F., Li, Q., Ge, Q., Shi, W., Su, T., Tang, L., Pan, Y., Liang, R., Zhang, L., & Shao, Y. (2021). Alternations of interhemispheric functional connectivity in children with strabismus and amblyopia: A resting-state fMRI study. *Scientific Reports*, 11(1), Article 1.  
<https://doi.org/10.1038/s41598-021-92281-1>
- Pfurtscheller, G., & Lopes da Silva, F. H. (1999). Event-related EEG/MEG synchronization and desynchronization: Basic principles. *Clinical Neurophysiology*, 110(11), 1842–1857.  
[https://doi.org/10.1016/s1388-2457\(99\)00141-8](https://doi.org/10.1016/s1388-2457(99)00141-8)
- Philpot, B. D., Sekhar, A. K., Shouval, H. Z., & Bear, M. F. (2001). Visual experience and deprivation bidirectionally modify the composition and function of NMDA receptors in visual cortex. *Neuron*, 29(1), 157–169. [https://doi.org/10.1016/s0896-6273\(01\)00187-8](https://doi.org/10.1016/s0896-6273(01)00187-8)
- Piccolino, M. (1998). Animal electricity and the birth of electrophysiology: The legacy of Luigi Galvani. *Brain Research Bulletin*, 46(5), 381–407. [https://doi.org/10.1016/s0361-9230\(98\)00026-4](https://doi.org/10.1016/s0361-9230(98)00026-4)
- Pitcher, D., Duchaine, B., & Walsh, V. (2014a). Combined TMS and FMRI reveal dissociable cortical pathways for dynamic and static face perception. *Current Biology: CB*, 24(17), 2066–2070. <https://doi.org/10.1016/j.cub.2014.07.060>

- Pitcher, D., Duchaine, B., & Walsh, V. (2014b). Combined TMS and fMRI reveal dissociable cortical pathways for dynamic and static face perception. *Current Biology: CB*, *24*(17), 2066–2070. <https://doi.org/10.1016/j.cub.2014.07.060>
- Pitcher, D., Japee, S., Rauth, L., & Ungerleider, L. G. (2017). The Superior Temporal Sulcus Is Causally Connected to the Amygdala: A Combined TBS-fMRI Study. *The Journal of Neuroscience*, *37*(5), 1156–1161. <https://doi.org/10.1523/JNEUROSCI.0114-16.2016>
- Pittenger, C., & Duman, R. S. (2008). Stress, Depression, and Neuroplasticity: A Convergence of Mechanisms. *Neuropsychopharmacology*, *33*(1), Article 1. <https://doi.org/10.1038/sj.npp.1301574>
- Polson, M. J., Barker, A. T., & Freeston, I. L. (1982). Stimulation of nerve trunks with time-varying magnetic fields. *Medical & Biological Engineering & Computing*, *20*(2), 243–244. <https://doi.org/10.1007/BF02441362>
- Posse, S., Wiese, S., Gembris, D., Mathiak, K., Kessler, C., Grosse-Ruyken, M. L., Elghahwagi, B., Richards, T., Dager, S. R., & Kiselev, V. G. (1999). Enhancement of BOLD-contrast sensitivity by single-shot multi-echo functional MR imaging. *Magnetic Resonance in Medicine*, *42*(1), 87–97. [https://doi.org/10.1002/\(sici\)1522-2594\(199907\)42:1<87::aid-mrm13>3.0.co;2-o](https://doi.org/10.1002/(sici)1522-2594(199907)42:1<87::aid-mrm13>3.0.co;2-o)
- Power, J. D., Mitra, A., Laumann, T. O., Snyder, A. Z., Schlaggar, B. L., & Petersen, S. E. (2014a). Methods to detect, characterize, and remove motion artifact in resting state fMRI. *NeuroImage*, *84*, 10.1016/j.neuroimage.2013.08.048. <https://doi.org/10.1016/j.neuroimage.2013.08.048>

Power, J. D., Mitra, A., Laumann, T. O., Snyder, A. Z., Schlaggar, B. L., & Petersen, S. E. (2014b).

Methods to detect, characterize, and remove motion artifact in resting state fMRI.

*NeuroImage*, 84. <https://doi.org/10.1016/j.neuroimage.2013.08.048>

Power, J. D., Plitt, M., Gotts, S. J., Kundu, P., Voon, V., Bandettini, P. A., & Martin, A. (2018a).

Ridding fMRI data of motion-related influences: Removal of signals with distinct spatial and physical bases in multiecho data. *Proceedings of the National Academy of Sciences*,

115(9), E2105–E2114. <https://doi.org/10.1073/pnas.1720985115>

Power, J. D., Plitt, M., Gotts, S. J., Kundu, P., Voon, V., Bandettini, P. A., & Martin, A. (2018b).

Ridding fMRI data of motion-related influences: Removal of signals with distinct spatial and physical bases in multiecho data. *Proceedings of the National Academy of Sciences*,

115(9), E2105–E2114. <https://doi.org/10.1073/pnas.1720985115>

Quandt, F., Bönstrup, M., Schulz, R., Timmermann, J. E., Mund, M., Wessel, M. J., & Hummel, F.

C. (2019). The functional role of beta-oscillations in the supplementary motor area during reaching and grasping after stroke: A question of structural damage to the corticospinal tract. *Human Brain Mapping*, 40(10), 3091–3101.

<https://doi.org/10.1002/hbm.24582>

Rafique, S. A., Richards, J. R., & Steeves, J. K. E. (2016). RTMS reduces cortical imbalance

associated with visual hallucinations after occipital stroke. *Neurology*, 87(14), 1493–

1500. <https://doi.org/10.1212/WNL.0000000000003180>

Rafique, S. A., Richards, J. R., & Steeves, J. K. E. (2018). Altered white matter connectivity

associated with visual hallucinations following occipital stroke. *Brain and Behavior*, 8(6),

e01010. <https://doi.org/10.1002/brb3.1010>

- Rafique, S. A., Solomon-Harris, L. M., & Steeves, J. K. E. (2015). TMS to object cortex affects both object and scene remote networks while TMS to scene cortex only affects scene networks. *Neuropsychologia*, *79*(Pt A), 86–96.  
<https://doi.org/10.1016/j.neuropsychologia.2015.10.027>
- Rafique, S. A., & Steeves, J. K. E. (2022). Modulating intrinsic functional connectivity with visual cortex using low-frequency repetitive transcranial magnetic stimulation. *Brain and Behavior*, e2491. <https://doi.org/10.1002/brb3.2491>
- Rahnev, D., Kok, P., Munneke, M., Bahdo, L., de Lange, F. P., & Lau, H. (2013a). Continuous theta burst transcranial magnetic stimulation reduces resting state connectivity between visual areas. *Journal of Neurophysiology*, *110*(8), 1811–1821.  
<https://doi.org/10.1152/jn.00209.2013>
- Rahnev, D., Kok, P., Munneke, M., Bahdo, L., de Lange, F. P., & Lau, H. (2013b). Continuous theta burst transcranial magnetic stimulation reduces resting state connectivity between visual areas. *Journal of Neurophysiology*, *110*(8), 1811–1821.  
<https://doi.org/10.1152/jn.00209.2013>
- Raichle, M. E. (2011). The Restless Brain. *Brain Connectivity*, *1*(1), 3–12.  
<https://doi.org/10.1089/brain.2011.0019>
- Raichle, M. E., & Snyder, A. Z. (2007). A default mode of brain function: A brief history of an evolving idea. *NeuroImage*, *37*(4), 1083–1090; discussion 1097-1099.  
<https://doi.org/10.1016/j.neuroimage.2007.02.041>
- Rao, B., Wang, S., Yu, M., Chen, L., Miao, G., Zhou, X., Zhou, H., Liao, W., & Xu, H. (2022). Suboptimal states and frontoparietal network-centered incomplete compensation

revealed by dynamic functional network connectivity in patients with post-stroke cognitive impairment. *Frontiers in Aging Neuroscience*, *14*, 893297.

<https://doi.org/10.3389/fnagi.2022.893297>

Ridding, M. C., & Ziemann, U. (2010). Determinants of the induction of cortical plasticity by non-invasive brain stimulation in healthy subjects. *The Journal of Physiology*, *588*(Pt 13), 2291–2304. <https://doi.org/10.1113/jphysiol.2010.190314>

Rolinski, M., Griffanti, L., Szewczyk-Krolkowski, K., Menke, R. A. L., Wilcock, G. K., Filippini, N., Zamboni, G., Hu, M. T. M., & Mackay, C. E. (2015). Aberrant functional connectivity within the basal ganglia of patients with Parkinson's disease. *NeuroImage. Clinical*, *8*, 126–132. <https://doi.org/10.1016/j.nicl.2015.04.003>

Romei, V., Gross, J., & Thut, G. (2010). On the role of prestimulus alpha rhythms over occipito-parietal areas in visual input regulation: Correlation or causation? *The Journal of Neuroscience*, *30*(25), 8692–8697. <https://doi.org/10.1523/JNEUROSCI.0160-10.2010>

Rossini, P. M., Burke, D., Chen, R., Cohen, L. G., Daskalakis, Z., Di Iorio, R., Di Lazzaro, V., Ferreri, F., Fitzgerald, P. B., George, M. S., Hallett, M., Lefaucheur, J. P., Langguth, B., Matsumoto, H., Miniussi, C., Nitsche, M. A., Pascual-Leone, A., Paulus, W., Rossi, S., ... Ziemann, U. (2015). Non-invasive electrical and magnetic stimulation of the brain, spinal cord, roots and peripheral nerves: Basic principles and procedures for routine clinical and research application. An updated report from an I.F.C.N. Committee. *Clinical Neurophysiology*, *126*(6), 1071–1107. <https://doi.org/10.1016/j.clinph.2015.02.001>

Rossini, P. M., & Rossi, S. (1998). Clinical applications of motor evoked potentials.

*Electroencephalography and Clinical Neurophysiology*, 106(3), 180–194.

[https://doi.org/10.1016/s0013-4694\(97\)00097-7](https://doi.org/10.1016/s0013-4694(97)00097-7)

Schaworonkow, N., Triesch, J., Ziemann, U., & Zrenner, C. (2019). EEG-triggered TMS reveals stronger brain state-dependent modulation of motor evoked potentials at weaker stimulation intensities. *Brain Stimulation*, 12(1), 110–118.

<https://doi.org/10.1016/j.brs.2018.09.009>

Seeley, W. W., Menon, V., Schatzberg, A. F., Keller, J., Glover, G. H., Kenna, H., Reiss, A. L., & Greicius, M. D. (2007). Dissociable intrinsic connectivity networks for salience processing and executive control. *The Journal of Neuroscience*, 27(9), 2349–2356.

<https://doi.org/10.1523/JNEUROSCI.5587-06.2007>

Shao, Y., Li, Q.-H., Li, B., Lin, Q., Su, T., Shi, W.-Q., Zhu, P.-W., Yuan, Q., Shu, Y.-Q., He, Y., Liu, W.-F., & Ye, L. (2019). Altered brain activity in patients with strabismus and amblyopia detected by analysis of regional homogeneity: A resting-state functional magnetic resonance imaging study. *Molecular Medicine Reports*, 19(6), 4832–4840.

<https://doi.org/10.3892/mmr.2019.10147>

Shatz, C. J. (1992). The developing brain. *Scientific American*, 267(3), 60–67.

<https://doi.org/10.1038/scientificamerican0992-60>

Shi, Y.-D., Ge, Q.-M., Lin, Q., Liang, R.-B., Li, Q.-Y., Shi, W.-Q., Li, B., & Shao, Y. (2022). Functional connectivity density alterations in children with strabismus and amblyopia based on resting-state functional magnetic resonance imaging (fMRI). *BMC Ophthalmology*, 22(1), 49. <https://doi.org/10.1186/s12886-021-02228-3>

- Shinomoto, S., Kim, H., Shimokawa, T., Matsuno, N., Funahashi, S., Shima, K., Fujita, I., Tamura, H., Doi, T., Kawano, K., Inaba, N., Fukushima, K., Kurkin, S., Kurata, K., Taira, M., Tsutsui, K.-I., Komatsu, H., Ogawa, T., Koida, K., ... Toyama, K. (2009). Relating Neuronal Firing Patterns to Functional Differentiation of Cerebral Cortex. *PLoS Computational Biology*, 5(7), e1000433. <https://doi.org/10.1371/journal.pcbi.1000433>
- Silvanto, J., Bona, S., Marelli, M., & Cattaneo, Z. (2018). On the Mechanisms of Transcranial Magnetic Stimulation (TMS): How Brain State and Baseline Performance Level Determine Behavioral Effects of TMS. *Frontiers in Psychology*, 9. <https://www.frontiersin.org/articles/10.3389/fpsyg.2018.00741>
- Silvanto, J., & Pascual-Leone, A. (2008). State-Dependency of Transcranial Magnetic Stimulation. *Brain Topography*, 21(1), 1–10. <https://doi.org/10.1007/s10548-008-0067-0>
- Singh, F., Shu, I.-W., Hsu, S.-H., Link, P., Pineda, J. A., & Granholm, E. (2020). Modulation of frontal gamma oscillations improves working memory in schizophrenia. *NeuroImage. Clinical*, 27, 102339. <https://doi.org/10.1016/j.nicl.2020.102339>
- Skipper, J. I., Goldin-Meadow, S., Nusbaum, H. C., & Small, S. L. (2007). Speech-associated gestures, Broca's area, and the human mirror system. *Brain and Language*, 101(3), 260–277. <https://doi.org/10.1016/j.bandl.2007.02.008>
- Smitha, K., Akhil Raja, K., Arun, K., Rajesh, P., Thomas, B., Kapilamoorthy, T., & Kesavadas, C. (2017). Resting state fMRI: A review on methods in resting state connectivity analysis and resting state networks. *The Neuroradiology Journal*, 30(4), 305–317. <https://doi.org/10.1177/1971400917697342>

- Solomon-Harris, L. M., Rafique, S. A., & Steeves, J. K. E. (2016). Consecutive TMS-fMRI reveals remote effects of neural noise to the “occipital face area.” *Brain Research*, *1650*, 134–141. <https://doi.org/10.1016/j.brainres.2016.08.043>
- Stewart, L. M., Walsh, V., & Rothwell, J. C. (2001). Motor and phosphene thresholds: A transcranial magnetic stimulation correlation study. *Neuropsychologia*, *39*(4), 415–419. [https://doi.org/10.1016/s0028-3932\(00\)00130-5](https://doi.org/10.1016/s0028-3932(00)00130-5)
- Stoby, K. S., Rafique, S. A., Oeltzschner, G., & Steeves, J. K. E. (2022). Continuous and intermittent theta burst stimulation to the visual cortex do not alter GABA and glutamate concentrations measured by magnetic resonance spectroscopy. *Brain and Behavior*, e2478. <https://doi.org/10.1002/brb3.2478>
- Stokes, M. G., Barker, A. T., Dervinis, M., Verbruggen, F., Maizey, L., Adams, R. C., & Chambers, C. D. (2013). Biophysical determinants of transcranial magnetic stimulation: Effects of excitability and depth of targeted area. *Journal of Neurophysiology*, *109*(2), 437–444. <https://doi.org/10.1152/jn.00510.2012>
- Talelli, P., Greenwood, R. J., & Rothwell, J. C. (2007). Exploring Theta Burst Stimulation as an intervention to improve motor recovery in chronic stroke. *Clinical Neurophysiology*, *118*(2), 333–342. <https://doi.org/10.1016/j.clinph.2006.10.014>
- Tesche, C. D., & Karhu, J. (2000). Theta oscillations index human hippocampal activation during a working memory task. *Proceedings of the National Academy of Sciences*, *97*(2), 919–924. <https://doi.org/10.1073/pnas.97.2.919>
- Thomson, A. C., Kenis, G., Tielens, S., de Graaf, T. A., Schuhmann, T., Rutten, B. P. F., & Sack, A. T. (2020). Transcranial Magnetic Stimulation-Induced Plasticity Mechanisms: TMS-

- Related Gene Expression and Morphology Changes in a Human Neuron-Like Cell Model. *Frontiers in Molecular Neuroscience*, 13.  
<https://www.frontiersin.org/articles/10.3389/fnmol.2020.528396>
- Thut, G., Veniero, D., Romei, V., Miniussi, C., Schyns, P., & Gross, J. (2011). Rhythmic TMS Causes Local Entrainment of Natural Oscillatory Signatures. *Current Biology*, 21(14), 1176–1185. <https://doi.org/10.1016/j.cub.2011.05.049>
- Tupak, S. V., Dresler, T., Badewien, M., Hahn, T., Ernst, L. H., Herrmann, M. J., Deckert, J., Ehlis, A., & Fallgatter, A. J. (2011). Inhibitory transcranial magnetic theta burst stimulation attenuates prefrontal cortex oxygenation. *Human Brain Mapping*, 34(1), 150–157.  
<https://doi.org/10.1002/hbm.21421>
- Uddin, L. Q. (2015). Salience processing and insular cortical function and dysfunction. *Nature Reviews. Neuroscience*, 16(1), 55–61. <https://doi.org/10.1038/nrn3857>
- Van Essen, D. C., Glasser, M. F., Dierker, D. L., Harwell, J., & Coalson, T. (2012). Parcellations and Hemispheric Asymmetries of Human Cerebral Cortex Analyzed on Surface-Based Atlases. *Cerebral Cortex (New York, NY)*, 22(10), 2241–2262.  
<https://doi.org/10.1093/cercor/bhr291>
- Van Essen, D. C., & Ugurbil, K. (2012). The Future of the Human Connectome. *Neuroimage*, 62(2), 1299–1310. <https://doi.org/10.1016/j.neuroimage.2012.01.032>
- Van Essen, D. C., Ugurbil, K., Auerbach, E., Barch, D., Behrens, T. E. J., Bucholz, R., Chang, A., Chen, L., Corbetta, M., Curtiss, S. W., Della Penna, S., Feinberg, D., Glasser, M. F., Harel, N., Heath, A. C., Larson-Prior, L., Marcus, D., Michalareas, G., Moeller, S., ... WU-Minn HCP Consortium. (2012). The Human Connectome Project: A data acquisition

perspective. *NeuroImage*, 62(4), 2222–2231.

<https://doi.org/10.1016/j.neuroimage.2012.02.018>

Van Ombergen, A., Van Rompaey, V., Maes, L. K., Van de Heyning, P. H., & Wuyts, F. L. (2016).

Mal de débarquement syndrome: A systematic review. *Journal of Neurology*, 263(5),

843–854. <https://doi.org/10.1007/s00415-015-7962-6>

van Wijk, B. C. M., Beek, P. J., & Daffertshofer, A. (2012). Neural synchrony within the motor system: What have we learned so far? *Frontiers in Human Neuroscience*, 6.

<https://doi.org/10.3389/fnhum.2012.00252>

Voigt, J. D., Leuchter, A. F., & Carpenter, L. L. (2021). Theta burst stimulation for the acute treatment of major depressive disorder: A systematic review and meta-analysis.

*Translational Psychiatry*, 11(1), 1–12. <https://doi.org/10.1038/s41398-021-01441-4>

Walsh, V. (1998). Brain mapping: Faradization of the mind. *Current Biology: CB*, 8(1), R8-11.

[https://doi.org/10.1016/s0960-9822\(98\)70098-3](https://doi.org/10.1016/s0960-9822(98)70098-3)

Wang, X.-J. (2010). Neurophysiological and Computational Principles of Cortical Rhythms in Cognition. *Physiological Reviews*, 90(3), 1195–1268.

<https://doi.org/10.1152/physrev.00035.2008>

Wassermann, E. M. (1998). Risk and safety of repetitive transcranial magnetic stimulation:

Report and suggested guidelines from the International Workshop on the Safety of

Repetitive Transcranial Magnetic Stimulation, June 5-7, 1996. *Electroencephalography*

*and Clinical Neurophysiology*, 108(1), 1–16. <https://doi.org/10.1016/s0168->

[5597\(97\)00096-8](https://doi.org/10.1016/s0168-5597(97)00096-8)

- Watkins, J. C., & Jane, D. E. (2006). The glutamate story. *British Journal of Pharmacology*, *147*(S1), S100–S108. <https://doi.org/10.1038/sj.bjp.0706444>
- Wen, Z., Zhou, F.-Q., Huang, X., Dan, H. D., Xie, B.-J., & Shen, Y. (2018). Altered functional connectivity of primary visual cortex in late blindness. *Neuropsychiatric Disease and Treatment*, *14*, 3317–3327. <https://doi.org/10.2147/NDT.S183751>
- Whitfield-Gabrieli, S., & Nieto-Castanon, A. (2012a). Conn: A functional connectivity toolbox for correlated and anticorrelated brain networks. *Brain Connectivity*, *2*(3), 125–141. <https://doi.org/10.1089/brain.2012.0073>
- Whitfield-Gabrieli, S., & Nieto-Castanon, A. (2012b). Conn: A Functional Connectivity Toolbox for Correlated and Anticorrelated Brain Networks. *Brain Connectivity*, *2*(3), 125–141. <https://doi.org/10.1089/brain.2012.0073>
- Xia, M., & He, Y. (2022). Connectome-guided transcranial magnetic stimulation treatment in depression. *European Child & Adolescent Psychiatry*, *31*(10), 1481–1483. <https://doi.org/10.1007/s00787-022-02089-1>
- Yamasaki, T., Ogawa, A., Osada, T., Jimura, K., & Konishi, S. (2018). Within-Subject Correlation Analysis to Detect Functional Areas Associated With Response Inhibition. *Frontiers in Human Neuroscience*, *12*, 208. <https://doi.org/10.3389/fnhum.2018.00208>
- Yeung, P. Y., Wong, L. L. L., Chan, C. C., Yung, C. Y., Leung, L. M. J., Tam, Y. Y., Tang, L. N., Li, H. S., & Lau, M. L. (2020). Montreal Cognitive Assessment—Single Cutoff Achieves Screening Purpose. *Neuropsychiatric Disease and Treatment*, *16*, 2681–2687. <https://doi.org/10.2147/NDT.S269243>

- Young-Bernier, M., Tanguay, A. N., Davidson, P. S. R., & Tremblay, F. (2014). Short-latency afferent inhibition is a poor predictor of individual susceptibility to rTMS-induced plasticity in the motor cortex of young and older adults. *Frontiers in Aging Neuroscience*, *6*, 182. <https://doi.org/10.3389/fnagi.2014.00182>
- Yu-Lei, X., Shan, W., Ju, Y., Yu-Han, X., Wu, Q., & Yin-Xu, W. (2022). Theta burst stimulation versus high-frequency repetitive transcranial magnetic stimulation for poststroke dysphagia: A randomized, double-blind, controlled trial. *Medicine*, *101*(2), e28576. <https://doi.org/10.1097/MD.00000000000028576>
- Zalesky, A., Fornito, A., & Bullmore, E. T. (2010). Network-based statistic: Identifying differences in brain networks. *NeuroImage*, *53*(4), 1197–1207. <https://doi.org/10.1016/j.neuroimage.2010.06.041>
- Zhang, Z., Zhang, D., Wang, Z., Li, J., Lin, Y., Chang, S., Huang, R., & Liu, M. (2018). Intrinsic Neural Linkage between Primary Visual Area and Default Mode Network in Human Brain: Evidence from Visual Mental Imagery. *Neuroscience*, *379*, 13–21. <https://doi.org/10.1016/j.neuroscience.2018.02.033>
- Zhu, D. C., Tarumi, T., Khan, M. A., & Zhang, R. (2015). Vascular coupling in resting-state fMRI: Evidence from multiple modalities. *Journal of Cerebral Blood Flow & Metabolism*, *35*(12), 1910–1920. <https://doi.org/10.1038/jcbfm.2015.166>
- Ziemann, U., Ilić, T. V., & Jung, P. (2006). Long-term potentiation (LTP)-like plasticity and learning in human motor cortex—Investigations with transcranial magnetic stimulation (TMS). *Supplements to Clinical Neurophysiology*, *59*, 19–25. [https://doi.org/10.1016/s1567-424x\(09\)70007-8](https://doi.org/10.1016/s1567-424x(09)70007-8)



## 5 Appendix

**Table A-1: Schaefer-200 node conversion to MNI coordinates**

Schaefer Atlas	MNI Coordinates			Corresponding MNI region
	x	y	z	
Vis1 (L)	-24	-53	-9	51% lingual gyrus, 33% temporal occipital fusiform cortex
Vis2 (L)	-26	-77	-14	64% occipital fusiform gyrus, 6% lingual gyrus
Vis3 (L)	-45	-69	-8	71 % lateral occipital cortex
Vis4 (L)	-10	-67	-4	67% lingual gyrus, 6% occipital fusiform gyrus
Vis5 (L)	-27	-95	-12	55 % occipital pole, 10% lateral occipital cortex (inferior division)
Vis6 (L)	-14	-44	-3	40 % lingual gyrus, 30 % cingulate gyrus posterior division,
Vis7 (L)	-5	-93	-4	62 % occipital pole, 11% lingual gyrus, 11 % Intracalcarine cortex
Vis8 (L)	-47	-70	10	66% lateral occipital
Vis9 (L)	-23	-97	6	56% occipital pole
Vis10 (L)	-11	-70	7	55% intracalcarine cortex, 10% lingual gyrus
Vis11 (L)	-40	-85	11	36 % lateral occipital cortex superior division, 32% lateral occipital inferior division
PCC1 (L)	-11	-56	13	46% precuneus cortex,
PCC2 (L)	-6	-54	42	75% precuneus cortex
Vis1 (R)	39	-35	-23	58% lingual gyrus, 30% occipital fusiform
Vis2 (R)	28	-36	-14	51% lingual gyri
Vis3 (R)	29	-69	-12	53 % occipital fusiform gyrus, 8% lingual gyrus
Vis4 (R)	12	-65	-5	68% lingual gyrus, 8% occipital fusiform gyrus
Vis5 (R)	48	-71	-6	68% lateral occipital cortex inferior division
Vis6 (R)	11	-92	-5	51% occipital pole, 10 lingual gyrus, 5% occipital fusiform gyrus
Vis7 (R)	16	-46	-1	48% lingual gyrus, 37% cingulate gyrus posterior division

Vis8 (R)	31	-94	-4	64% occipital pole, 6% lateral occipital cortex inferior division
Vis9 (R)	9	-75	9	64% intracalcarine cortex, 6% supracalcarine cortex,
Vis10 (R)	22	-60	7	37 % Intracalcarine cortex, 36% precuneus cortex
Vis11 (R)	42	-80	10	52% lateral occipital cortex inferior division, 29% lateral occipital superior cortex
Vis12 (R)	20	-90	22	31% occipital pole, 10% lateral occipital cortex superior division
PCC1 (R)	12	-55	15	60% precuneus cortex, 8% supracalcarine cortex
PCC2 (R)	7	-49	31	58% cingulate gyrus posterior division, 12% precuneus cortex
PCC3 (R)	6	-58	44	73% precuneus cortex
Stimulation site	1	-72	13	46% supracalcarine cortex, 23% Intracalcarine cortex

*Note.* ROIs in black and red were all included in ROI-to-ROI analysis. Only the ROIs in red were included in the seed-to-target analysis. 200-parcel 7-Network Schaefer atlas includes 1) Visual 2) Somatomotor 3) Dorsal attention 4) Ventral attention 5) Limbic 6) Frontoparietal 7) Default mode networks (Schaefer et al., 2018)

**Table A-2: Results of the rs-fMRI seed-to-target data analysis at three timepoints (Day 1 pre-TBS, Day 2 immediately post-TBS and Day 2 1 hr post-TBS).**

Seed: Stimulation site						
Contrast	Day 2 (immediately post-TBS) > Day1					
	<i>beta</i>	<i>t</i> (18)	<i>p</i> -unc	<i>p</i> -FDR		
iTBS > cTBS	PCC	0.02	0.26	0.80	0.98	
	R-OP	0.02	0.22	0.83	0.98	
	L-OP	0.02	0.15	0.88	0.98	
	R-SCC	0.03	0.39	0.69	0.98	
	L-SCC	0.03	0.33	0.75	0.98	
	R-ICC	0.08	0.71	0.49	0.98	
	L-ICC	0.03	0.33	0.75	0.98	
	MVN	0.02	0.20	0.84	0.98	
	OVN	0.05	0.45	0.66	0.98	
	L-LVN	-0.04	-0.48	0.64	0.98	
	R-LVN	-0.11	-1.10	0.29	0.98	
	L-CC	0.00	-0.03	0.98	0.98	
	R-CC	-0.06	-0.46	0.65	0.98	
	L-LOCi	-0.02	-0.15	0.88	0.98	
	R-LOCi	-0.02	-0.21	0.83	0.98	
	L-LOCs	-0.06	-0.71	0.49	0.98	
	R-LOCs	-0.20	-2.07	0.05	0.90	
Sham > cTBS	PCC	-0.06	-0.79	0.44	0.85	
	R-OP	0.03	0.32	0.75	0.85	
	L-OP	0.05	0.46	0.65	0.85	
	R-SCC	0.01	1.25	0.23	0.85	
	L-SCC	0.04	0.59	0.57	0.85	
	R-ICC	0.05	0.57	0.57	0.85	
	L-ICC	0.05	0.59	0.56	0.85	
	MVN	0.07	0.85	0.41	0.85	
	OVN	-0.01	-0.08	0.94	0.94	
	L-LVN	0.03	0.38	0.71	0.85	
	R-LVN	-0.07	-0.60	0.56	0.85	
	L-CC	0.12	1.21	0.24	0.85	
	R-CC	0.03	0.34	0.73	0.85	
	L-LOCi	0.04	0.49	0.63	0.85	
	R-LOCi	0.07	0.63	0.53	0.85	
	L-LOCs	0.01	0.17	0.87	0.85	
	R-LOCs	-0.23	-2.64	0.02	0.28	

	PCC	0.09	1.1	0.22	0.86
	R-OP	-0.01	-0.10	0.92	0.92
	L-OP	-0.03	-0.27	0.79	0.89
	R-SCC	-0.08	-0.98	0.34	0.86
	L-SCC	-0.04	-0.45	0.67	0.86
	R-ICC	0.03	0.21	0.83	0.89
	L-ICC	-0.02	-0.22	0.84	0.89
	MVN	-0.06	-0.50	0.63	0.87
	OVN	0.06	0.53	0.61	0.86
iTBS > Sham	L-LVN	-0.08	-0.98	0.34	0.86
	R-LVN	-0.04	-0.50	0.62	0.86
	L-CC	-0.12	-1.25	0.23	0.86
	R-CC	-0.09	-0.79	0.44	0.86
	L-LOCi	-0.06	-0.71	0.49	0.86
	R-LOCi	-0.09	-0.91	0.38	0.86
	L-LOCs	-0.06	-0.71	0.49	0.86
	R-LOCs	0.03	0.49	0.62	0.86

Contrast	Day 2 (1 hr post-TBS) > Day1				
	Target	<i>beta</i>	<i>t</i> (18)	<i>p</i> -unc	<i>p</i> -FDR
	PCC	0.01	0.15	0.90	0.91
	R-OP	-0.02	-0.15	0.88	0.91
	L-OP	0.01	0.14	0.89	0.91
	R-SCC	0.08	0.55	0.59	0.91
	L-SCC	0.30	3.05	0.007	0.12
	R-ICC	0.04	0.32	0.75	0.91
	L-ICC	0.14	10.3	0.32	0.91
	MVN	0.02	0.18	0.86	0.91
	OVN	0.02	0.23	0.82	0.91
iTBS > cTBS	L-LVN	-0.03	-0.34	0.74	0.91
	R-LVN	-0.01	-0.12	0.91	0.91
	L-CC	0.08	0.70	0.50	0.91
	R-CC	0.06	0.55	0.60	0.91
	L-LOCi	0.02	0.23	0.82	0.91
	R-LOCi	0.08	0.82	0.42	0.91
	L-LOCs	-0.03	-0.37	0.72	0.91
	R-LOCs	-0.10	-1.47	0.16	0.91
	PCC	-0.07	-0.74	0.47	0.82
	R-OP	0.05	0.42	0.68	0.82
Sham > cTBS	L-OP	0.11	0.95	0.35	0.82

	R-SCC	0.08	0.70	0.50	0.82
	L-SCC	0.12	1.52	0.14	0.82
	R-ICC	0.02	0.15	0.88	0.88
	L-ICC	0.12	0.89	0.38	0.82
	MVN	-0.03	-0.25	0.80	0.86
	OVN	0.08	0.56	0.59	0.82
	L-LVN	0.10	0.88	0.39	0.82
	R-LVN	0.05	0.43	0.68	0.82
	L-CC	-0.02	-0.24	0.83	0.82
	R-CC	-0.06	-0.49	0.63	0.82
	L-LOCi	0.25	1.23	0.23	0.82
	R-LOCi	0.12	1.03	0.32	0.82
	L-LOCs	0.15	1.23	0.24	0.82
	R-LOCs	-0.08	1.22	0.24	0.82
	PCC	0.05	1.15	0.27	0.99
	R-OP	-0.02	-0.23	0.82	0.99
	L-OP	-0.03	-0.33	0.75	0.99
	R-SCC	0.01	0.15	0.88	0.99
	L-SCC	0.19	3.01	0.007	0.13
	R-ICC	0.00	0.00	0.99	0.99
iTBS > Sham	L-ICC	0.05	0.75	0.46	0.99
	MVN	-0.04	-0.45	0.66	0.99
	OVN	0.03	0.31	0.76	0.99
	L-LVN	-0.02	-0.18	0.86	0.99
	R-LVN	0.00	0.05	0.96	0.99
	L-CC	0.04	0.54	0.59	0.99
	R-CC	0.02	0.32	0.75	0.99
	L-LOCi	0.03	0.31	0.76	0.99
	R-LOCi	0.05	0.57	0.57	0.99
	L-LOCs	-0.03	-0.71	0.48	0.99
	R-LOCs	0.01	0.10	0.92	0.99

Contrast	Day 2 (1 hr post-TBS) > Day2 (immediately post-TBS)				
	Target	<i>beta</i>	<i>t</i> (18)	<i>p</i> -unc	<i>p</i> -FDR
	PCC	-0.01	-0.15	0.88	0.99
	R-OP	-0.04	-0.29	0.77	0.99
	L-OP	0.00	-0.01	0.99	0.99
	R-SCC	0.05	0.46	0.65	0.99
iTBS > cTBS	L-SCC	0.30	3.59	0.002	0.036
	R-ICC	-0.04	-0.28	0.78	0.99
	L-ICC	0.11	0.87	0.40	0.99

	MVN	0.00	0.04	0.97	0.99
	OVN	-0.02	-0.16	0.88	0.99
	L-LVN	0.01	0.13	0.89	0.99
	R-LVN	0.01	0.73	0.47	0.99
	L-CC	0.08	0.76	0.45	0.99
	R-CC	0.12	1.00	0.33	0.99
	L-LOCi	0.04	0.45	0.65	0.99
	R-LOCi	0.11	0.99	0.34	0.99
	L-LOCs	0.03	0.27	0.79	0.99
	R-LOCs	0.09	0.85	0.41	0.99
	PCC	0.00	-0.05	0.96	0.96
	R-OP	-0.02	-0.20	0.84	0.96
	L-OP	-0.08	0.66	0.52	0.90
	R-SCC	-0.02	-0.20	0.35	0.96
	L-SCC	0.08	0.97	0.35	0.90
	R-ICC	-0.03	-0.33	0.75	0.90
	L-ICC	0.06	0.49	0.63	0.90
Sham > cTBS	MVN	-0.11	-1.29	0.21	0.90
	OVN	0.09	0.62	0.54	0.90
	L-LVN	0.07	0.59	0.56	0.90
	R-LVN	0.12	0.88	0.39	0.90
	L-CC	-0.14	-1.92	0.071	0.90
	R-CC	-0.09	-1.19	0.25	0.90
	L-LOCi	0.10	0.96	0.35	0.90
	R-LOCi	0.05	0.49	0.74	0.90
	L-LOCs	0.03	0.34	0.74	0.91
	R-LOCs	0.15	1.58	0.13	0.90
	PCC	-0.01	-0.11	0.91	0.97
	R-OP	-0.06	-0.73	0.47	0.83
	L-OP	-0.07	-0.79	0.44	0.83
	R-SCC	0.07	0.70	0.49	0.83
	L-SCC	0.22	3.03	0.007	0.12
	R-ICC	0.00	-0.04	0.97	0.97
	L-ICC	0.05	0.42	0.68	0.90
iTBS > Sham	MVN	0.11	1.02	0.32	0.83
	OVN	-0.11	-1.15	0.26	0.83
	L-LVN	-0.06	-0.57	0.57	0.83
	R-LVN	-0.02	-0.14	0.89	0.97
	L-CC	0.22	2.04	0.056	0.43
	R-CC	0.21	1.89	0.076	0.43
	L-LOCi	-0.07	-0.74	0.47	0.83
	R-LOCi	0.05	0.55	0.59	0.83
	L-LOCs	-0.01	-0.10	0.92	0.97

R-LOCs    -0.06    -0.71    0.49    0.83

*Note.* For the full list of ROIs (and their acronyms) refer to Figure 2. The only significant connection between the stimulation site and L-SCC is highlighted in red. p-unc = ROI-level uncorrected p values set at < 0.05, p-FDR = ROI-level false discovery rate corrected p-value set at < 0.05. Beta values represent the effect size based on Fisher-Z transformed correlation values.

**Figure A 1:** Individual pre- to post-stimulation phosphene thresholds.

